

12-2009

Probabilistic Remediation Evaluation Model for Chlorinated Solvents Considering Uncertainty

Hailian Liang

Clemson University, hailial@clemson.edu

Follow this and additional works at: https://tigerprints.clemson.edu/all_dissertations



Part of the [Environmental Engineering Commons](#)

Recommended Citation

Liang, Hailian, "Probabilistic Remediation Evaluation Model for Chlorinated Solvents Considering Uncertainty" (2009). *All Dissertations*. 462.

https://tigerprints.clemson.edu/all_dissertations/462

This Dissertation is brought to you for free and open access by the Dissertations at TigerPrints. It has been accepted for inclusion in All Dissertations by an authorized administrator of TigerPrints. For more information, please contact kokeefe@clemson.edu.

PROBABILISTIC REMEDIATION EVALUATION MODEL FOR CHLORINATED
SOLVENTS CONSIDERING UNCERTAINTY

A Dissertation
Presented to
the Graduate School of
Clemson University

In Partial Fulfillment
of the Requirements for the Degree
Doctoral of Philosophy
Environmental Engineering and Science

by
Hailian Liang
December 2009

Accepted by:
Dr. Ronald W. Falta, Jr, Committee Chair
Dr. Fred J. Molz, III
Dr. Lawrence C. Murdoch
Dr. Robert A. Fjeld

ABSTRACT

The complex processes and expensive costs of source and plume remediation of dense, non-aqueous phase liquid (DNAPL) complicate the decision-making process for site remediation. Selection of remediation alternatives has been a big challenge due to the lack of tools that simultaneously evaluate the effectiveness of source and plume remediation and access the uncertainties in all major parameters. In this research, a new probabilistic remediation model, Probabilistic Remediation Evaluation Model for Chlorinated solvents sites (PREMChlor), has been developed. This is achieved through linking the analytical model REMChlor to a Monte Carlo modeling simulation package GoldSim via a FORTRAN Dynamic Link Library (DLL) application. PREMChlor can simultaneously evaluate the effectiveness of source and plume remediation considering the inherent uncertainties in all major parameters. In PREMChlor, all of the uncertain input parameters are treated as stochastic parameters represented by probability density functions (PDFs). The outputs from the PREMChlor model are probability distributions and summary statistics of those distributions. This new model considers common technologies for DNAPL source removal and dissolved plume treatment. A license-free file containing the graphical user interfaces has been generated to make the PREMChlor model available for use by others.

In model demonstration, probabilistic simulations show the different probabilities of meeting a remediation goal for different combinations of source and plume remediation scenarios considering uncertainties in input parameters. The PREMChlor

model has been applied to a trichloroethene (TCE) plume in a shallow aquifer at a manufacturing plant. The calibrated model using a deterministic approach is able to closely match the pre-remediation site condition. Probabilistic simulations predicting the effects of remediation show the overall uncertainty in TCE concentration propagates over time given uncertainties in key input parameters. Probabilistic simulations capture most uncertainties in key parameters based on estimated PDFs. The PREMChlor model has also been used to conduct sensitivity analyses by assessing the influence or relative importance of each input parameter on plume behavior, in terms of contaminant mass concentration, for three different plume types. It is found that the degree of influence of different input parameters on the contaminant mass concentration varies widely for different plume types. The overall uncertainty of the contaminant mass concentration is reduced greatly by the remediation effort in all three plume types.

DEDICATION

To my family:

Your love and support gave me the strength to carry on ... Thank you.

ACKNOWLEDGEMENTS

I would like to thank all of the people who offered support and assistance for this work. In particular, I would like to thank my advisor, Dr. Ron Falta, for his guidance, encouragement, and understanding throughout this work. I would also like to thank my committee members, Dr. Fred Molz, Dr. Larry Murdoch and Dr. Robert Fjeld for their valuable comments and suggestions for this work.

Thanks also go to Dr. James Henderson, Mr. Steve Shoemaker and Mr. Kenneth Stuart from DuPont for their helps in providing detailed field data and valuable discussions during model application. Drs Charles Newell and Suresh Rao provided insightful discussions and suggestions during model development.

The United States Department of Defense through the Environmental Security Technology Certification Program (ESTCP) provided funding for this work (project ER-0704). This support is also acknowledged gratefully.

I would also like to acknowledge the GoldSim Technology Group for the use of GoldSim software. Mr. Andrew Burn and Mr. Rick Kossik were very helpful in providing the technical support.

Many individuals voluntarily offered model testing during the late stage of model development. Their detailed feedback and comments are very helpful, and the contributed significantly to the refinement of the final product.

Special thanks to my husband, Qingfeng, for his love, support and patience, and to the rest of my family and friends for their love and support.

TABLE OF CONTENTS

	Page
TITLE PAGE	i
ABSTRACT	ii
DEDICATION	iv
ACKNOWLEDGEMENTS	v
LIST OF TABLES	viii
LIST OF FIGURES	ix
LIST OF NOMENCLATURE AND SYMBOLS	xiii
CHAPTER	
1 INTRODUCTION	1
1.1 DNAPL Contamination and Remediation	1
1.2 Challenges in Evaluating DNAPL Remediation Alternatives	5
2 OBJECTIVES	11
3 MODEL DEVELOPMENT	12
3.1 REMChlor Model	12
3.1.1 REMChlor Source Model	13
3.1.2 REMChlor Plume Model	17
3.2 GoldSim Modeling Environment	24
3.3 Probabilistic Remediation Model	29
3.3.1 General Description	29
3.3.2 Model Structure	32
3.3.3. Interfaces	47
3.3.4 Distribution of Unit Cost and Remediation Efficiency	49
3.3.5 Remediation Cost Analysis	54
3.4 Model Demonstration	55
3.4.1 Problem Overview	55
3.4.2 Model Simulations	58

Table of Contents (Continued)

	Page
4 MODEL APPLICATION.....	69
4.1 Site Background and Field Remediation Activities	69
4.2 Calibration of Pre-remediation Condition	75
4.2.1 Model Settings and Parameters.....	75
4.2.2 Model Calibration Results and Discussion	79
4.3 Probabilistic Simulation of Field Remediation Activities.....	88
4.3.1 Model Settings and Parameters.....	88
4.3.2 Probabilistic Simulation Results and Discussions	96
5 SENSITIVITY ANALYSIS FOR DIFFERENT PLUME TYPES.....	113
5.1 Introduction	113
5.2 Case I: Stable Plume Connected to the Source	115
5.2.1 Base Case Description (Case I).....	115
5.2.2 Sensitivity Analysis (Case I).....	119
5.3 Case II: Growing Plume Disconnected from the Source.....	128
5.3.1 Base Case Description (Case II)	128
5.3.2 Sensitivity Analysis (Case II)	131
5.4 Case III: Growing Plume Connected to the Source.....	137
5.4.1 Base Case Description (Case III).....	137
5.4.2 Sensitivity Analysis (Case III).....	141
6 SUMMARY AND CONCLUSIONS.....	151
APPENDIX.....	155
REFERENCES	180

LIST OF TABLES

Table	Page
3.1 Key parameters used in model demonstration.	56
4.1 Source, transport and natural attenuation parameters used on model calibration.....	77
4.2 Stochastic parameters used in probabilistic simulation.	89
4.3 Percentage of mass removal and corresponding degradation rate for PRB wall used in probabilistic simulation.....	95
5.1 Input parameters tested in sensitivity analysis (Case I).	117
5.2 Ratio of 95 th /5 th percentiles for input parameters and resulting TCE concentration (Case I).	127
5.3 Input parameters tested in sensitivity analysis (Case II).	130
5.4 Ratio of 95 th /5 th percentiles for input parameters and resulting total concentration (Case II).	136
5.5 Input parameters tested in sensitivity analysis (Case III).....	140
5.6 Ratio of 95 th /5 th percentiles for input parameters and resulting VC concentration (Case III).....	149
5.7 Summary of sensitivity analysis for three plume types.	150

LIST OF FIGURES

Figure	Page
1.1 Illustration of DNAPL source zone and dissolved plume.....	3
1.2 Illustration of deterministic modeling approach.	8
1.3 Illustration of probabilistic modeling approach.	9
3.1 Power function illustration of source mass and source discharge relationship.....	14
3.2 Illustration of plume space-time zones [Falta, 2008].....	20
3.3 Schematic of Monte Carlo simulation approach [GoldSim User’s Guide, 2007].	28
3.4 Flow chart of the DLL linkage during the probabilistic simulation.....	30
3.5 Building structure and distribution of the initial source mass.....	34
3.6 Interface of the external DLL element.	36
3.7 Top level subgroups of the model structure.....	37
3.8 Building structures of source parameters.....	39
3.9 Building structure of source remediation efficiency parameters.	42
3.10 Probability histories of an output: Graphic view and Table view.....	45
3.11 Probability distribution summary of an output.	46
3.12 Interface of the source parameters.	48
3.13 Histograms generated from McDade et al.[2005] and interpolated beta distributions for unit costs ($\$/m^3$).....	51
3.14 Histograms generated from McGurie et al. [2006] and interpolated beta distributions for source removal fractions.....	53

List of Figures (Continued)

Figure	Page
3.15 Predicted total concentration over time at the compliance plane in the absence of remediation (model demonstration).	57
3.16 PDFs for uncertain parameters (model demonstration).	59
3.17 Predicted total concentration over time at the compliance plane from simulation 1 (model demonstration).	60
3.18 Predicted total concentration over time at the compliance plane from simulation 2 (model demonstration).	61
3.19 Predicted total concentration over time at the compliance plane from simulation 3 (model demonstration).	64
3.20 Predicted total concentration over time at the compliance plane from simulation 4 (model demonstration).	65
3.21 Probability distribution summary of source remediation cost from simulation 4 (model demonstration).	66
3.22 Probability distribution summary of plume remediation cost from simulation 4 (model demonstration).	67
3.23 Probability distribution summary of total remediation cost from simulation 4 (model demonstration).	68
4.1 Site map of Kinston plant with monitoring wells.	71
4.2 Comparison of TCE concentrations between modeled results and field data for MW-30A (model calibration).	82
4.3 Comparison of TCE concentrations between modeled results and field data for MW-29 (model calibration).	83
4.4 Comparison of TCE concentrations between modeled results and field data for MW-35 (model calibration).	84
4.5 Comparison of TCE concentrations between modeled results and field data for MW-37 (model calibration).	85
4.6 Comparison of TCE concentrations between modeled results and field data for MW-38 (model calibration).	86

List of Figures (Continued)

Figure	Page
4.7 Comparison of TCE concentrations between modeled results and field data for MW-36 (model calibration).....	87
4.8 The PDFs of the stochastic variables used in the probabilistic simulation.	90
4.9 Plume reaction zones, including the PRB treatment, simulated in the model.....	92
4.10 Simulated mean behavior of TCE concentrations in 1999 prior to source remediation or plume PRB wall installation from probabilistic simulation.	97
4.11 Simulated mean behavior of TCE concentrations in 2009 from probabilistic simulation.....	98
4.12 Comparison of TCE concentrations between modeled results and field data for MW-30A (probabilistic simulation).....	101
4.13 Comparison of TCE concentrations between modeled results and field data for MW-47 (probabilistic simulation).....	102
4.14 Comparison of TCE concentrations between modeled results and field data for MW-59 (probabilistic simulation).....	103
4.15 Comparison of TCE concentrations between modeled results and field data for MW-58 (probabilistic simulation).....	104
4.16 Comparison of TCE concentrations between modeled results and field data for MW-29 (probabilistic simulation).....	105
4.17 Comparison of TCE concentrations between modeled results and field data for MW-60 (probabilistic simulation).....	107
4.18 Comparison of TCE concentrations between modeled results and field data for MW-35 (probabilistic simulation).....	108
4.19 Comparison of TCE concentrations between modeled results and field data for MW-37 (probabilistic simulation).....	109
4.20 Comparison of TCE concentrations between modeled results and field data for MW-38 (probabilistic simulation).....	110

List of Figures (Continued)

Figure	Page
4.21 Comparison of TCE concentrations between modeled results and field data for MW-36 (probabilistic simulation).....	111
4.22 Comparison of TCE concentrations between modeled results and field data for MW-57 (probabilistic simulation).....	112
5.1 Plume evolution over time without remediation (Case I).	118
5.2 Distributions of input parameters: $C_0, M_0, \Gamma, V_d, \phi$. (Case I).	120
5.3 Distributions of input parameters (cont.): $R, \alpha_L, X_{rem}, \lambda_{TCE}, \lambda_{TCE_{rem}}$. (Case I).	121
5.4 Tornado chart of TCE concentration variation at $x=100m$ and $t=32$ yr (Case I).	122
5.5 Tornado chart of TCE concentration variation at $x=100m$ and $t=42$ yr (Case I).	126
5.6 Plume evolution over time without remediation (Case II).	129
5.7 Tornado chart of total concentration variation at $x=250m$ and $t=10$ yr (Case II).	132
5.8 Tornado chart of total concentration variation at $x=250m$ and $t=25$ yr (Case II).	135
5.9 Plume evolution over time without remediation (Case III).	139
5.10 Tornado chart of VC concentration variation at $x=300m$ and $t=30$ yr (Case III).	142
5.11 Tornado chart of VC concentration variation at $x=300m$ and $t=55$ yr (Case III).	144

LIST OF NOMENCLATURE AND SYMBOLS

Nomenclature

C	Contaminant mass concentration
C_0	Initial source concentration
M	Contaminant mass
M_0	Initial source mass
Γ	Power function exponent
W	Source width
D	Source depth
X_{rem}	Fraction of source removal
V_d	Groundwater Darcy velocity
ϕ	Effective porosity
R	Retardation factor
α_x	Longitudinal dispersivity
α_y	Transverse dispersivity
α_z	Vertical dispersivity
λ	Plume decay rate
λ_{rem}	Plume enhanced decay rate
x	Distance from source

CHAPTER 1

INTRODUCTION

1.1 DNAPL Contamination and Remediation

Groundwater is a main source of drinking water worldwide. For example, in the United States, more than half the population relies on groundwater for domestic use (Fetter, 1993). Contamination of groundwater by non-aqueous phase liquids (NAPLs), especially by dense, non-aqueous phase liquids (DNAPLs) poses a widespread and serious threat to groundwater supplies due to their toxicity. While the solubilities of DNAPLs are very low, they are typically several orders of magnitude higher than drinking water standards [Pankow et al., 1996]. For example, the common DNAPL, tetrachloroethene (PCE), has a solubility of 150 mg/L in pure water [Verschueren, 2001] and its drinking water standard according to the U.S. Environmental Protection Agency (EPA) Maximum Contaminant Level (MCL) is 5 ug/L as [http://www.epa.gov/ogwdw000/contaminats/dw_contamfs/tetrachl.html].

Common DNAPLs include coal tar, creosote, and chlorinated solvents (chlorinated volatile organic compounds, CVOCs). The most common chlorinated solvents are the chlorinated ethenes and chlorinated ethanes and their breakdown products. The chlorinated ethenes include PCE and its sequential degradation products, trichloroethene (TCE), cis-1,2-dichloroethene (cis-1,2-DCE) and vinyl chloride (VC). The most common chlorinated ethanes are trichloroethane (TCA) and dichloroethane (DCA) [Bedient et al., 1999]. Chlorinated solvents have been widely used in the

manufacturing, aerospace, semiconductor, and transportation industries since the 1940's. Because they are often resistant to biodegradation and dissolution, chlorinated solvents are common contaminants at Superfund sites, Department of Defense (DOD) sites and Department of Energy (DOE) sites [USEPA, 1997 and 2004a].

DNAPLs tend to act as continuous long-term sources of groundwater contamination. When DNAPL is spilled to the environment, it initially forms a separate free-phase because of the low aqueous solubilities. Due to the heavy densities, DNAPL migrates down through the vadose zone, penetrates the groundwater table and enters into the saturated zone, sometimes to depths over one hundred meters. In the saturated zone, much of the DNAPL mass spreads laterally before being trapped by capillary forces and distributed as ganglia and discontinuous pools. These act as highly concentrated source zones of contamination (Figure 1.1). As groundwater flows through these source zones, DNAPL dissolves into the flowing groundwater, slowly creating large dissolved contaminant plumes from relatively small volumes of DNAPL (Figure 1.1).

Technologies have been developed for both DNAPL source control and plume treatment. Source control includes either removal or destruction of the contaminant source, or its physical isolation. For chlorinated solvent source remediation, in-situ technologies include thermal methods (e.g. steam flooding and electrical heating), chemical oxidation, surfactant flooding and cosolvent flooding, soil vapor extraction, and air sparging [Reddi, 1996; Brusseau et al., 1999; Kaluarachchi, 2001; US EPA, 2004b; Mayer and Hassanizadeh, 2005]. Controlled field experiments have shown a range of 60% to more than 90% DNAPL source removal [US EPA 2004b]. To prevent or reduce

the source contaminant loading to the plume, source containment methods, such as slurry walls, clay caps and sealable joint sheet pile walls can be used for isolating the contaminant source.

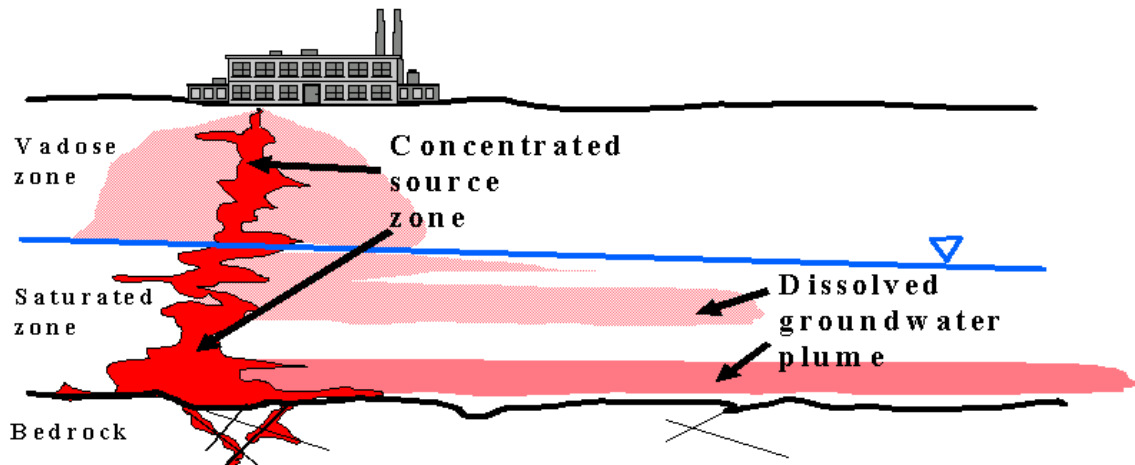


Figure 1.1 Illustration of DNAPL source zone and dissolved plume.

Researchers have shown that the primary benefit of source remediation efforts is to reduce the mass discharge to the plume, by removing source mass [Rao et al., 2001; Rao and Jawitz, 2003; Falta et al., 2005a; Fure et al., 2005; Jawitz et al. 2005]. The reduced plume loading following source remediation may or may not be sufficient to keep the plume within acceptable limits under natural attenuation processes [Falta et al., 2005a, b]. It is rarely possible to remove all of the contaminant source mass due to technical infeasibility or economical impracticability [US EPA, 2004b]. In most cases,

the more practical goal is to remediate contaminated sites through different combinations of source and plume remediation.

Chlorinated solvents in dissolved plumes can be removed by pump-and-treat (PAT) systems, by natural attenuation processes including biodegradation processes, or they can be controlled by reactive barriers. Currently, enhanced in-situ biodegradation is commonly employed if the natural attenuation as a remedy is not sufficient. These enhanced biodegradation processes can include reductive dechlorination, aerobic oxidation, anaerobic oxidation, and aerobic co-metabolism [Wiedemeier et al. 1999; National Research Council (NRC), 2000; Alvarez and Illman, 2006]. Enhancements of these processes involve adding the electron donors, such as hydrogen, molasses, lactate, or hydrogen-releasing compounds, to enhance anaerobic processes or adding electron acceptors, such as oxygen, H₂O₂, or oxygen-releasing compounds, to enhance aerobic processes [Chapelle et al., 2003; Alvarez and Illman, 2006]. Enhanced in-situ biodegradation can reduce plume concentrations in locations that are disconnected from the source, or allow the plume to attenuate in a shorter distance [Falta, 2008].

These source and plume remediation efforts are capital intensive. Partial source removal can cost from several hundred thousand dollars to tens of millions of dollars [McDade et al., 2005]. Due to the lower capital costs, plume remediation costs are normally considered to be smaller than those for source remediation. Plume remediation would be the most cost-effective strategy for sites where the source is almost depleted by natural dissolution or other processes. However, at some sites, source mass is significant. Without source removal, the resulting plume longevity would require a long period of

time to treat and manage. The operating and managing cost of plume remediation systems for such sites can be comparable to the source remediation costs [Falta, 2008]. For many sites, a cost-effective remediation design requires some combination of source and plume remediation. It is therefore essential to couple the transient effects of simultaneous source remediation and plume remediation.

1.2 Challenges in Evaluating DNAPL Remediation Alternatives

The complex processes and expensive costs of source and plume remediation complicate the decision-making process for the site remediation strategy. Simulation is a useful tool for decision-making because it provides a way in which alternative designs can be evaluated without having to experiment on a real site, which may be prohibitively costly, time-consuming, or simply impractical to do. Such decision-making related to remediation alternatives, however, has been a big challenge due to the lack of tools that simultaneously evaluate the effectiveness of source and plume remediation while considering the uncertainties in system parameters.

Most site modeling tools have tended to focus on either the dissolved plume behavior (natural attenuation models), or the source behavior (DNAPL remediation models), with little or no coupling between the two regions. The widely used screening-level models, BIOSCREEN [Newell et al. 1996] and BIOCHLOR [Aziz et al. 2000] simulate remediation by natural attenuation of dissolved hydrocarbons at petroleum fuel release sites and dissolved solvents at chlorinated solvent release sites, respectively. Several three-dimensional multiphase numerical models focus on the source zone behavior, such as T2VOC [Falta et al., 1992] and UTCHEM [Pope and Nelson, 1978;

Delshad et al., 1996]. These models have been used to improve the understanding of the physical and chemical processes that control the contaminant fate, transport, and removal in the source zone [Brown et al., 1994; Freeze, et al., 1994; Liang and Falta, 2008]. However, predicting the effect of the source remediation on plume behavior has been limited by the lack of easy-to-use tools that explicitly link source and plume remediation.

A recent analytical model, Remediation Evaluation Model for Chlorinated solvent sites (REMChlor) [Falta et al., 2005ab; Falta, 2008] was developed to evaluate the transient effects of groundwater source and plume remediation at a more generic and strategic level. REMChlor includes a source model that is based on a power function relationship linking the source zone mass to the source discharge and it can include any aggressive partial source remediation. REMChlor also includes an analytical plume model, based on one dimensional advection, with three-dimensional dispersion. The plume model can simulate plume natural attenuation or plume remediation for multiple compounds (up to four compounds) spatially and temporally. The plume model considers a first-order sequential decay and yield of parent to daughter products. The decay rates and parent/daughter yield coefficients are independently variable in space and time [Falta, 2008]. Cancer risks posed by carcinogenic compounds in the plume are calculated assuming that the contaminated water is used in a house for drinking, bathing, and other household uses [Falta, 2007].

Process and parameter uncertainty that occurs in source and plume remediation is a key factor that has made decision-making between remediation alternatives difficult. Uncertainties arise from hydrogeological and biogeochemical properties (e.g. hydraulic

conductivity), from the site condition and history (e.g. size and timing of contaminant releases and discharge to groundwater), from the effectiveness of remediation (e.g. fraction of source removed), and from the cost of remediation. Besides simultaneously evaluating the effectiveness of source and plume remediation, it is also essential to fully assess the uncertainties and variability inherent in process and system parameters in order to select the best remediation alternative.

The conventional deterministic modeling approach used in the models summarized above does not reflect these uncertainties. For example, Liang and Falta [2008] showed that deterministic simulations using complex multiphase flow codes predicted the delivery of remediation fluids to desired locations with a fairly high degree of certainty, while deterministic predictions of DNAPL recovery showed large uncertainties. One way to capture this uncertainty is by using a probabilistic modeling approach, where the model is run repeatedly using the statistical distributions of the uncertain parameters. At some sites, however, it may be hard to justify such an intensive modeling effort, and more idealized probabilistic simulation models of the remediation process could complement the deterministic process-based simulation models [Liang and Falta, 2008].

A deterministic modeling approach takes a single value for each parameter and yields into a single prediction of the system response (Figure 1.2). Typically, these single values selected for different parameters are “best estimates” or sometimes “worst estimates”, resulting in overestimates or underestimates of results. In reality, however, the hydrogeologic, geochemical, and process parameters used in a model are either

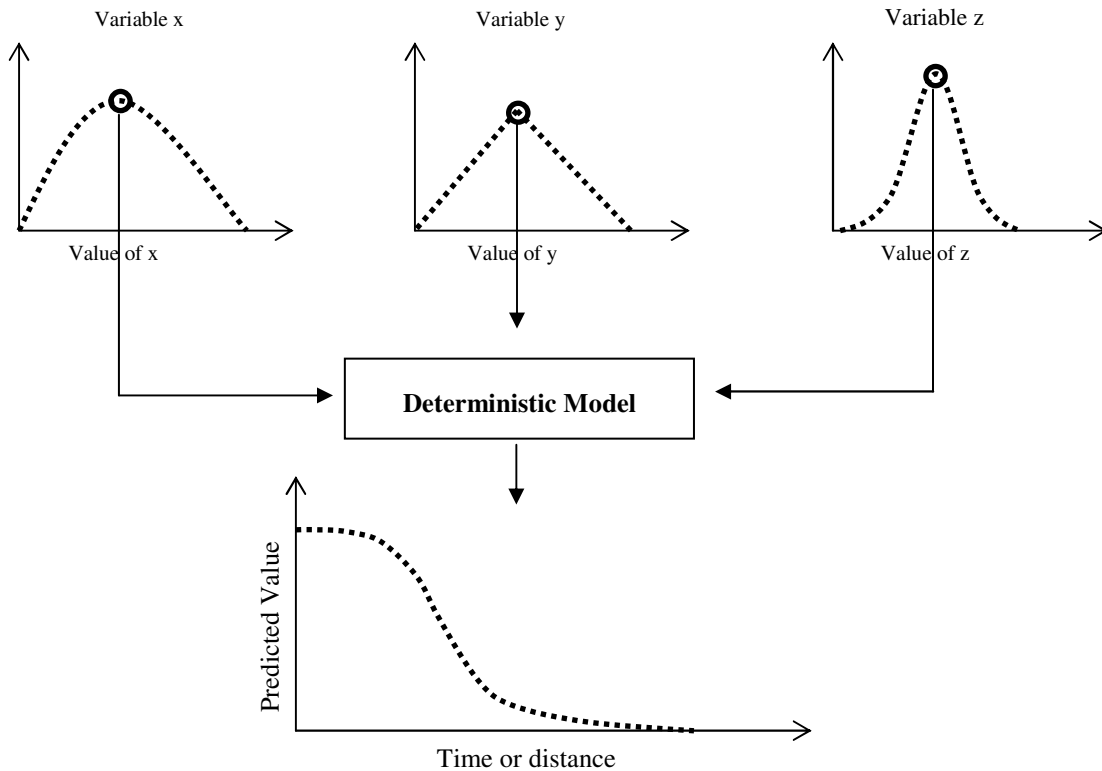


Figure 1.2 Illustration of deterministic modeling approach.

variable, uncertain, or both variable and uncertain. The deterministic model does not consider the nature of overall uncertainty in a simulation. A widely used approach for incorporating this uncertainty is probabilistic modeling (e.g., using the Monte Carlo technique), where uncertain parameters are represented by probability density functions (PDFs), and the result itself is also represented by a probability distribution (Figure 1.3).

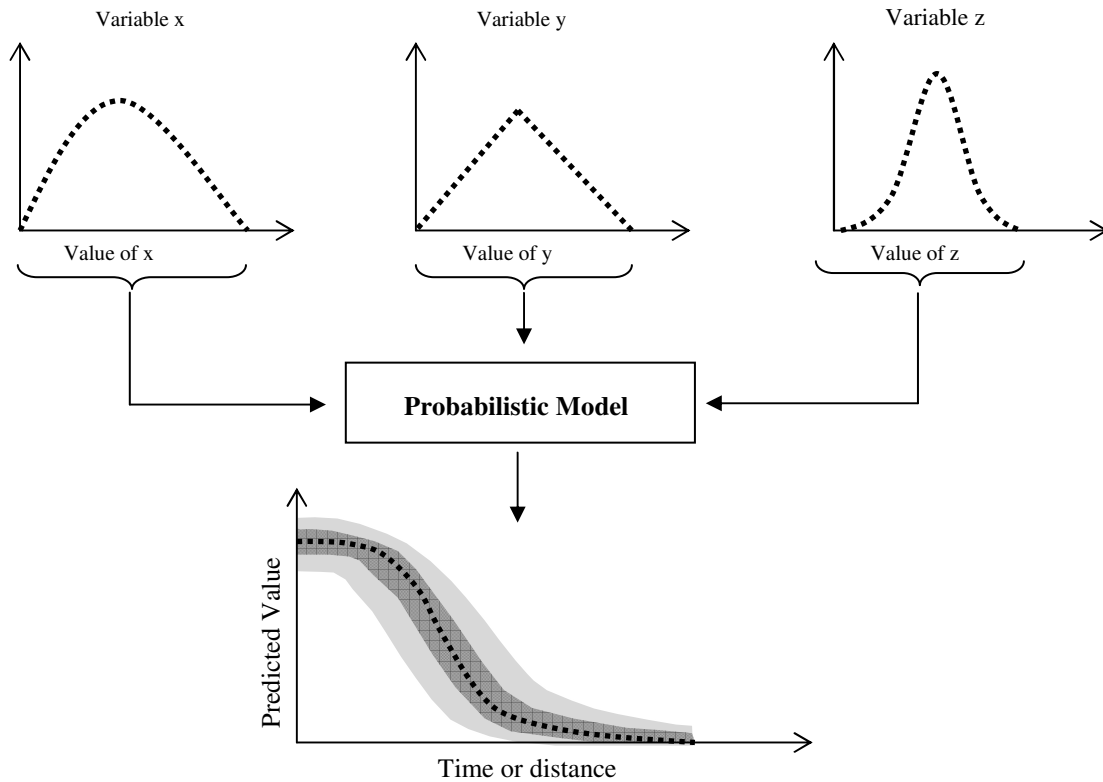


Figure 1.3 Illustration of probabilistic modeling approach.

The probabilistic modeling approach has been widely used to perform risk assessment in contaminated sites (US EPA, 1997; Hope and Stock, 1998; Slob and Pieters, 1998; Chang, 1999; US EPA, 2001; Liu et al., 2004; Li et al., 2007). However only a few models allow running Monte Carlo simulations and stochastic analysis regarding contaminant fate and transport, such as MODFLOW2000 within GMS v5.0

(<http://www.scisoft-gms.com/>) and Groundwater Vistas v4.0 (<http://www.groundwatermodels.com/>). To the author's knowledge, there is no such model that utilizes a probabilistic approach to gain the insight into the uncertainties related to the contaminant source and plume remediation for chlorinated solvents sites.

In this study, a new probabilistic remediation model, Probabilistic Remediation Evaluation Model for Chlorinated solvents sites (PREMChlor) has been developed through the linkage between the deterministic REMChlor model and the probabilistic simulation package GoldSim (<http://www.goldsim.com/>). The new PREMChlor model takes into account the uncertainties in all major parameters and allows for quick simulations of different combinations of source and plume remediation scenarios to evaluate remediation alternatives.

CHAPTER 2

OBJECTIVES

The research objective is to develop a quantitative probabilistic simulation model that can evaluate chlorinated solvent site remediation alternatives in the face of uncertainty. Specific objectives for this study include:

- Develop a probabilistic remediation model that evaluates the effectiveness of source and plume remediation considering uncertainties in all major input parameters.
- Apply the probabilistic remediation model to a real field site.
- Explore the importance of key input variables on the source and plume behavior by assessing the influence or relative importance of each input parameter on the effectiveness of both source and plume remediation in terms of different plume categories.

CHAPTER 3

MODEL DEVELOPMENT

The probabilistic remediation model is developed by linking the REMChlor analytical model to the GoldSim Monte Carlo simulation software package via a FORTRAN Dynamic Link Library (DLL) application. The REMChlor model simultaneously couples source remediation to plume remediation in a deterministic manner. GoldSim is a commercial probabilistic simulation software package. By linking the REMChlor model to the GoldSim probabilistic framework, the new model is capable of simulating the effects of source and plume remediation considering the uncertainties in major input parameters.

3.1 REMChlor Model

The REMChlor transport model fully links source remediation to plume remediation. It is not specific to any remediation technology. The contaminant source remediation is simulated as a fractional removal of the source mass at a future time; plume remediation is modeled considering first-order sequential decay rates of parent and daughter compounds that are variable in space and time. The following description of REMChlor model is based mainly on several works [Falta et al., 2005a, Falta, 2008].

3.1.1 REMChlor Source Model

The source model is based on a mass balance of the source zone where mass is removed by dissolution and advection with some type of additional decay [Falta et al., 2005a, Falta, 2007 and 2008]:

$$\frac{dM(t)}{dt} = -Q(t)C_s(t) - \lambda_s M(t) \quad (1)$$

where $Q(t)$ is the water flow rate through the source zone due to infiltration or groundwater flow, $C_s(t)$ is the average contaminant concentration leaving the source zone, $M(t)$ is the contaminant mass in the source zone, and λ_s is the additional decay term to account for chemical or biological destruction of mass in the source zone.

The source mass is linked to the source discharge through a power function [Rao et al. 2001; Rao and Jawitz, 2003; Parker and Park, 2004; Zhu and Sykes, 2004; Falta et al., 2005a; Falta, 2008]:

$$\frac{C_s(t)}{C_0} = \left(\frac{M(t)}{M_0} \right)^\Gamma \quad (2)$$

where C_0 is the flow-averaged source concentration corresponding to the initial source mass, M_0 . The exponent, Γ determines the shape of the source discharge response to changing source mass (Figure 3.1). When $\Gamma=1$, the source mass and source discharge decline exponentially with time [Newell and Adamson, 2005 and Newell et al., 2006].

When $\Gamma > 1$, the source is never fully depleted, and the source discharge is always greater than zero. When $\Gamma < 1$, the source is eventually depleted, and the source discharge equals zero in the end. When $\Gamma = 0.5$, the source discharge declines linearly with time. When $\Gamma = 0$, the source discharge remains constant until the source is completely depleted [Falta et al., 2005a, Falta, 2007 and 2008]:

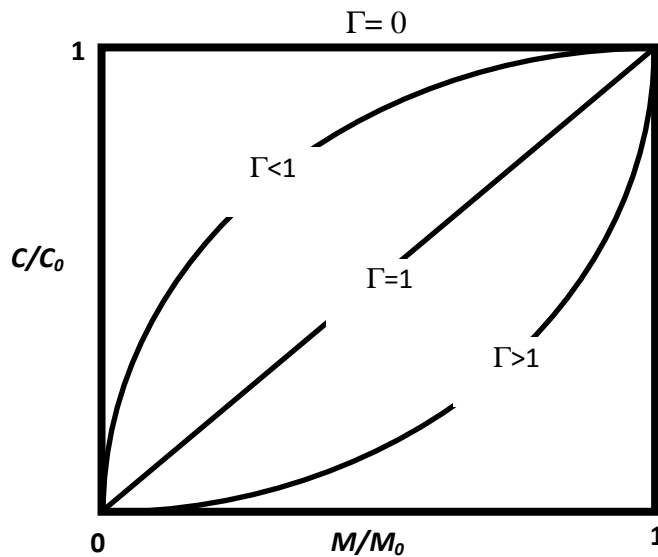


Figure 3.1 Power function illustration of source mass and source discharge relationship.

Field, laboratory, and theoretical evaluations of the source mass/source discharge response suggest that Γ may vary between about 0.5 and 2 at real sites [Rao and Jawitz, 2003; Falta et al., 2005a; Newell and Adamson, 2005; Jawitz et al., 2005; Fure et al.,

2005, McGuire et al., 2006, Newell et al., 2006]. Simulation studies suggest that sites with DNAPL located predominantly in low permeability zones exhibit $\Gamma > 1$ and sites with DNAPL in high permeability zones exhibit $\Gamma < 1$ [Falta et al., 2005 a, b]. Park and Parker [2005] suggest Γ values greater than 1 for finger-dominated residual DNAPL and less than 1 for DNAPL pools. Essentially, Γ should be considered as an uncertain parameter, whose mean value can be roughly estimated, but whose actual value will never be exactly known at a site.

The solution of Equation (1) with the power function (Equation (2)) can be used to predict the time-dependent depletion of the source zone mass by dissolution and perhaps some other form of biological or chemical decay. If Q is constant, substituting Equation (2) into Equation (1) results in a nonlinear differential equation and its solution was given by Falta et al. [2005b] as shown in Equation (3). Parker and Park [2004] and Zhu and Sykers [2004] give similar solutions for the case where λ_s equals to zero.

$$M(t) = \left\{ \frac{-QC_0}{\lambda_s M_0^\Gamma} + \left(M_0^{1-\Gamma} + \frac{QC_0}{\lambda_s M_0^\Gamma} \right) e^{(\Gamma-1)\lambda_s t} \right\}^{\frac{1}{1-\Gamma}} \quad (3)$$

The time-dependent mass is then used in Equation (2) to calculate the time-dependent source discharge:

$$C_s(t) = \frac{C_0}{M_0^\Gamma} \left\{ \frac{-QC_0}{\lambda_s M_0^\Gamma} + \left(M_0^{1-\Gamma} + \frac{QC_0}{\lambda_s M_0^\Gamma} \right) e^{(\Gamma-1)\lambda_s t} \right\}^{\frac{1}{1-\Gamma}} \quad (4)$$

This source model can account for aggressive source remediation efforts (such as excavation, thermal treatment, alcohol or surfactant flooding, or chemical oxidation) that remove a substantial fraction of the source mass over a short period of time [Falta et al., 2005a]. By rescaling the equations following the removal of source mass, the source mass and source discharge due to source remediation are presented by Falta et al. [2005b] as:

$$M(t) = \left\{ \frac{-QC_2}{\lambda_s M_2^\Gamma} + \left(M_2^{1-\Gamma} + \frac{QC_2}{\lambda_s M_2^\Gamma} \right) e^{(\Gamma-1)\lambda_s(t-t_2)} \right\}^{\frac{1}{1-\Gamma}} \quad (5)$$

$$C_s(t) = C_2 \left(\frac{M(t)}{M_2} \right)^\Gamma \quad (6)$$

$$M_2 = (1-X)M_1 \quad (7)$$

$$C_2 = C_0 \left(\frac{(1-X)M_1}{M_0} \right)^\Gamma \quad (8)$$

where t_2 is the time when the remediation ends; M_1 is the source mass before remediation, and M_2 is the source mass at t_2 ; X is the fraction of source mass removed

during the remediation. This approach is not technology specific, and it allows for a realistic and mass conservative assessment of the effects of source remediation on source longevity and discharge. The source model serves also as a time-dependent mass flux boundary condition to the analytical plume model as described later.

3.1.2 REMChlor Plume Model

The plume model considers 1-D advection, retardation, and 3-D dispersion with first order decay of parent compound into daughter products. The governing equation for the dissolved concentration of each contaminant compound in the plume is as follows [Falta et al., 2005b and Falta, 2008]:

$$R \frac{\partial C}{\partial t} = -v \frac{\partial C}{\partial x} + \alpha_x v \frac{\partial^2 C}{\partial x^2} + \alpha_y v \frac{\partial^2 C}{\partial y^2} + \alpha_z v \frac{\partial^2 C}{\partial z^2} + rxn(x, t) \quad (9)$$

where C is the dissolved concentration, and R is the retardation factor, α_x , α_y and α_z are the longitudinal, transverse, and vertical dispersivities, respectively, v is the pore velocity, and $rxn(x, t)$ is the rate of generation (+) or destruction (-) of the dissolved compound due to biological or chemical reactions that may vary temporally and spatially.

This plume model is coupled with the source zone mass balance (Equation (1)), using the power function relationship for C_s vs. M described by Equation (2). A specified flux condition at $x=0$ ensures that the rate of discharge leaving the source zone is equal to the rate of contaminants entering the plume. The total mass flux entering the plume from the source is specified as [Falta et al., 2005b and Falta, 2008]:

$$\frac{Q(t)C_s(t)}{A} = \left[\phi v C(t) - \phi \alpha_x v \frac{\partial C(t)}{\partial x} \right]_{x=0} \quad (10)$$

where ϕ is the porosity, and A is the area over which the contaminant flux enters the ground water flow system. If sources are located below the water table, A would be the cross-sectional area of the source zone perpendicular to the groundwater flow. If sources are located above the water table, A would be the cross-sectional area at the top of the water table perpendicular to flow that was used to accommodate the infiltration rate from the source.

A streamtube approach is used to decouple the solute advection and reactions from the longitudinal dispersion. The reactive plume model is based on a one-dimensional streamtube characterized by a constant pore velocity and solute retardation factor. Since only advection is considered in the streamtube, the flux boundary condition at the edge of the source zone is [Falta et al., 2005b]:

$$C(t)|_{x=0} = \frac{Q(t)C_s(t)}{\phi v A} \quad (11)$$

If the source is located below the water table and $Q = \phi v A$, then the flux boundary is the time-dependent source concentration:

$$C(t)|_{x=0} = C_s(t) \quad (12)$$

where $C_s(t)$ could be calculated by Equations (4) and (6). In this 1-D advective transport model, the time of solute release from the source at any time or distance is:

$$t_{release} = t - Rx/v \quad (13)$$

If there is not any plume degradation, the solute concentration at a location (x,t) is:

$$C(x,t) = C(t_{release})|_{x=0} \quad (14)$$

Plume reactions are included in this advective streamtube model. As a solute particle travels downstream in the streamtube, it is not subject to any mixing process, so it is conceptually equivalent to a batch reaction with an initial concentration of $C(t_{release})|_{x=0}$, and a reaction period equal to the travel time to that location, Rx/v [Falta et al., 2005b]. For example, if the solute reaction is first order decay in the aqueous phase with a decay rate of k , the equivalent batch reaction is:

$$R \frac{dC}{dt} = -kC \quad \text{with} \quad C|_{t=0} = C(t_{release})|_{x=0} \quad (15)$$

Then the solute concentration at a location (x,t) will be:

$$C(x,t) = C(t - Rx/v)|_{x=0} \exp\left(\frac{-kx}{v}\right) \quad (16)$$

This analysis is extended to the case of time and distance dependent reaction rates by dividing the distance-time domain into different zones [Falta, 2007 and 2008]. As illustrated in Figure 3.2, nine reaction zones are used in REMChlor to represent different conditions downgradient from a contaminant source over the life of a plume. The first time zone after the release, $0 < t < t_1$, could represent a period of natural attenuation following the contaminant spill. The second time zone after the release, $t_1 < t < t_2$ could represent a temporary period of active plume remediation (i.e. enhanced reductive dechlorination). The final time zone, $t > t_2$, could represent long term conditions in the

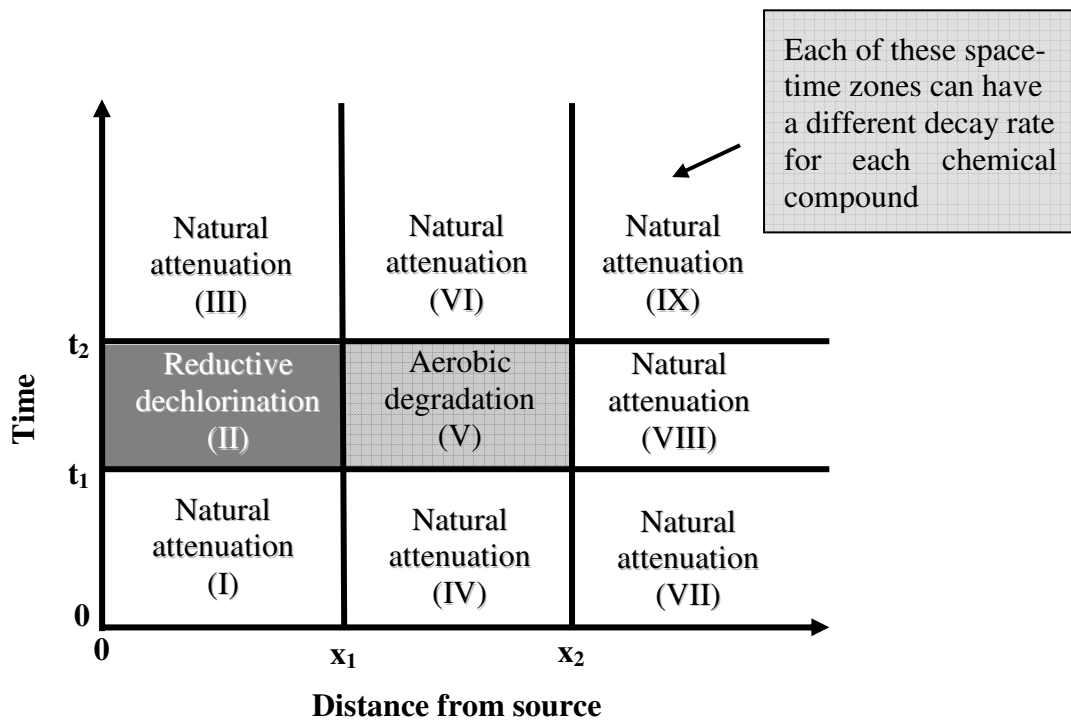


Figure 3.2 Illustration of plume space-time zones [Falta, 2008].

plume after the plume remediation ended (another period of natural attenuation). Similarly, the distance from the source is divided into three zones. For $x < x_1$, one set of natural or engineered biogeochemical conditions are present, while downstream, at $x_1 < x < x_2$, another set of conditions could predominate. For $x > x_2$, conditions could again revert back to natural background conditions. This “reaction-zone” approach provides REMChlor with flexibility to simulate the effect of plume natural attenuation or plume remediation on different contaminant compounds spatially and temporally.

The analytical solution for these multiple reaction zones is derived using the residence time in each zone to develop the batch reaction solution for that zone. The initial conditions for the batch reaction in a given zone are the final conditions from the previously encountered reaction zone. For first-order decay in the aqueous phase, a set of nine reaction rates are defined ($k_{(I)}-k_{(IX)}$) (Figure 3.2). At a given location (x,t), the solute concentration is given by Falta [2008]:

$$C(x,t) = C(t - Rx/v) |_{x=0} \exp\left\{-\sum_{n=I}^{IX} \frac{t_{(n)} k_{(n)}}{R}\right\} \quad (17)$$

This plume model considers first order parent-daughter decay/production reactions for a four-component system. The batch reaction equations for compounds A, B, C, and D in zones (n) are:

$$R \frac{dC_{A(n)}}{dt} = -k_{A(n)} C_{A(n)} \quad I.C. \rightarrow C_{A(n)}(0) = C_{A(n-1)} \quad (18)$$

$$R \frac{dC_{B(n)}}{dt} = y_{BA(n)} k_{A(n)} C_{A(n)} - k_{B(n)} C_{B(n)} \quad I.C. \rightarrow C_{B(n)}(0) = C_{B(n-1)} \quad (19)$$

$$R \frac{dC_{C(n)}}{dt} = y_{CB(n)} k_{B(n)} C_{B(n)} - k_{C(n)} C_{C(n)} \quad I.C. \rightarrow C_{C(n)}(0) = C_{C(n-1)} \quad (20)$$

$$R \frac{dC_{D(n)}}{dt} = y_{DC(n)} k_{C(n)} C_{C(n)} - k_{D(n)} C_{D(n)} \quad I.C. \rightarrow C_{D(n)}(0) = C_{D(n-1)} \quad (21)$$

where $y_{ij(n)}$ are the yield coefficients for each parent-daughter reaction. These yield coefficients also depend on distance and time if the nature of a reaction changes.

Longitudinal dispersion is accounted for by considering a collection of streamtubes with a normally distributed pore velocity [Falta, 2008]. Longitudinal dispersivity, α_x , at (x, t) is calculated by Equation (22) [Falta, 2008].

$$\alpha_x = \frac{1}{2} \frac{\sigma_v^2}{\bar{v}} t = \frac{1}{2} \frac{\sigma_v^2}{\bar{v}^2} \bar{x} = a\bar{x} \quad (22)$$

where \bar{v} is the mean pore velocity, σ_v is the standard deviation of pore velocity, \bar{x} is the mean front location. With a fixed inlet concentration, C_0 , the concentration at (x, t) using the streamtube approach is given by Falta [2008]:

$$\frac{C}{C_0} = \frac{1}{2} \operatorname{erfc} \left(\frac{x - \bar{v}t}{\sigma_y t \sqrt{2}} \right) \quad (23)$$

With a longitudinal dispersivity expressed in Equation (22), Equation (23) would become to the analytical solution of 1-D advection dispersion equation for an infinite system where the initial concentration is C_0 for $x < 0$ and $C=0$ for $x > 0$ [Charbeneau, 2000 and Falta, 2008]:

$$\frac{C}{C_0} = \frac{1}{2} \operatorname{erfc} \left(\frac{x - \bar{v}t}{2\sqrt{\alpha_x \bar{v}t}} \right) \quad (24)$$

Transverse and vertical dispersions are modeled using Domenico's [1987] approximation. The longitudinal, transverse and vertical dispersivities are made scale dependent by being different linear functions of the mean front location. The plume model assumes dispersion occurring in the positive and negative y directions, but only in the positive z direction [Falta, 2008]. The solution with 3-D dispersion constructed from the 1-D solution (Equation (17)) is given by Falta [2008]:

$$C(x, y, z, t) = C(x, t) f_y(y) f_z(z) \quad (25)$$

where the transverse and vertical functions are:

$$f_y(y) = \frac{1}{2} \left(\operatorname{erf} \left\{ \frac{y + Y/2}{2\sqrt{\alpha_y x}} \right\} - \operatorname{erf} \left\{ \frac{y - Y/2}{2\sqrt{\alpha_y x}} \right\} \right) \text{ and}$$

$$f_z(z) = \frac{1}{2} \left(\operatorname{erf} \left\{ \frac{z + Z}{2\sqrt{\alpha_z x}} \right\} - \operatorname{erf} \left\{ \frac{z - Z}{2\sqrt{\alpha_z x}} \right\} \right) \quad (26)$$

Cancer risks posed by carcinogenic compounds in the plume are calculated assuming that the contaminated water is used in a house for drinking, bathing, and other household uses [Falta et al., 2005b]. The plume model currently considers the inhalation and ingestion cancer risk from water that is piped into the house from a well, but it does not consider vapor transport through the vadose zone. The calculation approach follows US EPA's method [US EPA, 1989 and Falta, 2007].

3.2 GoldSim Modeling Environment

GoldSim is a probabilistic simulation software package for visualizing and conducting dynamic, probabilistic simulation to support management and decision-making in business, engineering and science [GoldSim User's Guide, 2007]. It has a great flexibility to link to other external programs and process models. GoldSim was chosen for this work partly because it provides a capability to easily build graphical user interfaces. It has been used in the nuclear industry for conducting performance/safety assessment calculations [Robinson et al., 2003]. It was also used to conduct the economic evaluation of geological CO₂ storage [Zhang et al., 2007]. A geochemical model was linked to GoldSim [Eary, 2007].

The GoldSim modeling environment is highly-graphical and completely object-oriented [GoldSim User's Guide (v9.60), 2007]. The model is constructed, documented, and presented by creating and manipulating graphical objects representing model components: data and relationships between the data. The objects within a model are the basic model building blocks, referred to as elements. Most elements accept at least one input and produce one or more outputs. A GoldSim model is constructed by linking the outputs of one (or more) elements to the inputs of other elements. A complex model can have hundreds (or thousands) of elements and links.

GoldSim provides a variety of elements, such as input elements, function elements, results elements and others. This section briefly describes elements that have been heavily used to construct the probabilistic model. Input elements are designed for defining basic input data in the model. There are two main types of input elements: Data and Stochastic. Data elements allow the user to specify a single scalar value or an array of related values. One important feature of a data element is that it can be linked to the edit input field to build the graphical interface. Stochastic elements allow the user to specify an uncertain value by defining it as a probability distribution. GoldSim provides various probability distributions, such as log, log-normal, triangular, uniform, and so forth.

The main function elements are the Expression element and the Selector element. The Expression element is designed for defining mathematical expressions by using various mathematical operators and functions, or logical expressions by using conditional operators and logic expression (*if, then*). The Selector element defines expressions with

nested *if, then* logic. With the expressions set up appropriately, a selector element can allow the switch or selection among several different values or conditions. During the construction of the probabilistic model, many selector elements are used in order to establish a switch between the probabilistic value and the deterministic value for a stochastic input parameter.

The most advanced and powerful element is the External (DLL) element. The External (DLL) element allows the modeler to dynamically link an external computer program (such as a FORTRAN program) directly to GoldSim. To do so, the modeler needs to specify the inputs and outputs for an external DLL element. The inputs of a DLL element are the parameters that the modeler wishes to send to the external program. The inputs usually are the outputs of other existing GoldSim elements. The outputs of a DLL element are the parameters that the external program will return to GoldSim. The external computer program must to be compiled as the dynamic link library (DLL) and linked to GoldSim through the external (DLL) element. In order to communicate with (i.e., be dynamically called by) GoldSim, some modifications to the external program code are necessary. GoldSim allows almost any computer program to be dynamically linked into GoldSim [GoldSim User's Guide, 2007].

Result elements are designed to provide a convenient and powerful method to assemble, analyze and display probabilistic simulation results. There are four types of result elements: time history, distribution, multi-variate, and array. Time history shows the result of a certain output as a function of time, and is probably the most common and useful form of result display. Distribution results show the probability distribution (in the

form of a histogram) based on the final values of a particular uncertain output, as well as summary statistics, such as percentiles, mean, standard deviation etc. Multi-variate results provide a way to analyze multiple outputs to support sensitivity and uncertainty analysis. Array results allow the users to view vectors and matrices.

GoldSim conducts the probabilistic simulation using a Monte Carlo approach. The Monte Carlo approach is the common technique for propagating the uncertainty in the input parameters of a system to the predicted results and performance. In Monte Carlo simulation, the entire system is simulated a large number of times. Each simulation is independent and equally likely, referred to as a realization of the system. For each realization, all of the uncertain parameters are sampled from the specified distributions. The performance of the system from one realization is then computed or evaluated and the result is saved. After repeating many realizations, the results of the independent simulations are assembled into probability statistics and distributions. Figure 3.3 shows a schematic of Monte Carlo simulation.

The GoldSim Dashboard Authoring Module [GoldSim Dashboard Authoring Module User's Guide, 2007] allows the modeler to design and build graphical user interfaces for the model. The GoldSim Dashboard Authoring Module also lets the modeler to create GoldSim Player files which can be run under GoldSim Player, a free program. The Player file containing graphical user interfaces makes a model that can be easily used by other users without having the GoldSim license and without being familiar with the details of the specific model and the GoldSim simulation environment.

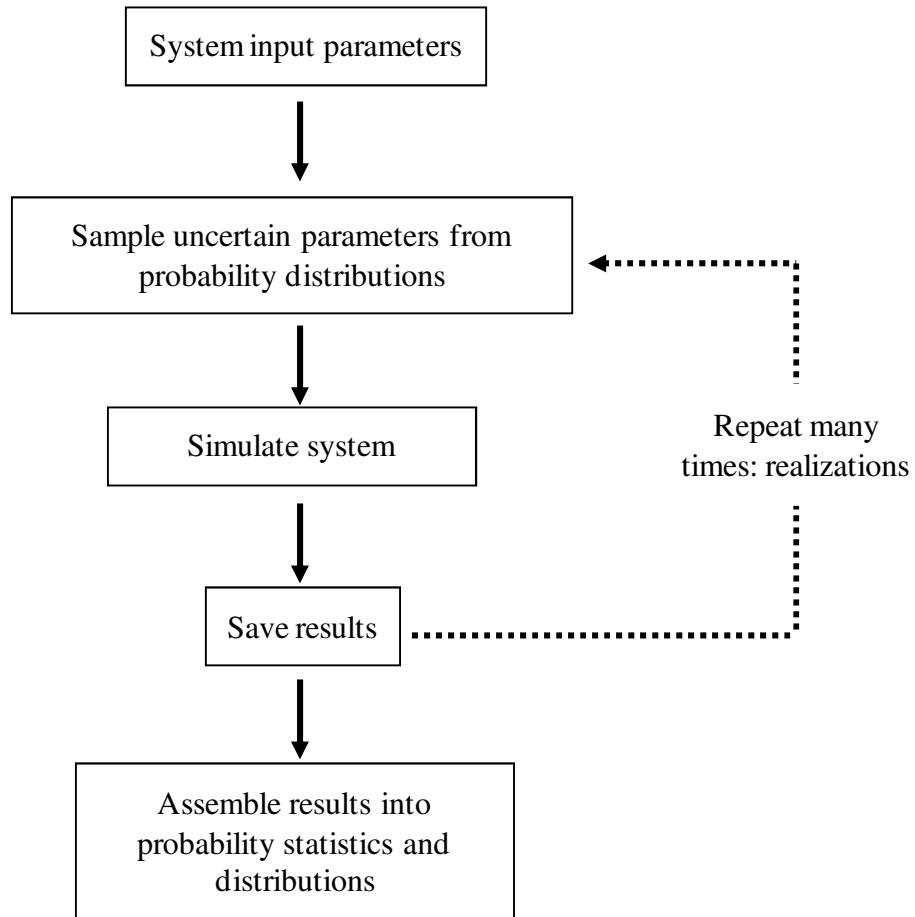


Figure 3.3 Schematic of Monte Carlo simulation approach [GoldSim User's Guide, 2007].

3.3 Probabilistic Remediation Model

3.3.1 General Description

The PREMChlor probabilistic remediation model is developed by linking the REMChlor model to the GoldSim software via a FORTRAN Dynamic Link Library (DLL) application. A probabilistic simulation consists of hundreds or thousands of deterministic Monte Carlo realizations. As illustrated in Figure 3.4, during the probabilistic simulation, GoldSim is used to specify the probability distributions for all stochastic parameters and specify the Monte Carlo parameters, such as the total simulation duration, time step, and the total realization number for the probabilistic simulation. Inside the Monte Carlo loop, for each realization, GoldSim is used to sample the value for each uncertain parameter through its PDF and specify the value to each deterministic parameter and assigns the values to REMChlor. The REMChlor model is called via FORTRAN DLL application to perform the analytical calculation and the results are passed back to GoldSim. After all of the realizations are completed, all of the results of REMChlor calculations are stored in GoldSim and assembled into probability distributions and probability statistics.

In the probabilistic simulation model, all of the input uncertain parameters (e.g., source mass, power function exponent, source removal percentage, groundwater velocity, retardation factor, plume decay rates etc.) are treated as stochastic parameters represented by PDFs. Probabilistic simulation can be performed to evaluate the influence of the uncertainty in input parameters on the effectiveness of both source and plume remediation. The outputs from the probabilistic simulation model (e.g., contaminant

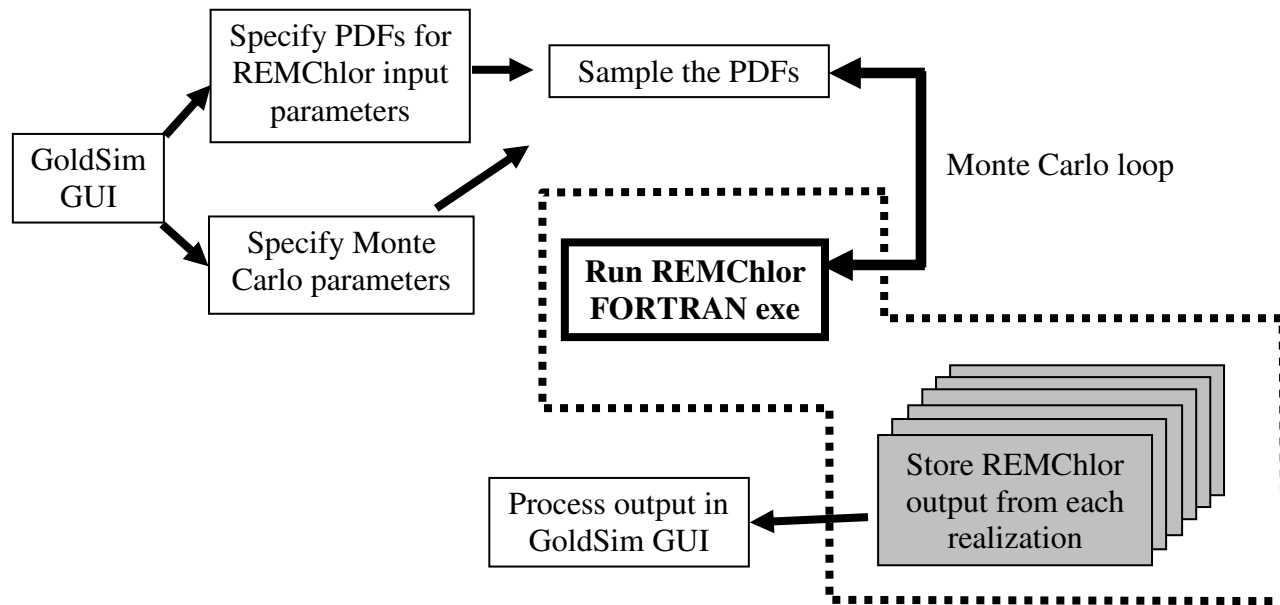


Figure 3.4 Flow chart of the DLL linkage during the probabilistic simulation.

concentrations and mass discharges etc.) are also probability distributions or probability statistics.

The probabilistic model can be run in two different modes: the probabilistic simulation mode and the deterministic simulation mode. Under the probabilistic simulation mode, model runs multiple realizations. Each realization is deterministic and uses a different probabilistic value for a stochastic parameter. Under the deterministic simulation mode, only one realization is run in which a deterministic value is used for every parameter.

The probabilistic model allows two different types of input information, either deterministic or probabilistic values. Deterministic values are provided as the inputs to the model when the user knows the specific values the model requires. When the required information is uncertain, the user provides probability distribution parameters, such as mean, standard deviation etc., as the inputs.

In the PREMChlor model, thirteen pages of graphical user interfaces have been built to allow other users to easily enter the input values, run the model and view the results. A GoldSim player file containing the graphical user interfaces has been generated to make the probabilistic simulation model easily used by users without having the GoldSim license and without being familiar with the details of the probabilistic model and the GoldSim simulation environment.

3.3.2 Model Structure

3.3.2.1 Model Inputs and Elements

There are 86 input parameters in the PREMChlor probabilistic model (74 are linked to the DLL element). Among those, 18 are treated as deterministic and 68 are treated as stochastic. Deterministic parameters usually have less or no variability and can be defined in a certain way. For example, two parameters, the times when remediation starts and ends, are treated as deterministic because they are known parameters for a remediation design. Stochastic parameters are normally associated with much uncertainty. For example, groundwater Darcy velocity is treated as stochastic because it is inherently uncertain.

In the PREMChlor probabilistic model, a deterministic input parameter requires a single GoldSim data element in which a scalar value is specified. A stochastic input parameter requires several different types of GoldSim elements, including several data elements, a single stochastic element, and a single selector element. One data element is used to specify a deterministic value for that stochastic input parameter. To define the probabilistic value sampled from a PDF for that stochastic input parameter, a single stochastic element and other several data elements are involved. The single stochastic element is used to specify the type of distribution and gives the probabilistic value. Another single data element is used to generate a true/false condition controlling the deterministic value and the probabilistic value for that stochastic input parameter. A selector element is used to establish a switch between the probabilistic value and the deterministic value. During the simulation, either the probabilistic value or the

deterministic value can be used for a stochastic input parameter, depending on the user's choice.

In order to edit the probabilistic value from interfaces, data elements, instead of numerical values, are used to specify the parameters describing the shape of the distribution. The number of GoldSim data elements used to describe the shape of the distribution depends on the type of the distribution. For example, a normal distribution requires two data elements, one for the mean and the other for the standard deviation (Stdv) of the normal distribution. A triangular distribution requires three data elements, for minimum value, most likely value and maximum value of the triangular distribution, respectively.

An example is given here to illustrate the building structure of a stochastic variable, the initial source mass, M_0 . As shown in Figure 3.5, M_0 uses six GoldSim elements: Mzero, Mzero_switch, Mzero_determ, Mzero_prob, Mo_Min, Mo_Likely and Mo_Max. Mzero is a selector element and it is used to assign the input value, either probabilistic or deterministic, to M_0 in the REMChlor analytical model via the FORTRAN DLL. The Mzero_switch is a data element allowing users control between the probabilistic distribution and the deterministic value. Mzero_determ is a data element which defines a single value for M_0 under the overall probabilistic simulation mode. This is achieved by linking Mzero_determ to the deterministic simulation value for M_0 . Mzero_prob is a stochastic element which determines the type of the distribution and gives a probabilistic value. Here M_0 is assumed to have a triangular distribution, and its distribution parameters are the minimum value, most likely value and the maximum

value. Three data elements, Mo_Min, Mo_Likely and Mo_Max, are used for entering the value for the minimum, most likely and the maximum value parameters for such triangular distribution, respectively. To allow the user enter the value from the interface, each data element is linked to a certain input field on the graphical interface.

Other stochastic input parameters are constructed using a similar approach. The resulting PREMChlor model contains 604 various GoldSim elements.

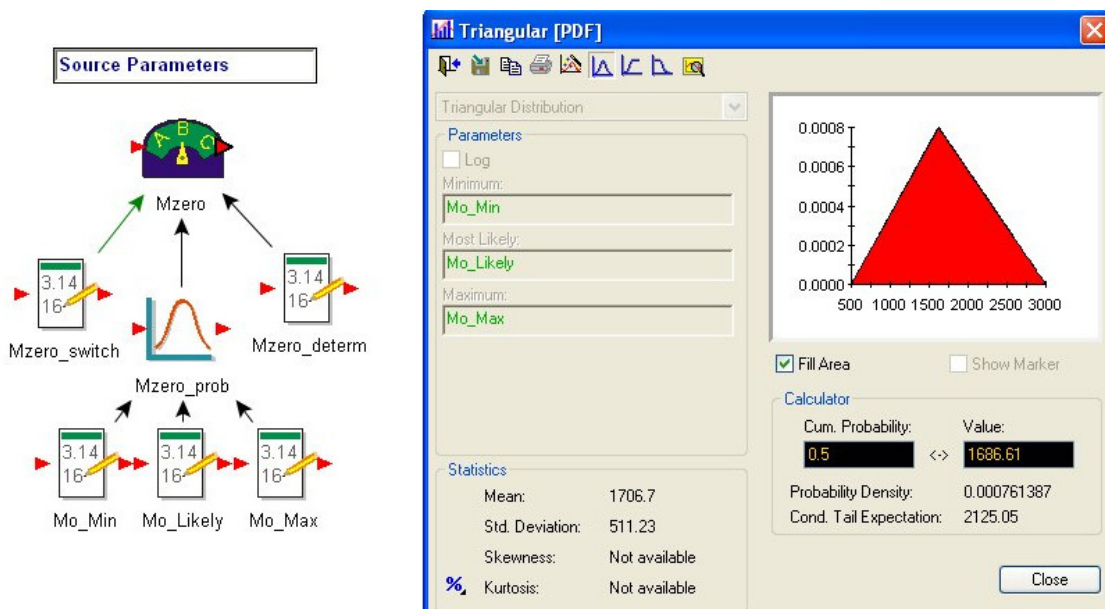


Figure 3.5 Building structure and distribution of the initial source mass.

3.3.2.2 *DLL Linkage Element*

Among all 604 elements, an external DLL element, SourcePlumeRiskDLL, is the key element in the probabilistic model. This DLL element provides the critical dynamic linkage between the REMChlor FORTRAN program and GoldSim platform. This external DLL element has 74 inputs and 15 outputs (Figure 3.6). Every input of the external DLL element corresponds to a certain input of the REMChlor FORTRAN code. These inputs are the outputs of the entire 74 input parameters in Transport_Model subgroup, which is described in the following section. Each of these 74 inputs has a value either probabilistic or deterministic depending on the type of the input parameter. These values are used to conduct the analytical calculations in the REMChlor model. Every output of the external DLL element corresponds to a certain calculation result from the REMChlor FORTRAN code. This model considers up to four compounds. The outputs are the concentrations of each compound and the total concentration, the mass discharges of each compound and the total mass discharge, and the cancer risks posed by each compound and the total cancer risk, respectively, at a specified point or plane. The detail about these outputs can be found in Model Outputs section.

To communicate with GoldSim, the necessary modifications have been made to the original REMChlor FORTRAN code. The modified FORTRAN program is compiled as the FORTRAN dynamic link library (DLL) and specified into the GoldSim external DLL element. The dynamic linkage is established by calling the REMChlor FORTRAN DLL through the simulation.

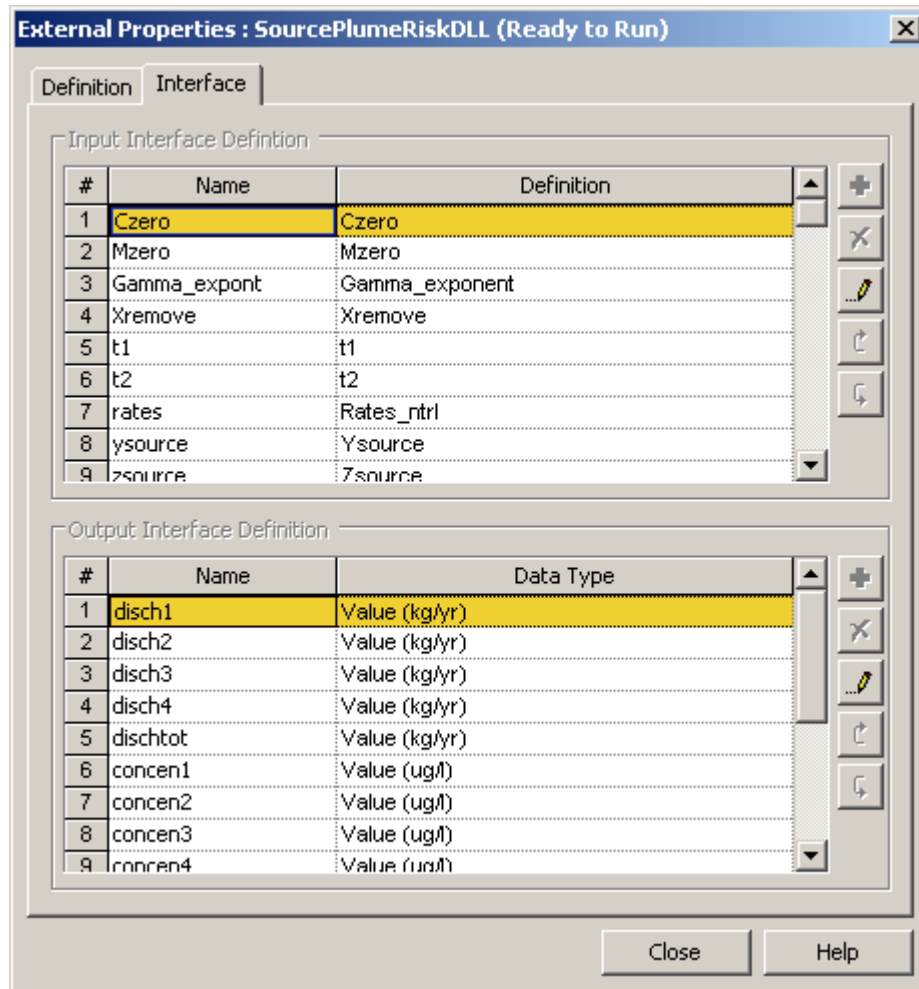


Figure 3.6 Interface of the external DLL element.

3.3.2.3 Model Subgroups

In order to organize, manage, and view the model, the elements are grouped into several different levels of subgroups and containers in a hierarchical “top-down” manner. This method allows the user to explore the model with increasing detail as they “drill down” into the model hierarchy. The PREMChlor model contains four top-level subgroups: Transport_Model, Remediation, Result, and Interface (Figure 3.7). Each subgroup consists of several containers. This section describes Transport_Model and Remediation subgroups. Result and Interface subgroups will be described in later sections.

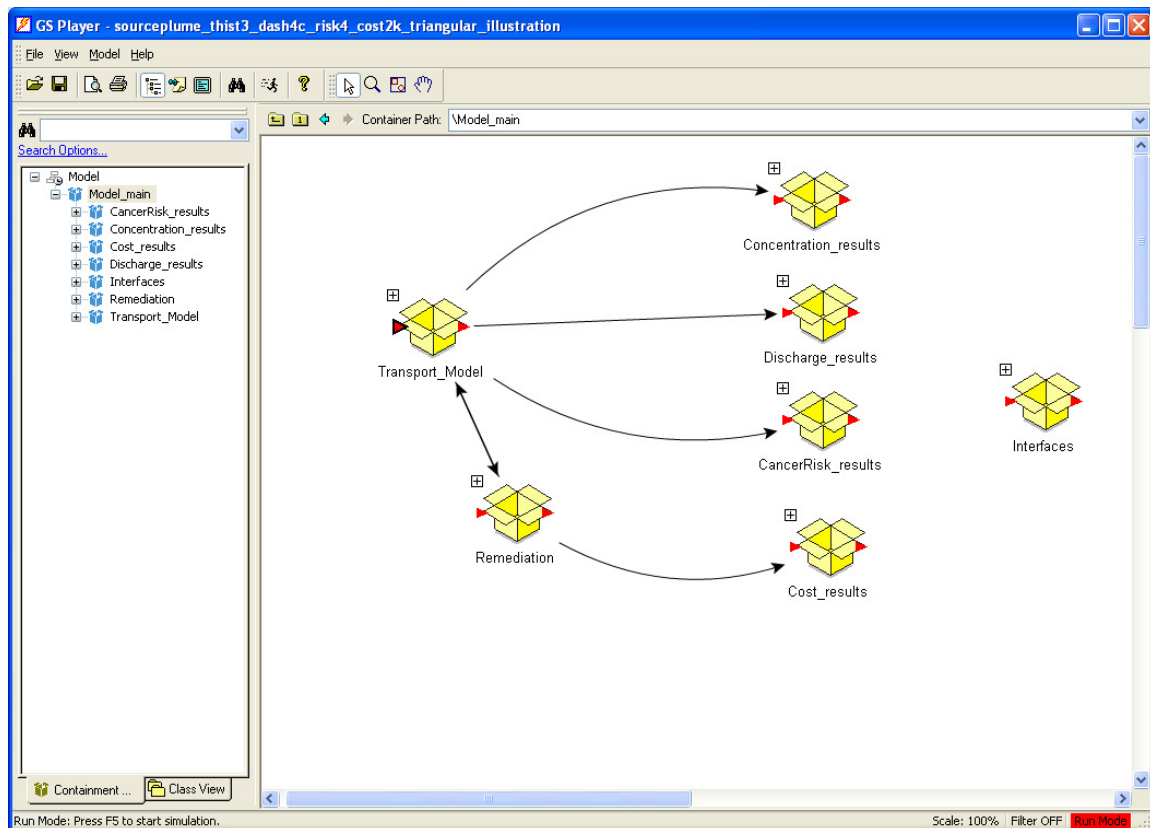


Figure 3.7 Top level subgroups of the model structure.

Transport_Model Subgroup

The Transport_Model subgroup is the most important subgroup in PREMChlor. It includes 74 input parameters and contains 436 GoldSim elements. Based on the nature of the input parameters, these parameters are grouped into six different containers: Source_Parameters, Transport_Parameters, Plume_DecayRates, SlopeFactor_Yield, Observation_Location and Run_Properties. These containers are connected to an external DLL element, SourcePlumeRiskDLL, to establish the linkage between REMChlor analytical code and GoldSim. The Source_Parameters container includes the input parameters related to the source zone, such as the initial source concentration (C_0), initial source mass (M_0), power function exponent (Γ), and the source dimensions. Each parameter in this container is treated as a stochastic variable and corresponds to several GoldSim elements. The building structures of source parameters are shown in Figure 3.8.

The Transport_Parameters container includes the retardation factor (R), Darcy velocity (V_d), effective porosity (ϕ), longitudinal, transverse and vertical scale-dependent dispersivity parameters (α_x , α_y and α_z). In PREMChlor, the longitudinal, transverse and vertical dispersivities are all scale-dependent, being the linear functions of the mean front location. Each parameter in this container is treated as a stochastic variable and corresponds to several GoldSim elements. The building structures of these parameters are similar to the source parameters.

The Plume_DecayRates container includes the lengths of space zones 1 and 2 (x_1 and x_2 in Figure 3.2) and the durations of time periods 1 and 2 for plume decay (t_1 and t_2 in Figure 3.2). These four parameters are treated as deterministic parameters. Each of

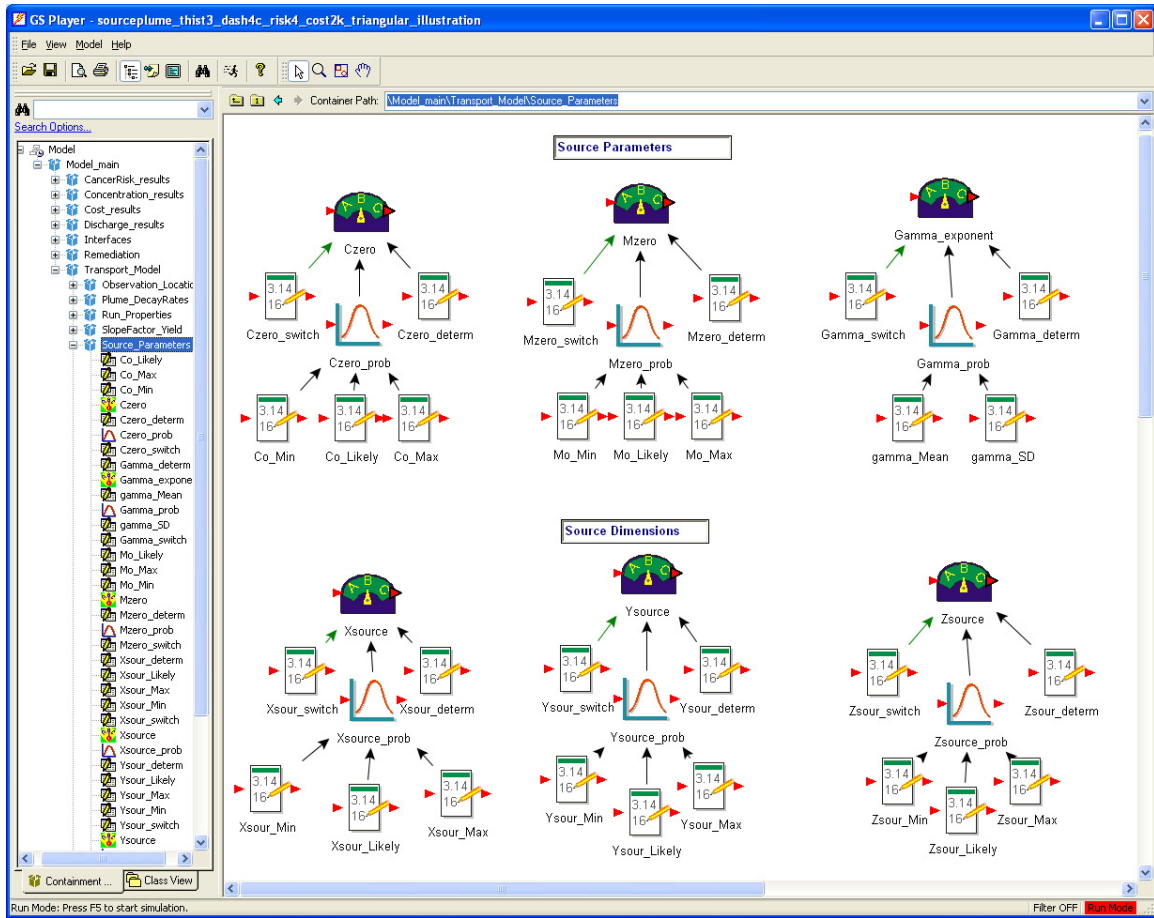


Figure 3.8 Building structures of source parameters.

them corresponds to a single GoldSim data element. The plume decay rates for four components in the different reactions (totally 36 decay rates) are considered as stochastic parameters. The building structures of parameters in the Plume_DecayRates container are similar to the source parameters.

The SlopeFactor_Yield container has three yield coefficients, including the yield of daughter 2 from parent 1, yield of daughter 3 from parent 2, and yield of daughter 4

from parent 3. This container also includes the lifetime cancer risk oral slope factors and inhalation slope factors for four compounds. All these parameters are treated as stochastic variables. The building structures of these parameters are similar to the source parameters.

The Observation_Location container includes four parameters: the number of streamtubes used in the transport model, and x , y , z coordinates for a certain location, such as the compliance point or potential receptor exposure point. These four parameters are treated as the deterministic variables and each of them corresponds to a single GoldSim data element. In the Run_Properties container, the simulation elapsed time and the time step are included. Each parameter is treated as the deterministic variable and corresponds to a single GoldSim data element.

Remediation Subgroup

The Remediation subgroup consists of source remediation parameters and plume remediation parameters. PREMChlor considers common technologies for DNAPL source removal and dissolved plume treatment. Source remediation methods are thermal treatments, surfactant/cosolvent flooding, chemical oxidation/reduction, and enhanced bioremediation. Source remediation parameters include the remediation start and end times, the remediation efficiencies and the unit costs (cost per volume treated) for different technologies, and the source decay rate. The remediation start and end times are known parameters for a remediation design therefore they are treated as the deterministic variables.

The plume treatment methods mainly are enhanced biodegradation, but the model can also simulate permeable reactive barriers (PRBs) and pump and treat (PAT) systems. In PREMChlor, plume PRB treatment can be modeled by assigning a very high first-order degradation rate for contaminant in a narrow reaction zone. The application of PREMChlor to the plume PRB treatment can be found in chapter 4. PAT systems can be approximated by a rough first-order decay rate, which can be derived from the percentage of removed contaminant mass during a period of time. Plume remediation parameters include enhanced degradation rates for different compounds, the dimensions of treated zones, the unit costs (cost per volume treated), and annual operation and management costs, etc. Most of these parameters are treated as stochastic variables.

In the PREMChlor model, efficiency of source remediation is represented by the fraction of mass removed (X_{rem}). In addition, efficiency of enhanced bioremediation has another option as it can alternately be represented by the enhanced decay rate. The fraction of source mass removed and the enhanced decay rate are treated as stochastic variables. The building structures of source remediation efficiency parameters are shown in Figure 3.9. For source remediation, the probabilistic model considers a one-time capital cost, which is the product of the unit cost of the source remediation and the volume of the source zone. The unit costs for different technologies are treated as the stochastic variables. The building structures of source remediation cost parameters are similar to other stochastic parameters. If enhanced source bioremediation is conducted and its efficiency is represented by the enhanced decay rate, PREMChlor uses the enhanced decay rate for source decay rate; otherwise, the natural source decay rate is

applied. Both the natural decay rate and enhanced decay rate are treated as stochastic variables.

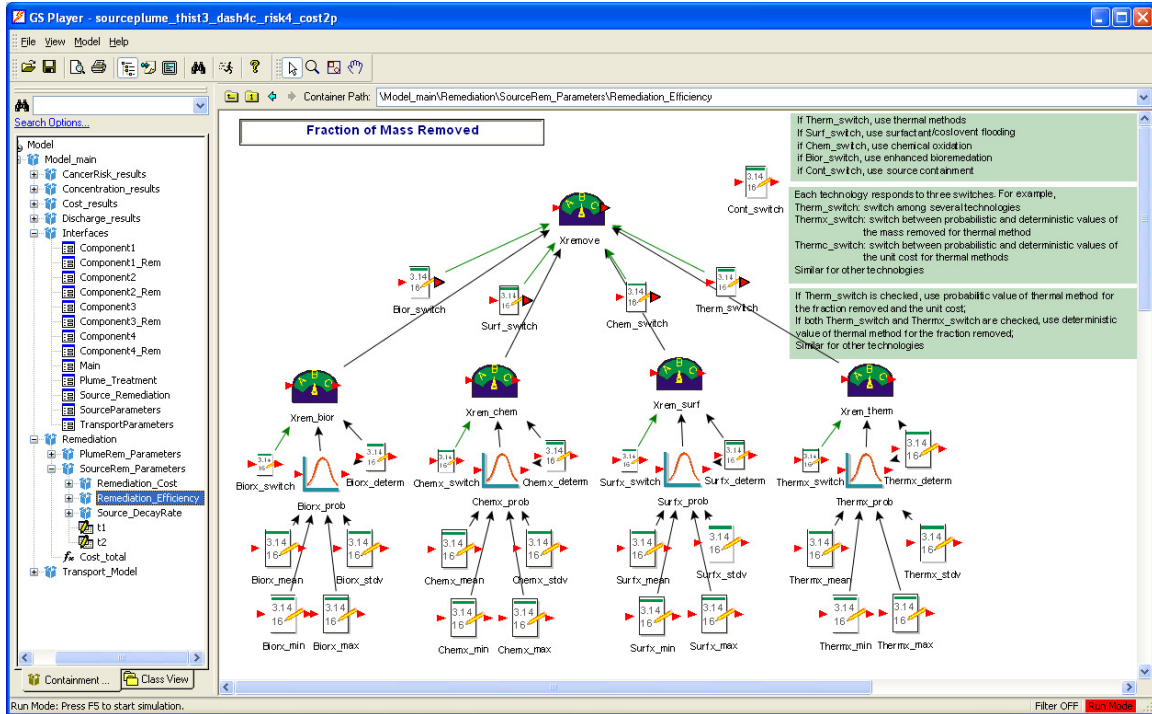


Figure 3.9 Building structure of source remediation efficiency parameters.

For plume remediation, cost includes a one-time capital cost and a total operation & management (O&M) cost in present net value (NPV) for a certain remediation period. The PREMChlor model allows two plume remediation zones in which different remediation activities can be simulated. The one-time capital cost of each remediation zone is the product of the unit cost of the plume remediation and the volume of the

remediation zone, respectively. The unit costs for two plume remediation zones and the annual O&M cost are treated as stochastic variables. More details about remediation costs are described in Remediation Cost Analysis section.

3.3.2.4 Model Outputs

The probabilistic model provides many intermediate and final outputs. Eighteen useful final outputs are included in the result subgroup. The probabilistic model considers up to four parent-daughter compounds. These results include the concentration of each component and the total concentration, the mass discharge of each component and the total mass discharge, and the cancer risk posed by each component and the total cancer risk. Contaminant concentration, mass discharge, and cancer risk are the commonly used metrics to assess the performance of the remediation. In PREMChlor model, the changes of concentrations, mass discharges and cancer risks over time (time-histories) are calculated for a specified location (x,y,z). PREMChlor allows users to specify such a location by entering any x, y and z values. The results also include the source remediation cost, the plume remediation cost, and the total remediation cost.

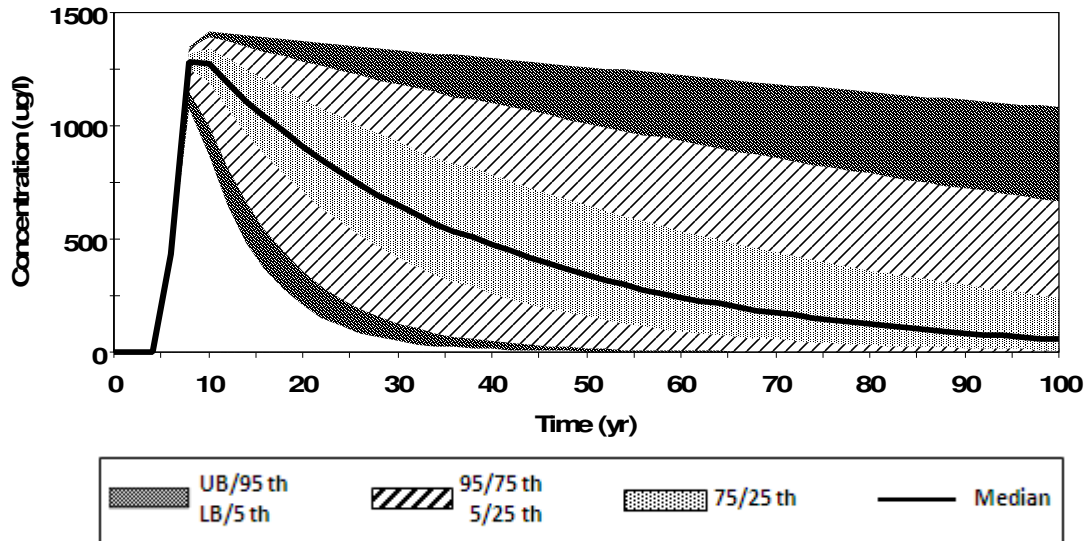
Each output has multiple values computed from different realizations. All these values/observations are assembled into the probability statistics and the probability distribution. Probability statistics include the lower and upper bounds, and different percentiles. Lower bound (LB) and upper bound (UB) are the lowest and highest values for an output among all of the realizations, respectively. A percentile is the value of an output below which a certain percent of observations fall. The 50th percentile, also known as the median, is the value below which 50 percent of the observations may be found.

Such probability statistics are useful to evaluate the remediation alternatives. For example, assume the remediation goal is to reach the MCL of a contaminant compound at a specific time. If the 95th percentile of predicted concentration has a value same as the MCL, it means that 95% of predicted concentrations are lower than the MCL and one may say that this remediation design would work with a 95% certainty.

The probability statistics of an output are displayed by the time histories in the form of the probability histories. An example of the probability histories display of concentration vs. time at a location (x, y, z) during the natural attenuation is shown as the top figure in Figure 3.10. The x axis is the simulation duration time and the y axis is the concentration. The concentration shown here is the plume centerline mass concentration and the location is defined by x=100 m, y=0 m, z=0 m. The solid line is the median of the concentration over the time among all of the realizations. From the median line upward, the outline of the light dot filled area is the 75th percentile, the outline of light upward diagonal filled area is the 95th percentile, and the outline of dark dot filled area is the upper bound. From the median line downward, the outline of the light dot filled area is the 25th percentile, the outline of light upward diagonal filled area is the 5th percentile, and the outline of dark dot filled area is the lower bound.

The probabilistic statistics also are displayed in tabular form (the bottom figure in Figure 3.10). In this natural attenuation example, the concentration at the 30th yr has the lower bound of 49 ug/L, 5th percentile of 128 ug/L, 25th of 419 ug/L, median of 647 ug/L, 75th of 929 ug/L, 95th of 1185 ug/L, and the upper bound of 1337 ug/L.

Concentration vs. Time (x=100 m, y=0 m, z=0 m)



Time (yr)	Mean	Lower Bound	5%	25%	Median	75%	95%	Upper Bound
0	0	0	0	0	0	0	0	0
2	0	0	0	0	0	0	0	0
4	0	0	0	0	0	0	0	0
6	428.79	410.21	417.6	426.66	429.98	432.86	434.75	435.7
8	1272.7	1075.7	1150.3	1247.7	1285.1	1318.2	1340.4	1351.5
10	1247.7	863.89	999.29	1192.1	1271.1	1342.8	1392.1	1417.3
12	1160.7	648.75	815.36	1076	1190.3	1297.2	1372.6	1411.7
14	1080.2	485.99	663.4	968.67	1112.1	1250.4	1350.5	1403.3
16	1007.8	364.34	539.82	872.14	1039	1205	1328.7	1394.8
18	942.46	273.36	439.34	785.25	970.84	1161.3	1307.1	1386.4
20	883.33	205.23	357.64	707.04	907.16	1119.1	1285.9	1378
22	829.63	154.16	291.19	636.64	847.71	1078.4	1265	1369.6
24	780.7	115.85	237.13	573.26	792.2	1039.1	1244.4	1361.3
26	735.98	87.097	193.13	516.22	740.37	1001.2	1224.1	1353.1
28	694.99	65.5	157.33	464.86	691.96	964.65	1204.1	1344.9
30	657.32	49.27	128.18	418.62	646.76	929.37	1184.5	1336.7
32	622.59	37.068	104.44	376.97	604.5	895.28	1165	1328.5
34	590.57	27.896	85.114	339.51	565.08	862.49	1146	1320.5
36	562.61	21.327	70.187	307.67	530.38	832.66	1128.2	1312.8

Figure 3.10 Probability histories of an output: Graphic view and Table view.

The probability distribution summary includes the distribution statistics, such as the mean, standard deviation, skewness and kurtosis, and the PDF for an output. The histogram of the PDF is generated by placing the final values of an output from all of the realizations into a discrete number of “bins”. The PDF of an output reflects the overall uncertainty posed by the uncertainties in the input parameters. An example of the probability distribution summary for an output is shown in Figure 3.11. The left table shows the distribution’s percentiles below which the distribution statistics are shown. The histogram on the right side is the PDF.

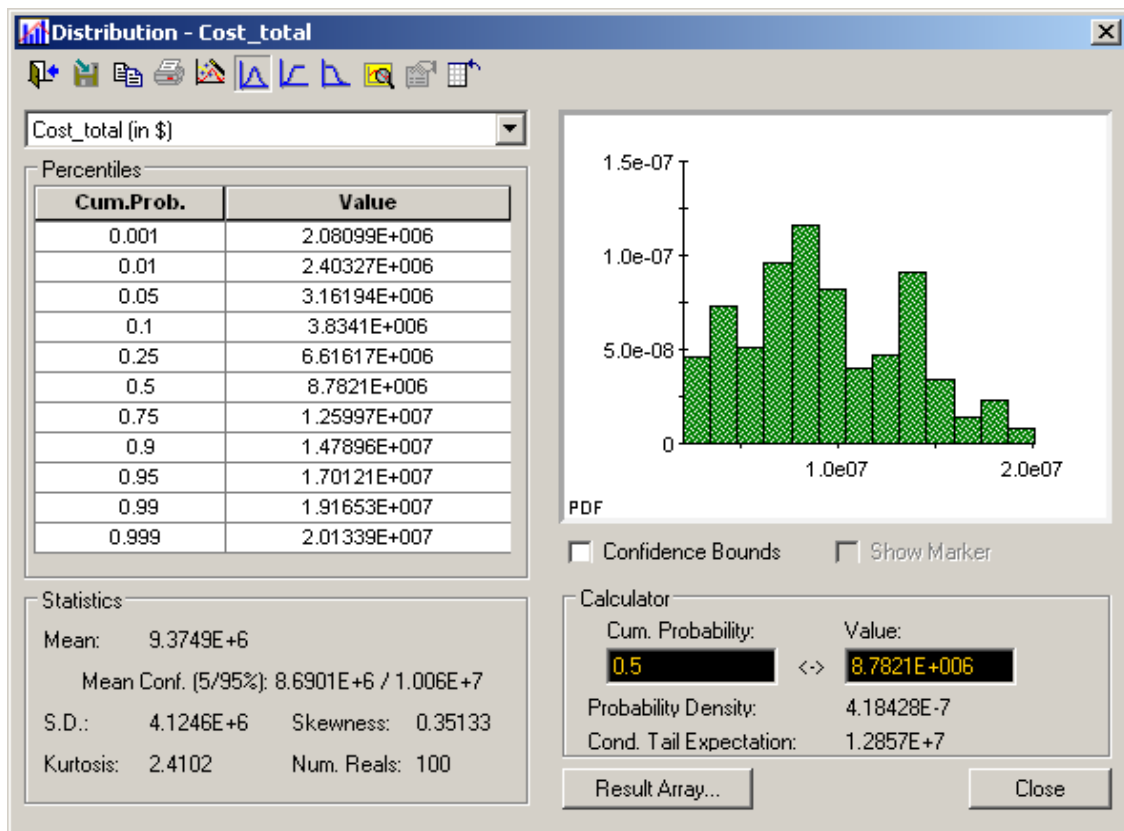


Figure 3.11 Probability distribution summary of an output.

3.3.3. Interfaces

In this probabilistic simulation model, thirteen pages of graphical user interfaces have been built to allow other users to easily enter the input values, run the model and view the results. The detailed descriptions of various interfaces are included in Appendix A. A GoldSim player file containing the graphical user interfaces has been generated to make the probabilistic simulation model available for use by others without having the GoldSim license and without being familiar with the details of the probabilistic model and the GoldSim simulation environment.

The user interfaces are designed and constructed by adding various buttons, gauges, sliders, input edit fields, text boxes, check boxes, display panels and imbedding instructions, and tool-tips. An example is given here to show how to build the interface and how to create the linkage between the front interface and the back model. Recall the example of a stochastic variable, the initial source mass, M_0 . The building structure of M_0 has been described earlier. As shown in Figure 3.12 (interface of source parameters), M_0 uses a triangular distribution with the minimum value, most likely value and the maximum value of 500, 1620 and 3000 kg, respectively. The distribution was shown in Figure 3.5. The deterministic value of M_0 is 1620 kg. The input fields of Min, Likely and Max on the interface (see Figure 3.12) are linked to data elements of Mo_Min, Mo_Likely and Mo_Max back in the model (see Figure 3.5), respectively. The check box (Figure 3.12) is linked to the data element Mzero_switch (Figure 3.5).

The switch box allows the selection between the probabilistic value and the deterministic value for a stochastic input parameter during the probabilistic simulation.

By default, the probabilistic model uses the probabilistic values for all stochastic parameters. If the switch box for a particular input parameter is checked, the model then uses the deterministic value for that parameter during the simulation. This switch feature is very useful for conducting the sensitivity analysis by holding some parameters constant and letting others be variable.

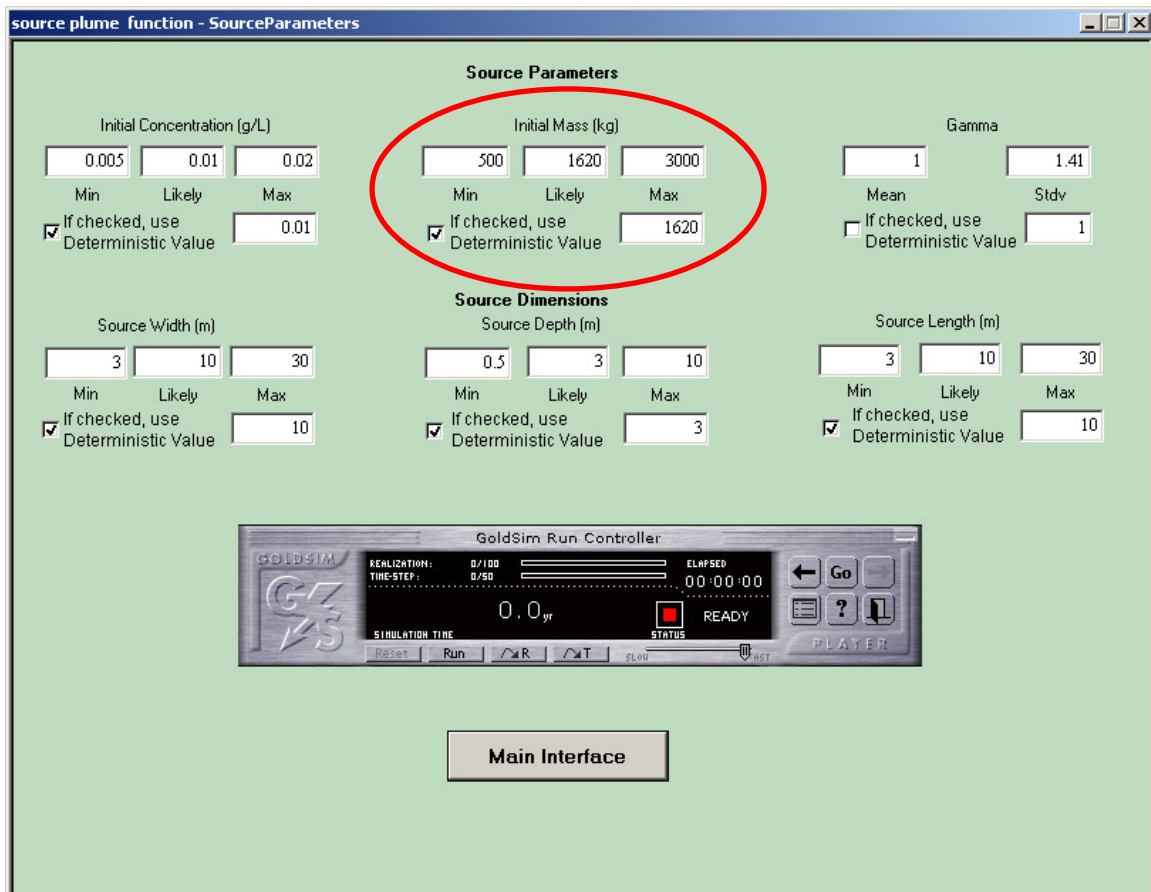


Figure 3.12 Interface of the source parameters.

3.3.4 Distribution of Unit Cost and Remediation Efficiency

In the probabilistic model, each remediation technology corresponds to a specific unit cost (cost per volume treated) and specific remediation efficiency. These parameters are treated as uncertain variables represented by the PDFs. The distributions and the parameters of unit costs and remediation efficiencies were interpolated based on literature resources.

McDade et al. [2005] presented a comprehensive cost analysis of DNAPL source depletion technologies. This study collected and compiled data from peer-reviewed literature, conference proceedings, site reports submitted to state and federal regulatory agencies, internet databases, and a survey of DNAPL source remediation projects across the United States. They reviewed more than 60 sites and performed the cost analysis for 36 field sites across the United States that had sufficient size, cost, and performance data to evaluate. The unit costs were reported for enhanced bioremediation (11 sites), chemical oxidation (13 sites), surfactant/cosolvent flooding (6 sites), and thermal treatment (6 sites). Statistics of each unit cost are presented as the minimum, 25th percentile, median, 75th percentile and maximum values.

The reported statistics were used to determine the distribution function of the unit cost. Different types of distribution functions available in GoldSim were tested to fit the reported values. It was found that the beta distribution fit the reported value best. The beta distribution is defined by a mean, a standard deviation, a minimum and a maximum. It can have different forms, such as exponential, positively or negatively skewed, or symmetrical. In GoldSim, the standard deviation is limited to ensure that the distribution

has a single peak and that the distribution is continuous [GoldSim User's Guide (v9.60), 2007]. In PREMChlor, the mean, minimum (min) and maximum (max) values of the interpolated beta distribution are the reported median, minimum and maximum values [McDade et al., 2005], respectively. The standard deviation of the beta distribution was adjusted by matching the interpolated PDF with the histogram generated based on the reported unit costs. In Figure 3.13, the histograms of unit costs generated based on the reported statistics are shown in the left column and the beta distributions of unit costs interpolated from the reported statistics are shown in the right column for four source depletion technologies. From top to bottom, the source depletion technologies are thermal treatment, surfactant/cosolvent flooding, chemical oxidation and enhanced bioremediation, respectively. Due to the lack of information, the unit cost for plume treatment is assumed to have a triangular distribution as well.

As mentioned earlier in Remediation Subgroup section, the remediation efficiency is represented by either the percentages of mass removal or the enhanced degradation rate. McGuire et al. [2006] presented a performance evaluation of DNAPL source remediation technologies at 59 chlorinated solvents contaminated sites. Data were collected and compiled from similar sources as in McDade et al. [2005]. The concentration reduction percentages of parent CVOC compound were reported for enhanced bioremediation (26 sites), chemical oxidation (23 sites), thermal treatment (6 sites) and surfactant/cosolvent flooding (4 sites). Since the mass reduction/removal data were not reported, we assumed the value of the exponent of Equation (2), Γ , in order to estimate the mass reduction/removal from concentration reduction percentage. By

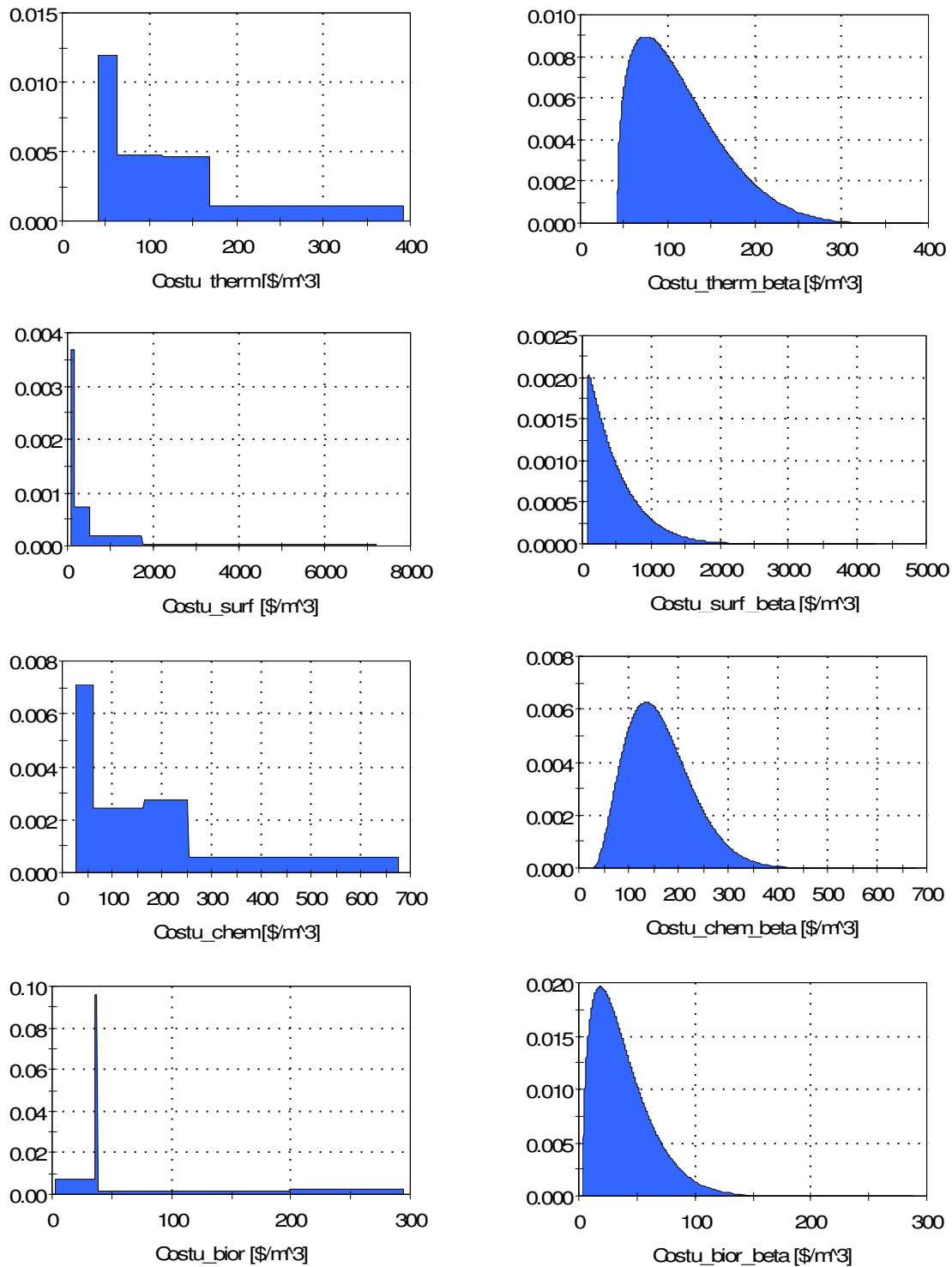


Figure 3.13 Histograms generated from McDade et al.[2005] and interpolated beta distributions for unit costs ($$/m^3$).

assuming Γ is equals to one, the ratio of mass reduction to concentration reduction is 1:1. In the model, only the parent CVOC compound was considered in the source zone. Therefore the reported concentration reduction percentages for parent CVOC compound [McGurie et al., 2006] were used as the source mass removal percentages in the probabilistic model.

The reported statistics of the concentration reduction percentages for parent CVOC compound were used to determine the distribution function for the source removal efficiency. Different types of distribution functions available in GoldSim were tested to fit the reported values. It was found that the beta distribution fit the reported value best. In PREMChlor, the mean, minimum (min) and maximum (max) values of the interpolated beta distribution are the reported median, minimum and maximum values [McGurie et al., 2006], respectively. The standard deviation of the beta distribution was adjusted by matching the interpolated PDF with the histogram generated based on the reported values. In Figure 3.14, the histograms of CVOC concentration reduction percentages generated based on the reported statistics are shown in the left column and the beta distributions of removal efficiencies interpolated from the reported statistics are shown in the right column for four source depletion technologies. From top to bottom, the source depletion technologies are thermal treatment, surfactant/cosolvent flooding, chemical oxidation and enhanced bioremediation, respectively. Due to lack of information, the enhanced decay rate, which is another option to represent the remediation efficiency of enhanced bioremediation, is assumed to have a triangular distribution.

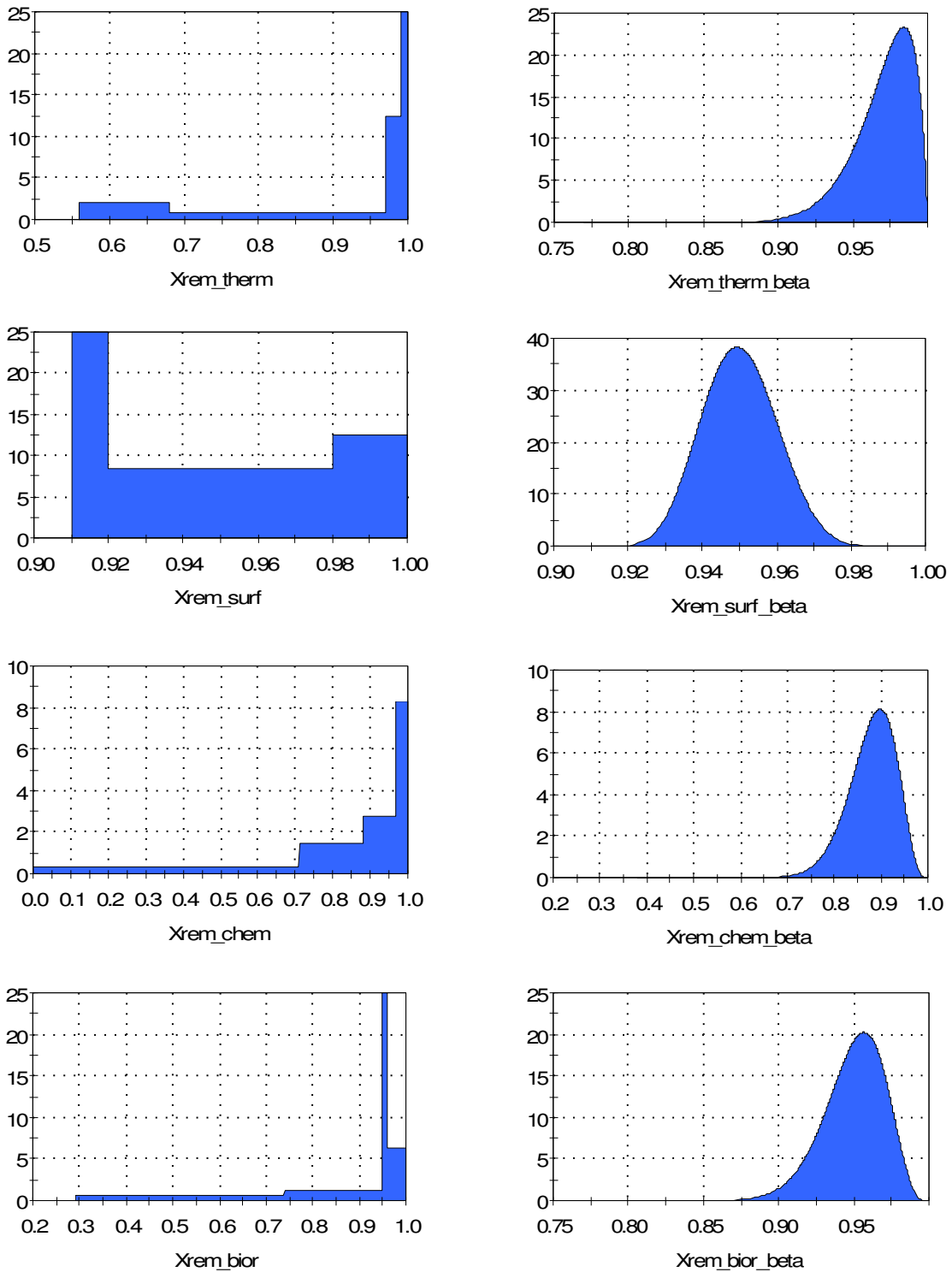


Figure 3.14 Histograms generated from McGurie et al. [2006] and interpolated beta distributions for source removal fractions.

3.3.5 Remediation Cost Analysis

Remediation costs of source removal and plume treatment are included in the probabilistic simulation model. Remediation cost analysis is performed outside the FORTRAN DLL link. The total remediation cost consists of the source remediation cost and the plume remediation cost.

For source remediation, the probabilistic model considers a one-time capital cost, which is the product of the unit cost of the source remediation and the volume of the source zone. For plume remediation, cost includes a one-time capital cost and a total operation & management (O&M) cost in present net value (NPV) for a certain remediation period. The probabilistic model allows two plume remediation zones. The one-time capital cost of each remediation zone is the product of the unit cost of the plume remediation and the volume of the remediation zone, respectively. The calculation of the total O&M cost in NPV is based on the formula in ITRC [2006]:

$$TotalNPV = AnnualCost \sum_1^n \frac{(1+i)^{t-1}}{(1+r)^{t-1}} \quad (27)$$

where *AnnualCost* is the current annual cost and it is assumed to be constant, *i* is the average annual inflation rate, *r*, is the average annual interest rate, and *t* is the year, and *n* is the total period of time for plume operation and management. In Equation (27), the numerator accounts for the total O&M cost in current dollar considering inflation, and the denominator accounts for the interest rate. This formula accounts for the inflation and interest factors at the beginning of the second year.

3.4 Model Demonstration

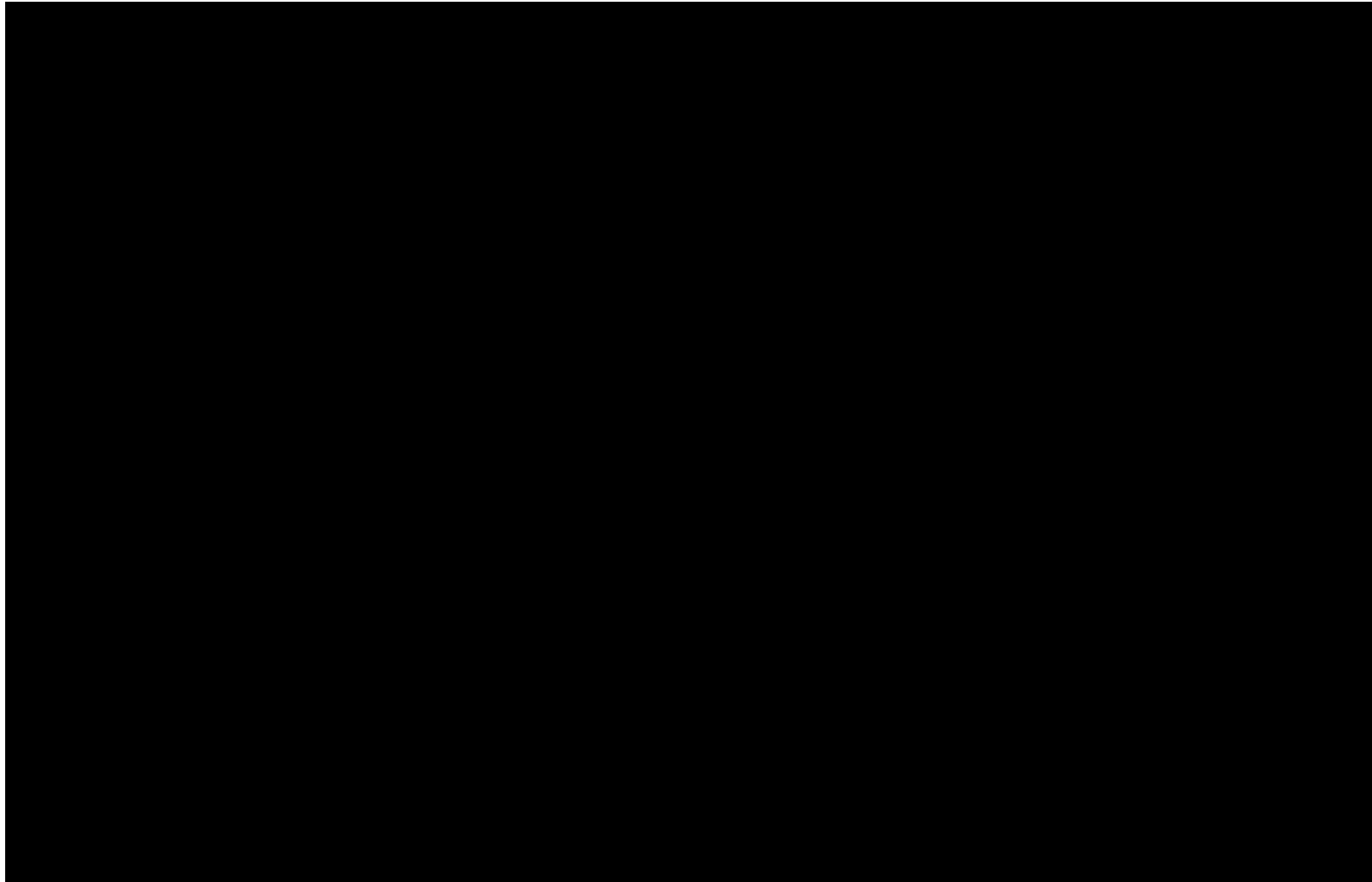
The probabilistic simulation model has been developed successfully by linking the analytical model REMChlor and the system-level Monte Carlo modeling software GoldSim via FORTRAN DLL application. This section demonstrates the model utility by applying the probabilistic model to a hypothetical problem.

3.4.1 Problem Overview

The example starts from a deterministic setup, involving a 1620 kg release of PCE from the source zone, with a groundwater Darcy velocity of 20 m/yr, and an average porosity of 0.33. The source zone has dimensions of X=10 m, Y=10 m and Z=3 m. The source is assumed to behave according to Equation (2) with an exponent, Γ , of 1. This type of source behavior gives an exponential decay of the source mass and concentration with time [Newell et al., 1996; Parker and Park, 2004; Zhu and Sykes, 2004; Newell and Adamson, 2005]. The release was assumed to have occurred in 1985, and the initial source concentration was 10 mg/l, leading to an initial source discharge of 6 kg of PCE per year.

PCE and its daughter products, TCE, DCE and VC were assumed to undergo natural attenuation. The decay rates of four compounds (as shown in Table 3.1) used the medians of the decay rates from the BIOCHLOR database [Aziz et al., 2000]. The compounds were assigned a retardation factor of 2, the longitudinal dispersivity was set equal to 1/100 times the travel distance, the transverse dispersivity was set of 1/10 of the longitudinal dispersivity, and the vertical dispersivity was set of 1/100 of the longitudinal dispersivity.

Table 3.1 Key parameters used in model demonstration.



It is assumed that the compliance plane was located at 100 meters downstream from the source. In the absence of any type of remediation, this release would result in a concentration around 3600 ug/l at the compliance plane in 2010 and 3400 ug/l in 2025 [Figure 3.15] due to the natural flushing process. Suppose some remediation effort is proposed in 2010, and the remediation goal was to reduce the total concentration to less than 200 ug/l in 15 years following the remediation (year 2025) at the compliance plane.

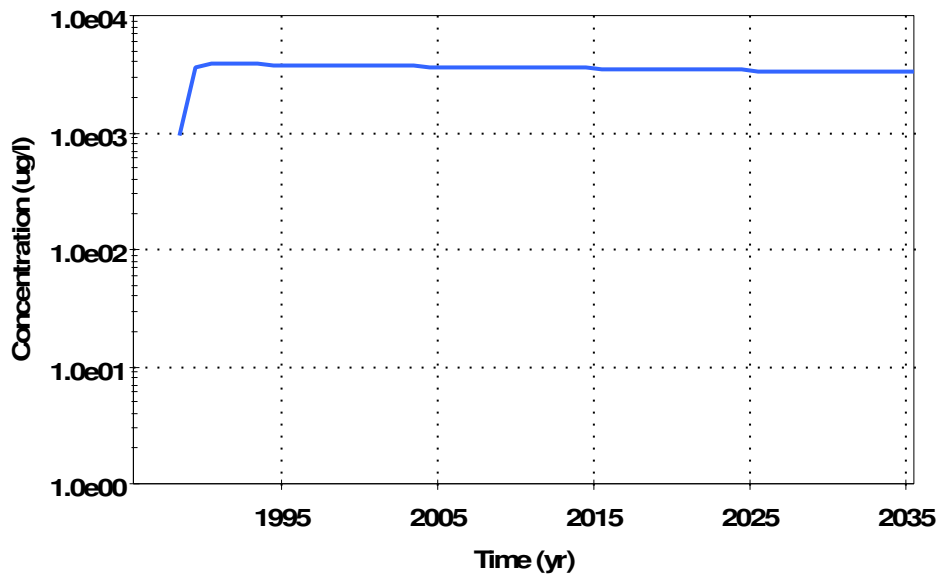


Figure 3.15 Predicted total concentration over time at the compliance plane in the absence of remediation (model demonstration).

3.4.2 Model Simulations

In this example demonstration, a total of four simulations were conducted using different combinations of uncertain parameters and remediation effort. Key parameters used in the four simulations are given in Table 3.1, and distributions of the uncertain parameters are shown in Figure 3.16. Simulation 1 is fully deterministic, and modeled a very effective deterministic thermal remediation of the source that removed 97% of the source mass. Simulation 2 used the same problem set up, except adding some uncertainties to the source parameters (M_0 , Γ). Simulation 3 was identical to the second simulation, except making the source remediation parameter (X_{rem}) uncertain. Simulation 4 was based on the third simulation, adding an enhanced bioremediation of the plume in the first 300m. The enhanced bioremediation decay rates of the compounds in plume treatment zone were treated as stochastic variables.

Simulation 1 modeled a partial source removal that removed 97% of the source mass, and is conducted in 2010 with a period of 0.2 year. This simulation used deterministic values for all input parameters. The deterministic output, total concentration at the compliance plane over time is shown in Figure 3.17. Due to this very effective partial source remediation, the total concentration drops sharply from 2948 ug/l in 2013 to 126 ug/l in 2013. The concentration continuously decreases slightly due to the natural flushing process. In year 2025, 15 years after the source removal, the total concentration is 98 ug/l, which meets the remediation goal. So this remediation may work, but it includes no uncertainty.

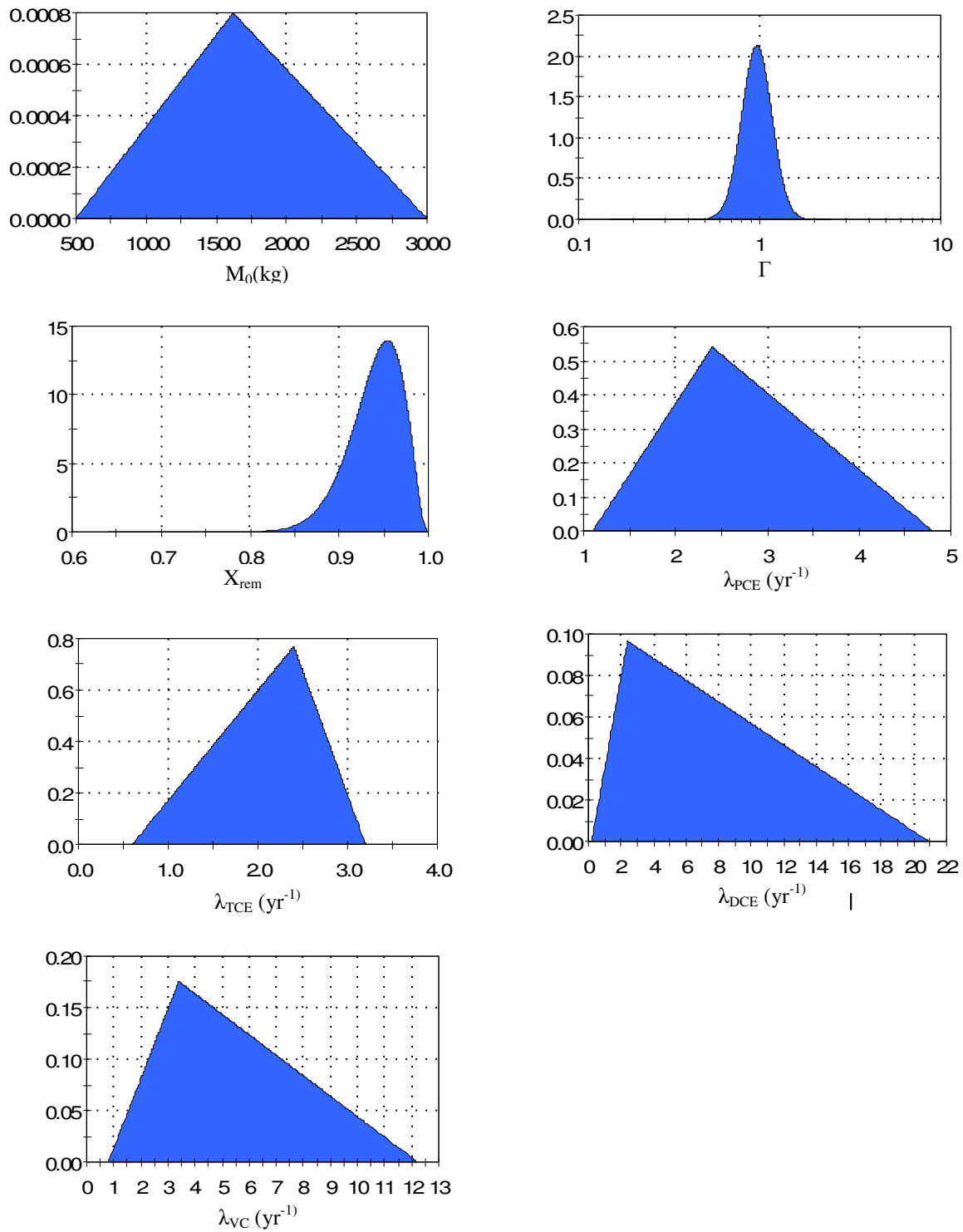


Figure 3.16 PDFs for uncertain parameters (model demonstration).

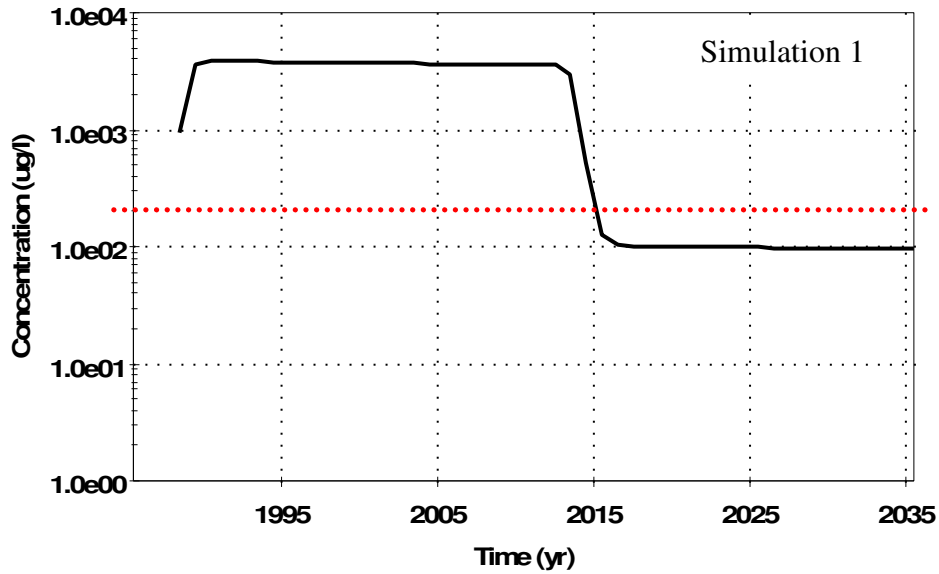


Figure 3.17 Predicted total concentration over time at the compliance plane from simulation 1 (model demonstration).

Simulation 2 used the same problem set up, except adding some uncertainties to the source parameters, including the initial source mass and the exponent of power function [Equation (2)]. The initial source mass, M_0 , was assumed to have a triangular distribution, with a minimum value of 500 kg, a most likely value of 1620 kg, and a maximum value of 3000 kg. The exponent in Equation (2), Γ , was assumed to have a log-normal distribution, with a geometric mean of 1 and a geometric standard deviation (Stdv) of 1.21. This resulted in that most Γ values falling in a range from 0.5 to 2. Many researchers have suggested that Γ may vary between about 0.5 and 2 at real sites [Rao and Jawitz, 2003; Falta et al., 2005a; Newell and Adamson, 2005; Jawitz et al., 2005;

Fure et al., 2005, McGuire et al., 2006, Newell et al., 2006]. The PDFs of M_0 and Γ are shown in Figure 3.16.

The probabilistic output of the total concentration over time obtained from Simulation 2 is shown in Figure 3.18. Shown are the mean and different percentiles of the total concentration corresponding to the uncertain input parameters. The upper bound concentration at 100m in 2025 is 324 ug/l. The 75th percentile concentration at 100m in 2025 is 154 ug/l. Given the uncertainties in the initial source mass and the power function exponent, the model predicts more than 75% probability of meeting the remediation concentration goal.

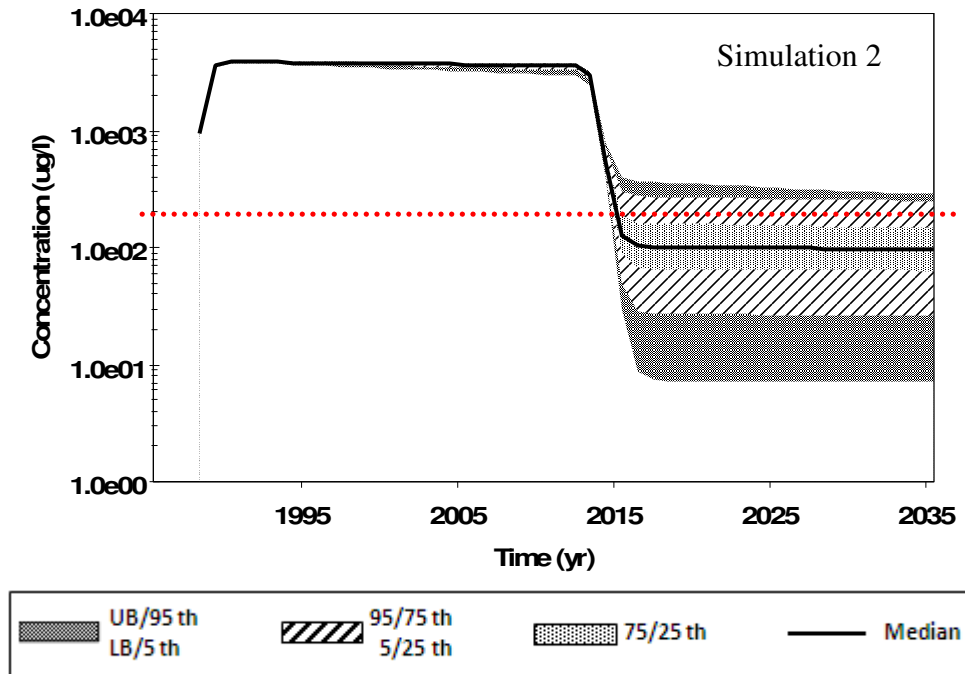


Figure 3.18 Predicted total concentration over time at the compliance plane from simulation 2 (model demonstration).

Simulation 3 was identical to Simulation 2, except making the source remediation efficiency (the fraction of mass removed, X_{rem}) uncertain. The removal efficiency was assumed to have a beta distribution, with a mean of 94%, a standard deviation of 3%, a minimum value of 56%, and a maximum value 100% (Table 3.1). The PDF is shown in Figure 3.16. The probabilistic output of the total concentration over time obtained from simulation 3 is shown in Figure 3.19. The upper bound concentration at 100m in 2025 is 900 ug/l, and the median concentration at 100m in 2025 is 203 ug/l. The remediation effort is predicted to meet the goal approximately 50% of the time given uncertainties in the initial source mass, the power function exponent, and the source remediation efficiency. Therefore, the model predicts a likely failure of the original design. Compared to Simulation 2, the uncertainty of the source remediation efficiency in Simulation 3 resulted in a lower chance of meeting the remediation goal.

Simulation 4 was based on the Simulation 3, but adding enhanced plume biodegradation in the first 300m. The treatment zone has dimensions of length = 300 m, width = 30 m, and depth = 5 m. Enhanced biodegradation was assumed to begin in 2010 and last for 75 years. The enhanced decay rates of the compounds in the treatment zone were treated as uncertain variables, with triangular distributions. The minimum, most likely, and the maximum values of the triangular distribution for each component are shown in Table 3.1 and Figure 3.16.

The probabilistic output of the total concentration over time obtained from Simulation 4 is shown in Figure 3.20. The upper bound concentration at 100m in 2025 is 213 ug/l. The 95th percentile concentration at 100m in 2025 is 165 ug/l. Therefore, the

remediation effort would meet the goal with more than 95% certainty. Compared to Simulation 3, the addition of the plume bioremediation in Simulation 4 along with the original source remediation increased the chance of meeting the remediation goal. The new design including the source remediation and the enhanced plume biodegradation appears to be robust.

A remediation cost analysis was also performed in Simulation 4. For source remediation, the unit cost used a beta distribution interpolated from McDade et al.[2005] , with a mean of 115 \$/m³, a standard deviation of 50 \$/m³, a minimum of 42 \$/m³ and a maximum of 392 \$/m³. For plume treatment, the unit cost of bioremediation was assumed to have a triangular distribution, with a minimum value of 1 \$/m³, a most likely value of 2 \$/m³, and a maximum value of 3 \$/m³. The annual operation and management cost used a deterministic value of \$10,000. The annual inflation rate and the interest rate used deterministic values of 4% and 6%, respectively. Based on these values, the predicted mean values of the source remediation, plume treatment, and the total remediation costs were \$34,500, \$493,000 and \$527,500, respectively. The distribution summaries of three remediation costs are shown in Figure 3.21, Figure 3.22 and Figure 3.23, respectively.

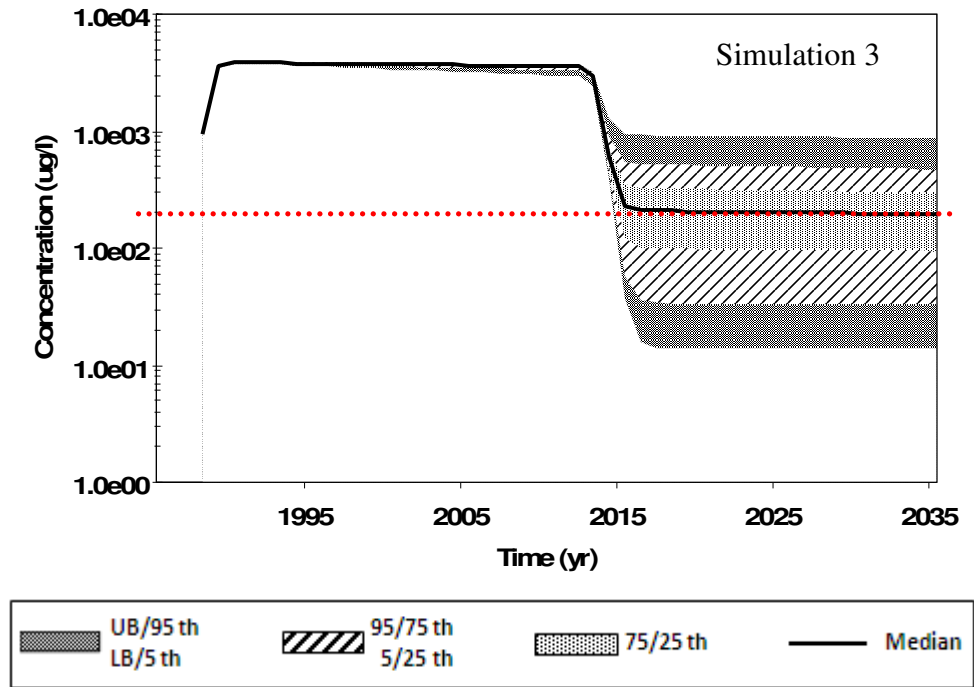


Figure 3.19 Predicted total concentration over time at the compliance plane from simulation 3 (model demonstration).

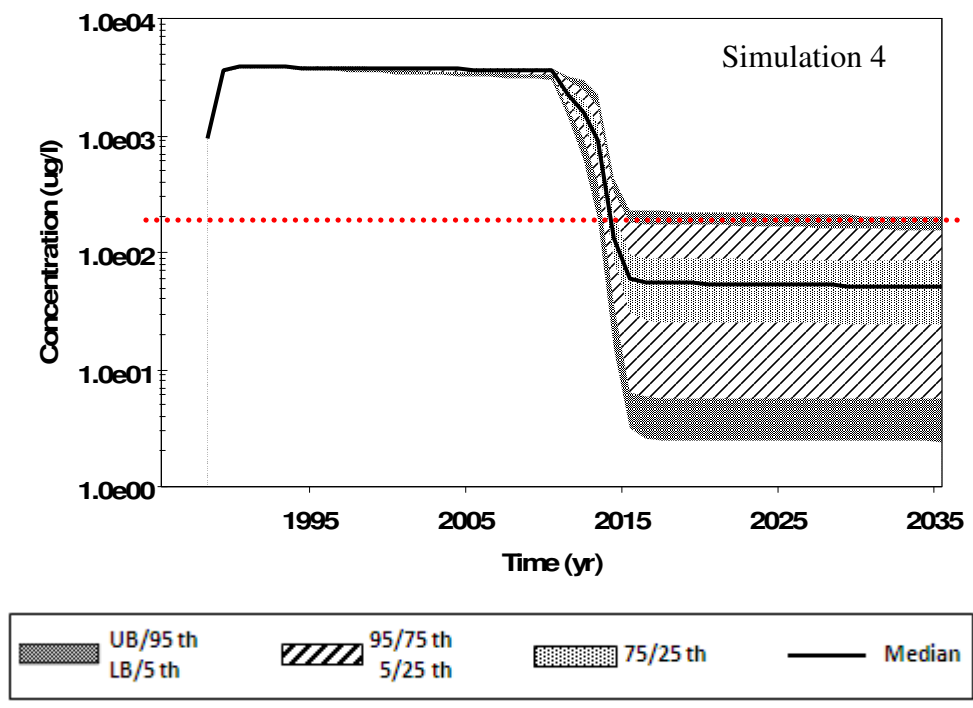


Figure 3.20 Predicted total concentration over time at the compliance plane from simulation 4 (model demonstration).

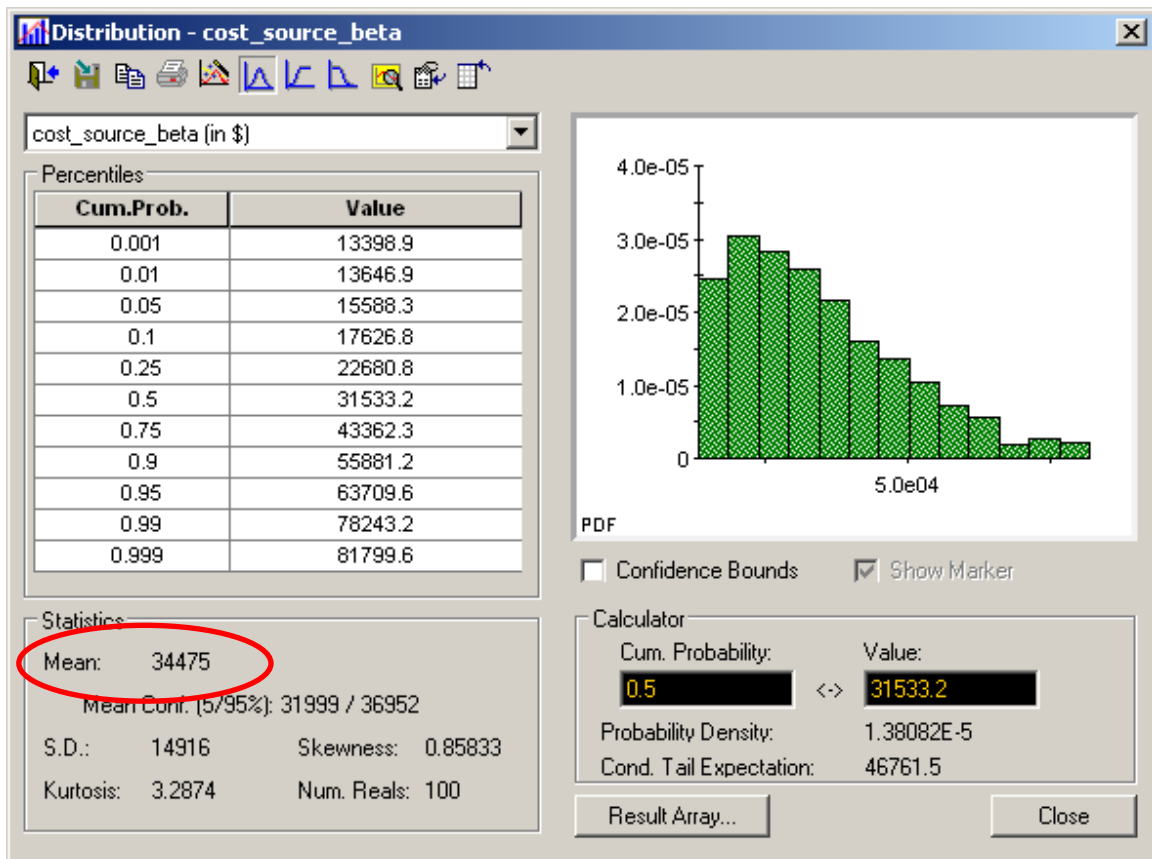


Figure 3.21 Probability distribution summary of source remediation cost from simulation 4 (model demonstration).

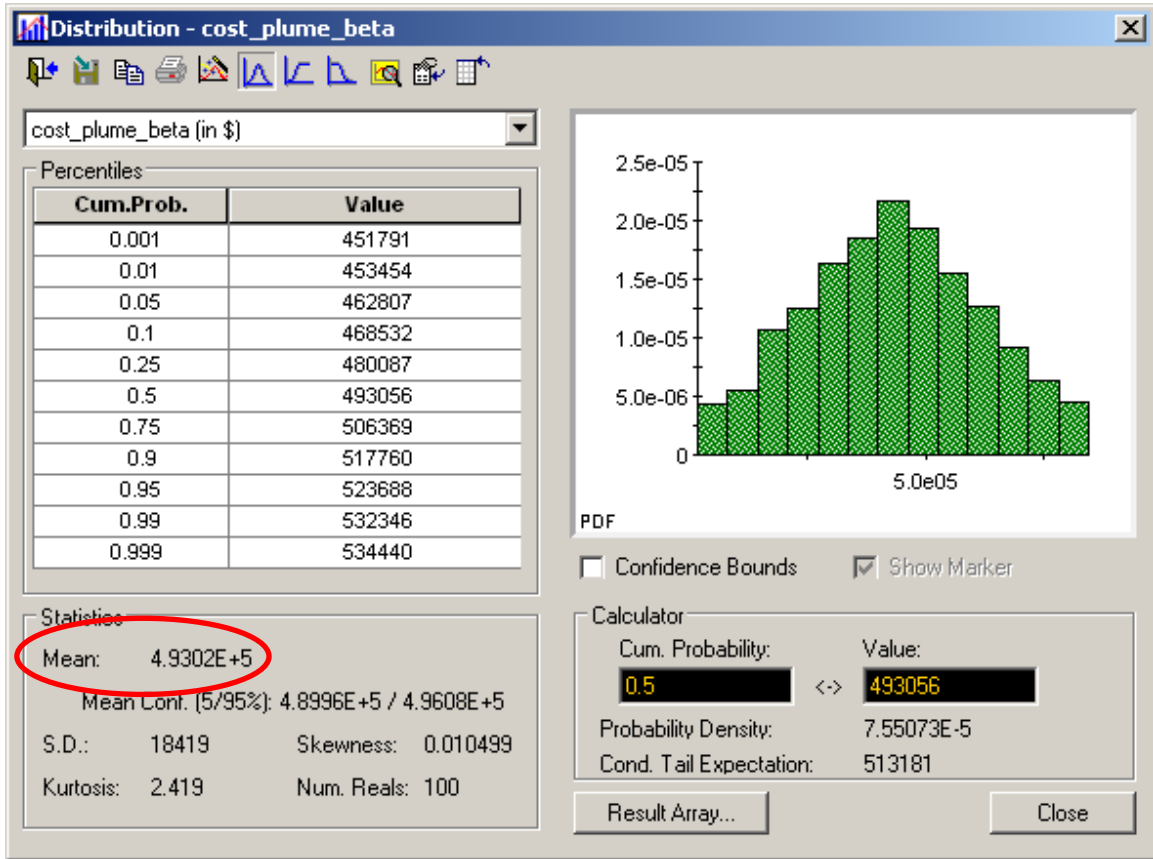


Figure 3.22 Probability distribution summary of plume remediation cost from simulation 4 (model demonstration).

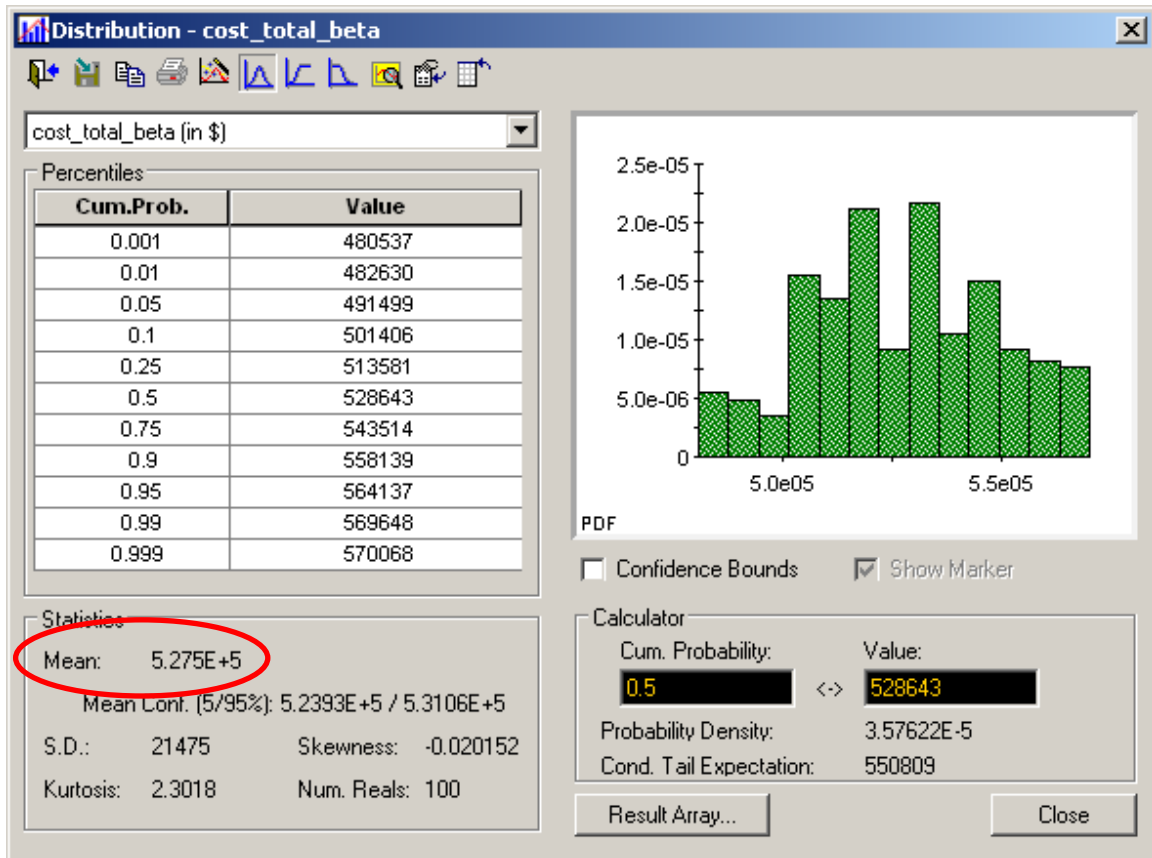


Figure 3.23 Probability distribution summary of total remediation cost from simulation 4 (model demonstration).

CHAPTER 4

MODEL APPLICATION

In this chapter, consisting of two sections, the probabilistic model is applied to a shallow aquifer contaminated with TCE at a manufacturing plant in North Carolina. This chapter consists of two sections. Section 1 describes the site background, including site geology and hydrogeology, contaminants of concern, and field remediation efforts. Section 2 describes the probabilistic model application. Model application is divided into two parts: model calibration and probabilistic simulation of field remediation efforts. Under model calibration, the probabilistic model is calibrated to match the site conditions prior to field remediation efforts, using a deterministic simulation. Probabilistic simulations are then conducted for predicting the field remediation efforts considering the uncertainty in key parameters. During the probabilistic simulation, seven key parameters associated with a high level of uncertainty were assigned values sampled from specified PDFs, and the other parameters were assigned deterministic values derived from the model calibration. Model settings and results for these two parts are presented and discussed respectively.

4.1 Site Background and Field Remediation Activities

The site is located at the DuPont Kinston Plant, northeast of Kinston, Lenoir County, North Carolina. The area of the plant is approximately 650 acres [CRG, 2002]. The plant began operations in 1953, and currently manufactures Dacron polyester resin

and fibers [CRG, 2002]. In 1986, the Plant initiated a facility-wide groundwater assessment program. In November 1989, site investigation data indicated that the surficial aquifer beneath the manufacturing area had been impacted by the release of TCE [DERS, 1994]. Site investigations have been unable to identify neither free-phase TCE nor definable origin of the release [DERS, 1998]. The impacted zone is limited to a surficial sand unit approximately 15 feet deep overlying a thick mudstone-confining layer.

Cone Penetrometer Tests (CPT) indicated that the surficial aquifer at the Kinston Plant is composed of unconsolidated and interbedded sand, silty sand, clayey silt, and clay, combined with a thickness of 7 to 25 feet [DERS, 1992]. The surficial saturated zone is underlain by the Beaufort Formation (Paleocene in age) consisting of a light to dark gray siliceous shale (mudstone), with some chert, siltstone, and sandstone. This formation is believed to be 20 to 25 feet in thickness [DERS, 1992]. The mudstone separates the upper aquifer from the Peedee Formation, which is composed of dark green or gray sand with layers of clay, silt, and indurated shell fragments. The Peedee is approximately 120 feet thick beneath the site [DERS, 1995]. A fault trending southwest to northeast is present between wells MW-43, MW-44, and MW-36 and MW-38 (Figure 4.1). The vertical displacement of the mudstone is approximately 36 feet across the fault. Based on the results of an investigation conducted in 1991, TCE appeared to be confined to the shallow unconsolidated sediments above the mudstone unit, and exists primarily in the lower region of the saturated zone of the sediments above a thin clay layer [DERS, 1992].

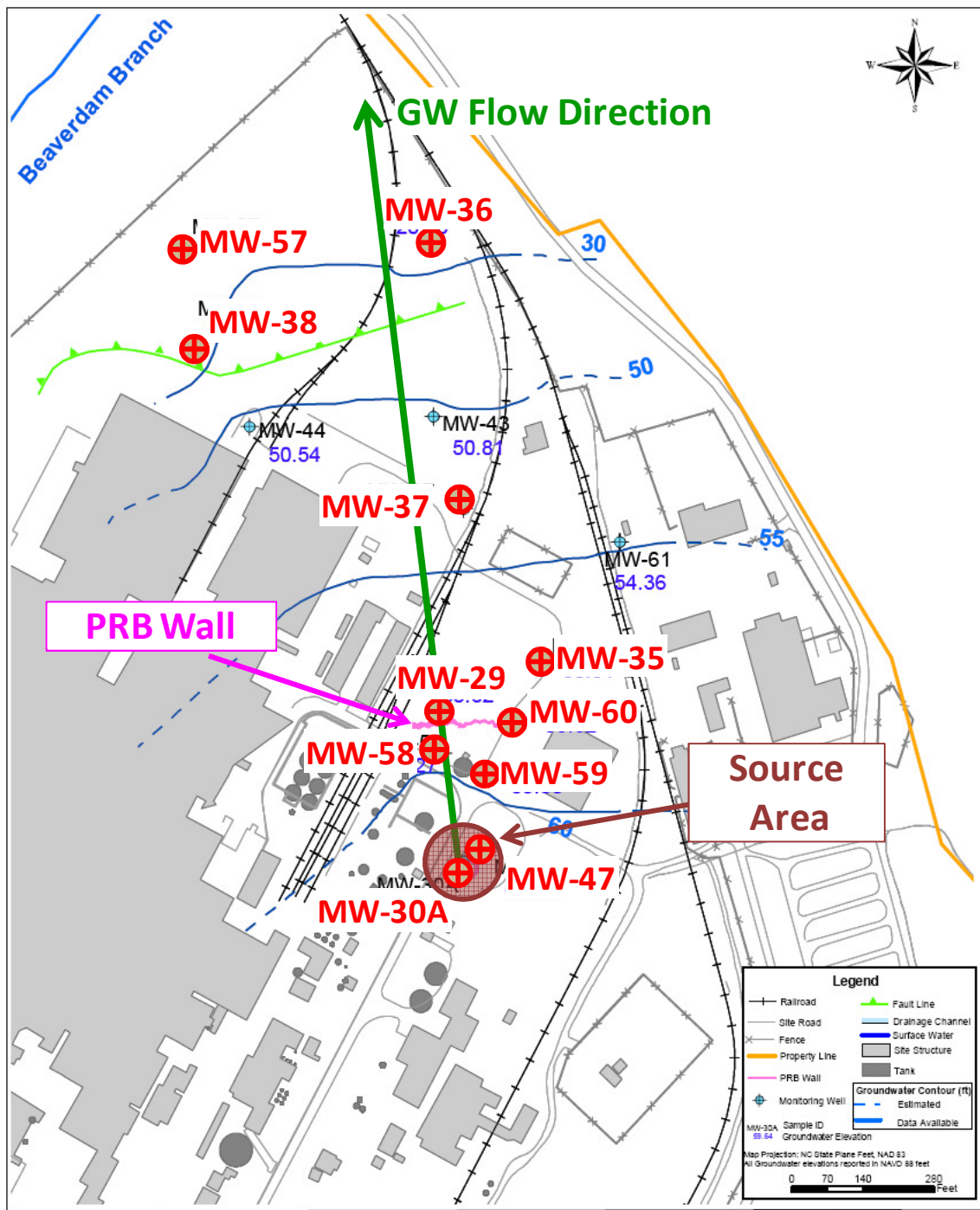


Figure 4.1 Site map of Kinston plant with monitoring wells.

Based on slug tests from monitoring wells (MW-30A and MW-31), the estimated average hydraulic conductivity for the surficial aquifer is 7.7×10^{-4} cm/sec [DERS, 1992]. Based on this and average hydraulic gradients, groundwater Darcy velocity in the upper aquifer has been estimated to be about 1.52 to 4.57 m/yr [DERS, 1994]. The average pore velocity is estimated to be about 5.56 to 11.13 m/yr [DERS, 1998], and the regional groundwater flow direction is from southeast to northwest [DERS, 1995]. The water table is located at about five feet below the ground surface (bgs) [DERS, 1998].

The TCE-impacted groundwater plume originated near the facility's chemical tank storage area [CRG, 2002], apparently resulting from undocumented waste handling activity prior to 1980 [Shoemakers, 2002]. Base on Geoprobe® soil core data, the source area was estimated to be 25 feet in diameter [CRG, 2002]. Analyses of soil and water sampling data indicate that about 300 lbs of TCE were present in the source area [DERS, 1994]. The aqueous concentration of TCE in the source region showed large fluctuations over time, ranging from 0.34 mg/L to 75 mg/L [DERS, 1992]. Extending several hundred feet in the downgradient (northwest) direction, the TCE plume is roughly 250 to 300 feet wide at a downgradient distance of 300 feet [CRG, 2002].

Site investigation indicated that TCE is the main contaminant at Kinston Site. According to the field sampling data, its daughter product, cis-1,2 DCE had a concentration below the detection limit from 1989 to 1991, was not sampled from 1992 to 2001, and was reported to have a concentration in the plume below the detection limit or less than 5 ug/L from 2002 to 2008. Concentration of cis-1,2 DCE in the source zone wells ranged from 1.3 ug/L to 130 ug/L; with most measurements less than 100 ug/L

from 2002 to 2008. The concentration of VC was not reported before 2002. After 2002, VC concentration was reported as below the detection limit or non-detected in plume, and was detected only from one source monitoring well (MW-30A) as a few ug/L, ranging from 2.9 ug/L to 8.3 ug/L.

In order to clean up the site, three remediation efforts have been conducted since 1995. Initially a pump and treat (PAT) system was installed to recover and treat TCE-impacted groundwater [DERS, 1994]. This TCE PAT system was operated from 1995 to 2001, resulting in a TCE mass extraction of 3 lbs. In 1999, an in-situ source area destruction pilot (a reductive dechlorination of TCE) using zero valent iron (ZVI) was implemented to destroy source zone soil contamination. This source area ZVI treatment was coupled with a permeable reactive barrier (PRB) wall, which was installed at a downgradient distance of about 300 feet to intercept and treat contaminated groundwater [DERS, 1998 and CRG, 2002].

During the source treatment, a slurry of ZVI and kaolinite clay was high-pressure jetted into the subsurface at the source region of TCE contamination. A total of 11 treatment columns of this material were emplaced to depths ranging from 15 to 18 feet to the top of the mudstone confining layer that exists at the Kinston Plant [CRG, 2002]. The installation of in-situ source ZVI treatment was completed in September, 1999. Soil and groundwater sampling were conducted before and after the source ZVI treatment. Source mass reduction was reported as 95% [<http://www.rtdf.org/PUBLIC/permbarr/prbsumms/profile.cfm?mid=92>]. However, there is lack of information on what objective evidence

this reported source mass reduction is based on. Thus, there is a large uncertainty associated with this source mass removal percentage.

Geoprobe® soil cores were obtained before and 11 months after the source ZVI installation. Soil samples were collected from two discrete vertical depth intervals at 16 locations in and around the source area. Prior to treatment, concentrations ranged from roughly 1 mg/kg to 100 mg/kg (on a wet weight basis), with higher concentrations generally observed at a gradational contact two to three feet above the mudstone interface. Based on the early coring, no free phase or residual phase DNAPL was observed. Eleven months after the treatment, the resampling effort took duplicate samples at the same source area locations sampled prior to treatment. Only two out of 16 previously contaminated locations contained concentrations of TCE and/or its breakdown products (cis-1,2- DCE and VC) in the post-treatment cores [CRG, 2002]. Groundwater sampling data from monitoring wells within and downgradient of the source area showed that while TCE concentrations have declined or remain non-detect in some locations, concentrations in others (e.g. MW-30A) remain at or near historical levels.

A similar ZVI technology was used to install a 400-foot long PRB wall emplaced across the groundwater plume approximately 290 feet downgradient of the source area (Figure 4.1) [CRG, 2002]. However, the slurry design for the PRB wall was changed to consist of ZVI and a guar gum slurry. Guar gum is a natural plant-derived viscosifying agent that is readily broken down by enzymes within a few days of emplacement, which restores permeability to the wall [DERS, 1998]. The resulting PRB wall has an effective thickness of four to six inches [DERS, 1998]. The deciding factors in choosing the PRB

wall thickness were the relatively low dissolved-phase concentrations of TCE (maximum influent concentration of about 0.3 mg/L) and slow groundwater flow (5.56 to 11.13 m/yr). The reported bench scale half-life of TCE in contact with ZVI was less than four hours [DERS, 1998]. Groundwater sampling data showed that dissolved TCE concentrations have declined or remain non-detect in monitoring wells downgradient of the PRB wall. TCE Concentrations from MW-29, which is nearest the PRB wall, have dropped by an order of magnitude since installation of the wall, from a high of 130 ug/L in September 1999 to 17 ug/L in January 2002 [CRG, 2002].

4.2 Calibration of Pre-remediation Condition

4.2.1 Model Settings and Parameters

The purpose of model calibration is to use a deterministic simulation approach to match the site condition prior to field remediation efforts. The TCE PAT system only removed about 3 lbs of mass during an operation period from 1995 to 2001, so it was not included in the model. During model calibration, the pre-remediation condition refers to the site condition prior to source remediation or plume PRB wall installation. Also, because TCE is the major contaminant, the model calibration focused on the TCE plume. To better present the site condition, the monitoring well sampling data that are variable both in space and time were used to compare with the simulation results. To be more specific, the simulated and measured time-series of TCE concentrations were compared for several monitoring wells located in different locations in the source zone and plume. The monitoring wells used for model calibration are MW-30A in the source area, along with MW-29, MW-35, MW-37, MW-38 and MW-36 in the plume area (see Figure 4.1).

During model calibration, the probabilistic model was set to use deterministic values for all parameters. Some parameters used values that fall in the reported range from previous site investigations, some were estimated during the model calibration, and some were calibrated to better match the site conditions. Transport and natural attenuation parameters used in model calibration are shown in Table 4.1. It is critical to estimate the source parameters during the model calibration. For the initial source concentration, C_0 , a value of 6 mg/L, estimated from the source well concentrations, was used in the model. The reported historical aqueous concentration of TCE in the source region showed large fluctuations over time, ranging from 0.34 mg/L to 75 mg/L during 1989 to 1992 [DERS, 1992]. For the initial source mass, M_0 , the reported value of 300 lb was used in the model [DERS, 1994]. The power function exponent, Γ , was estimated to be 1. This type of source behavior gives an exponential decay of the source mass and concentration with time. The source area was estimated to be a 25-foot diameter circle [CRG, 2002], so a value of 8 m was used for the source width in the model. The reported source thickness was about three or four meters, so a value of 3.5 m was used in the model. There is no information available for source decay, so a zero source decay rate was used in the model. Among these parameters, initial source concentrations and initial source mass are the parameters associated with high levels of uncertainty. Because data are available only from 1989 (at least 10 years after the initial release), it is not clear how C_0 and M_0 can be defined uniquely. There are likely to be several possible C_0 , M_0 combinations that represent available well data.

Table 4.1 Source, transport and natural attenuation parameters used on model calibration.

Parameter	Value	Comment
Initial source concentration, C_0 (mg/l)	6	Estimated
Initial source mass, M_0 (kg)	136	From site reports [DERS, 1994]
Power function exponent, Γ	1	Estimated
Source width, W (m)	8	From site reports [CRG, 2002]
Source depth, D (m)	3.5	From site reports [DERS, 1994]
Source decay rate (yr^{-1})	0	Estimated
Darcy velocity, V_d (m/yr)	8	Calibrated; reports had estimated 1.5 to 4.6 m/yr [DERS, 1994]
Porosity, ϕ	0.333	Estimated from reported Darcy velocity and pore velocity [DERS, 1994 and 1998],
Retardation Factor, R	2	Estimated
Longitudinal dispersivity, α_x	x/20	Calibrated
Transverse dispersivity, α_y	x/50	Calibrated
Vertical dispersivity, α_z	x/1000	Estimated
Overall plume degradation rate for TCE, λ (yr^{-1})	0.125	Calibrated (equal to $t_{1/2}$ of 5.5 yrs)

Transport parameters also play key role in the model. A groundwater Darcy velocity, V_d , of 8 m/yr resulted from the calibration process. Initially, a value of 4 m/yr was used for V_d , which was estimated from a hydraulic conductivity of 7.7×10^{-4} cm/sec and a gradient of 0.017 [DERS, 1992]. This value falls within the reported range of 1.5 to 4.6 m/yr [DERS, 1994]. By using $V_d=4$ m/yr, however, the simulated TCE concentration front moved slowly compared to field well data. This inconsistency could result from a variety of causes, including heterogeneity and transient variations of the gradient. The hydraulic conductivity of 7.7×10^{-4} cm/sec was based on slug tests from two monitoring wells (MW-30A and MW-31) and it might not represent the true conductivity of the entire area due to the heterogeneity nature. To better represent the site history based on data from MW-35, MW-37, MW-36 and MW-38, a calibrated value of 8 m/yr was used for V_d . Using reported groundwater Darcy velocity and pore velocity [DERS, 1994 and 1998], an effective porosity, ϕ , was estimated to be in the range of 0.28 to 0.41, and during the model calibration, a value of 0.33 was selected. No information was reported on retardation factor, R , for the Kinston site, so an estimated value of 2 was used in the model. In order to better match plume monitoring well data, longitudinal dispersivity, α_x , was calibrated to have a value of $x/20$, transverse dispersivity, α_y , was calibrated to have a value of $x/50$, and vertical dispersivity, α_z , was estimated to have a value of $x/1000$. The TCE first order degradation rate in the plume, λ , was calibrated to have a value of 0.125 yr^{-1} , which yields a half-life of 5.5 yrs. This TCE degradation rate is viewed as some type of average over the entire plume. As such, this value is also associated with some degree of uncertainty.

The initial TCE release date was not reported, but was at least prior to 1989. Based on the TCE plume extent in 1991 and the calibrated groundwater Darcy velocity and the estimated retardation factor, it was roughly estimated that the initial release occurred around 1967. The TCE plume in 1991 had a length about 280 m [DERS, 1992] and was assumed to be stable. Given $V_d=8\text{m/yr}$, $\phi=0.333$, $R=2$, the plume residence time of TCE was estimated as $t=(280)*(0.333)*(2)/(8)=23.31$ yr. Based on this number, the initial release would have occurred around 1967.

4.2.2 Model Calibration Results and Discussion

After model parameters have been estimated or calibrated, the probabilistic model was run in a deterministic way to match the site condition prior to source remediation or plume PRB wall installation. This section shows the model calibration results. The comparison of the historical time-series of TCE concentration before 1999 between the simulation results and the historical field sampling data from several monitoring wells are shown in Figures 4.2 through 4.7. The compared monitoring wells are located in different locations in the source zone and plume. For both model results and field data, TCE concentrations lower than 1 ug/L are not shown in the figures.

The comparison of TCE concentration before 1999 for source well MW-30A is shown in Figure 4.2. The simulated TCE concentrations for MW-30A are generally higher than the field sampling data. This discrepancy in the source well is probably caused by the initial source concentration used in the model. As discussed before, there is large uncertainty associated with this parameter. The comparison of TCE concentration before 1999 for plume well MW-29 is shown in Figure 4.3. The simulated TCE

concentrations for MW-29 are falling between the field sampling data. This indicates that with the combination of parameters discussed above, the simulated concentrations from the calibrated model match the field data in a reasonable degree for MW-29. The comparisons of TCE concentration before 1999 for plume wells MW-35 and MW-37 located in the middle of the plume are shown in Figure 4.4 and Figure 4.5. The simulated TCE concentrations match the field sampling data closely for both wells. This indicates that with the combination of parameters discussed above, the calibrated model captured the site condition for MW-35 and MW-37. The comparisons of TCE concentration before 1999 for plume well MW-38 is shown in Figure 4.6. The simulated TCE concentrations for MW-38 are higher than the field sampling data. This suggests that the initial source concentration might be too high or the TCE plume degradation rate might be too low. The TCE plume degradation rate is an averaged estimate for the entire plume. Because the entire plume is heterogeneous in terms of the TCE degradation rate, this averaged estimate is also associated with some degree of uncertainty. The uncertainty in other transport parameter also could cause such inconsistency for MW-38. The comparisons of TCE concentration before 1999 for plume well MW-36 is shown in Figure 4.7. One field sampling record is shown, which is higher than 1 ug/L, and the simulated results catch that value very well.

The compared monitoring wells are located in different locations in the source zone and plume within a large area (as shown in Figure 4.1). Also, the compared time-series of TCE concentration covered a period of time from 1989 to 1998. The agreements of time-series of TCE concentration between modeled results and field sampling data in

monitoring wells MW-29, MW-35, MW-37 and MW-36 show that with the given combination of parameters as discussed above, the calibrated model is able to closely match the pre-remediation site condition in term of time-series of TCE concentration. The disagreements in the source well MW-30A and plume well MW-36 show that the initial source concentration is associated with a high level of uncertainty and TCE plume degradation rate is associated with some degree of uncertainty. There are likely to be other possible combinations of such parameters that could match or represent available well data. To capture the uncertainty of these parameters, the probabilistic simulation of remediation efforts are conducted and presented in next section.

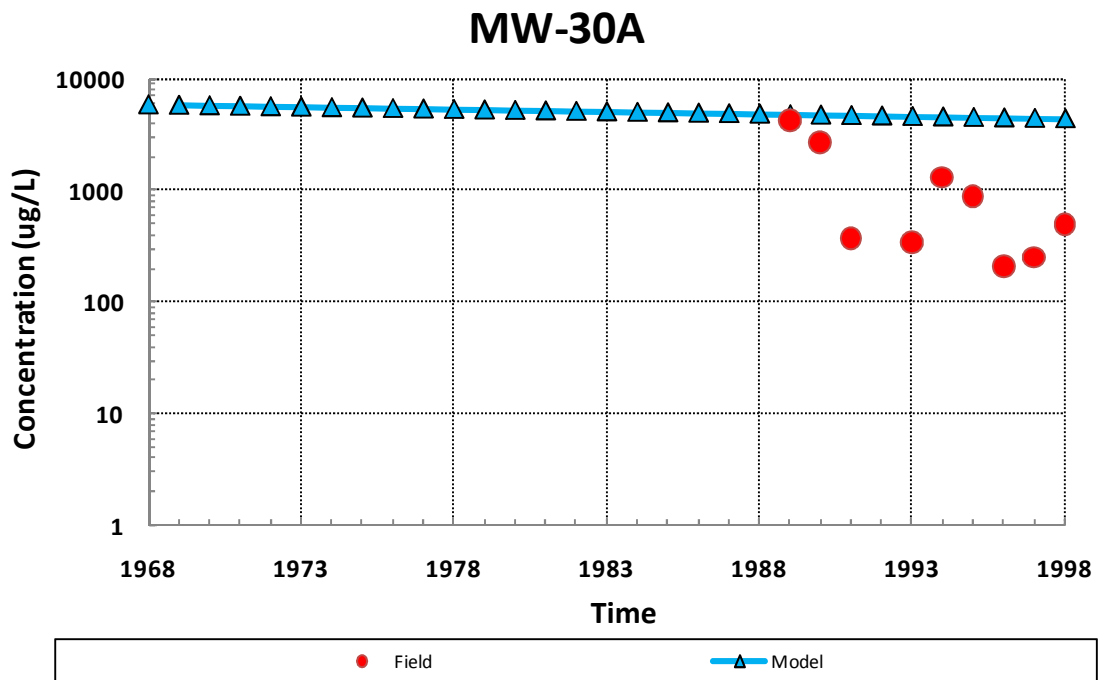


Figure 4.2 Comparison of TCE concentrations between modeled results and field data for MW-30A (model calibration).

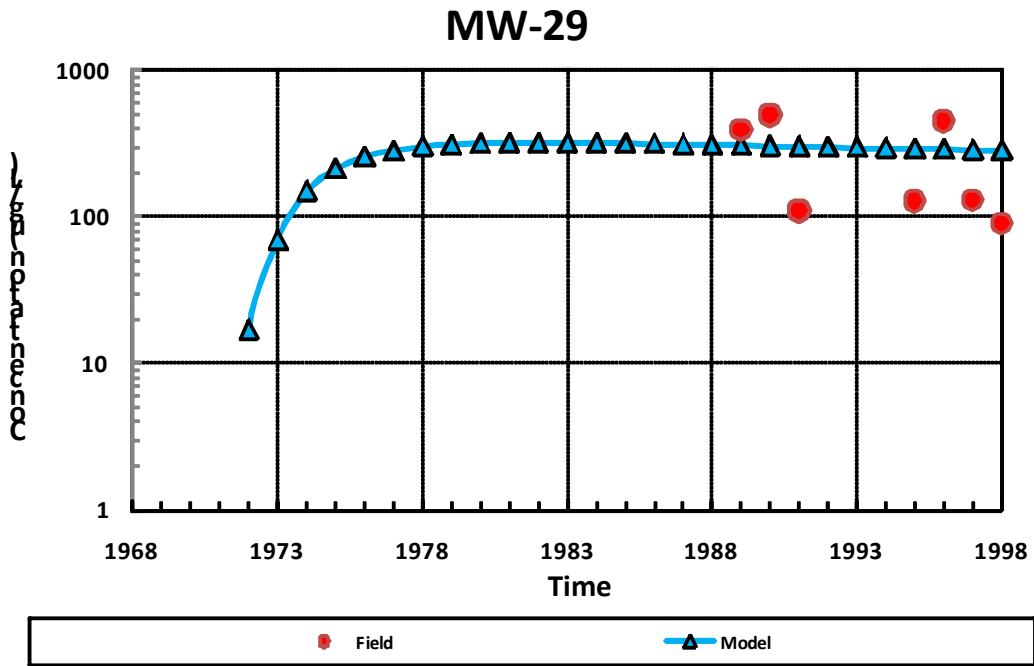


Figure 4.3 Comparison of TCE concentrations between modeled results and field data for MW-29 (model calibration).

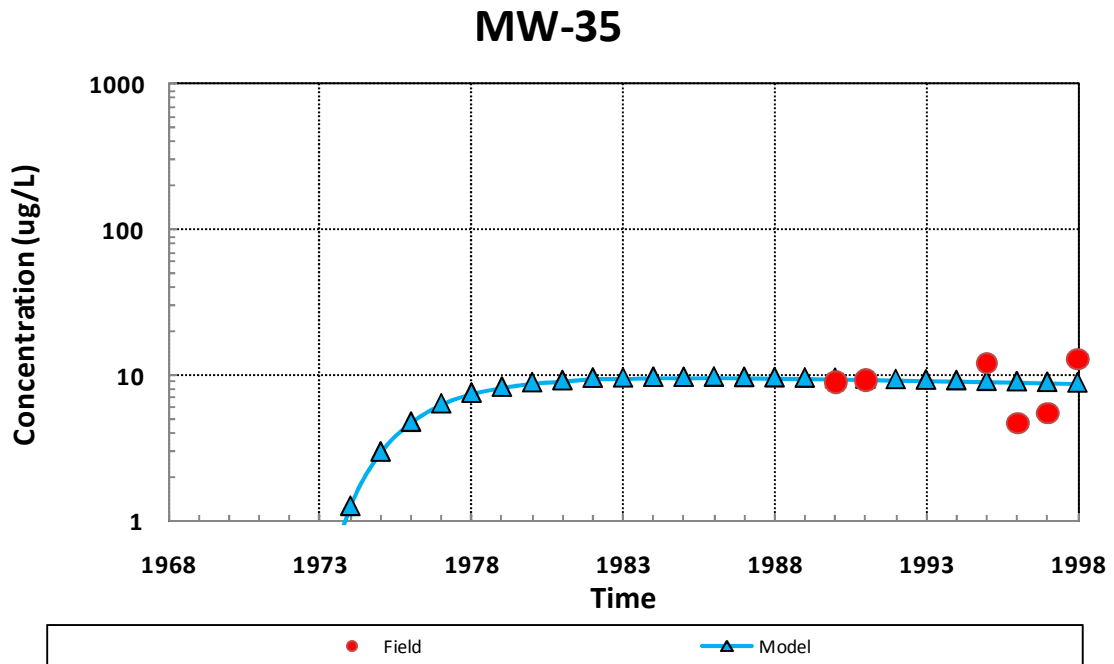


Figure 4.4 Comparison of TCE concentrations between modeled results and field data for MW-35 (model calibration).

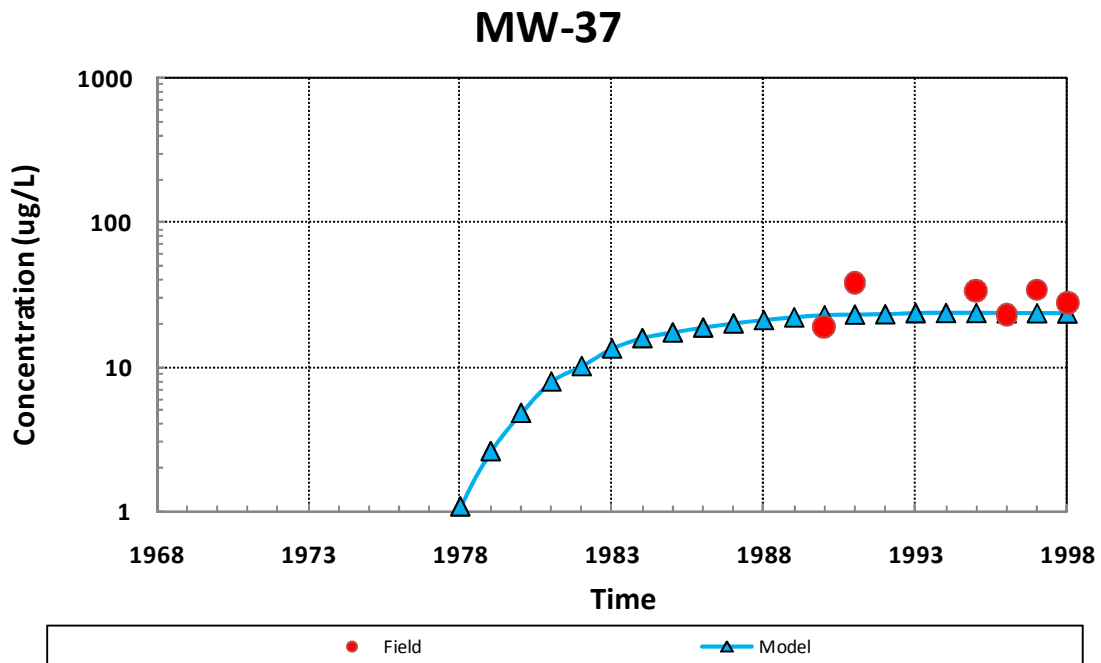


Figure 4.5 Comparison of TCE concentrations between modeled results and field data for MW-37 (model calibration).

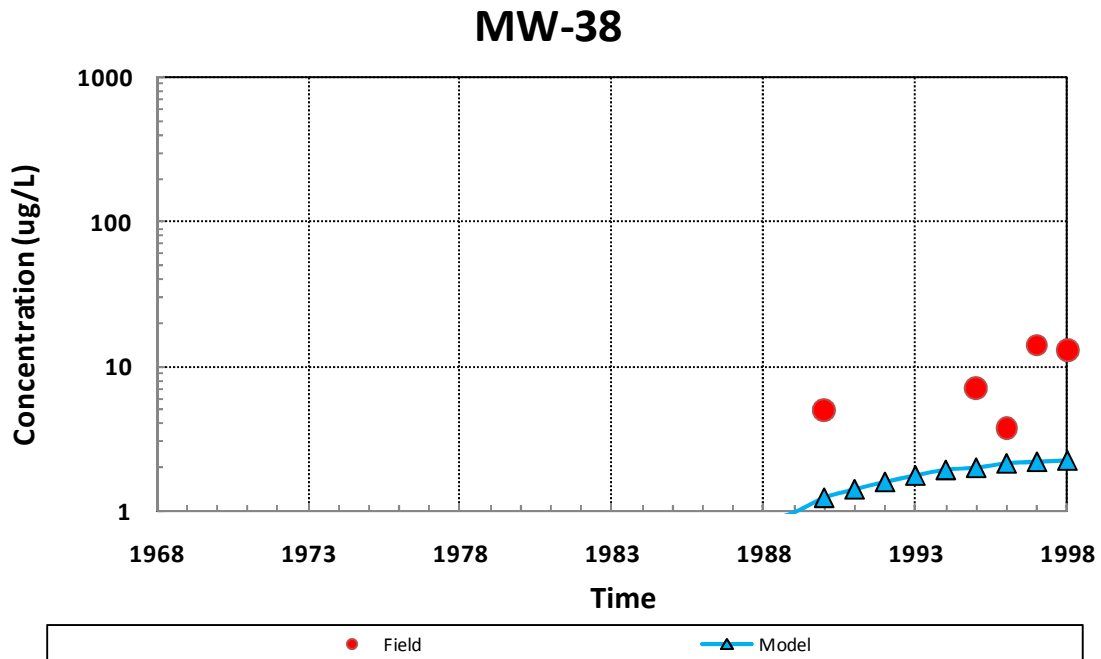


Figure 4.6 Comparison of TCE concentrations between modeled results and field data for MW-38 (model calibration).

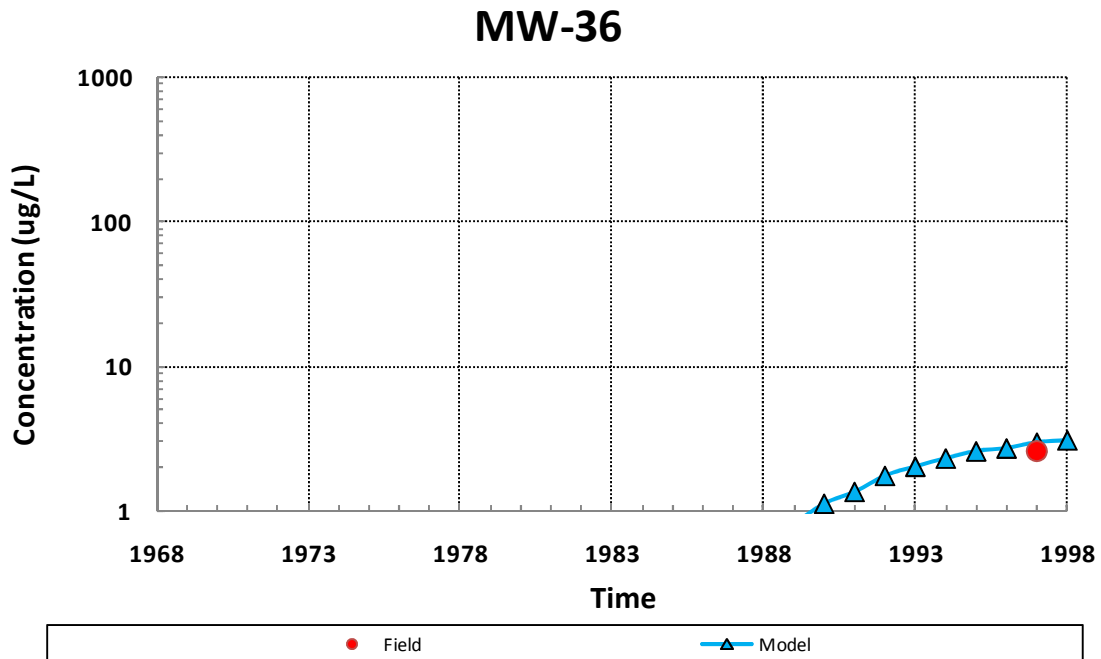


Figure 4.7 Comparison of TCE concentrations between modeled results and field data for MW-36 (model calibration).

4.3 Probabilistic Simulation of Field Remediation Activities

4.3.1 Model Settings and Parameters

Based on the previous calibrated model, probabilistic simulations are conducted to model both the source ZVI treatment and plume PRB treatment in order to evaluate the effectiveness of field remediation efforts by considering the uncertainty in key parameters. During the probabilistic simulation, seven key parameters associated with a high level of uncertainty used probabilistic values sampled from specified PDFs, and other parameters used deterministic values as used in model calibration. For the uncertainty parameters, the mean behaviors keep consistent with the values used in model calibration and the ranges keep close or reasonable to the site conditions. The distributions and values of uncertain parameters are shown in Table 4.2 and Figure 4.8. The deterministic transport parameters used in probabilistic simulation can be found in Table 4.1. Note that C_0 , M_0 and Γ are uncertainty parameters, so the deterministic values for these three parameters in Table 4.1 are not applied during the probabilistic simulation.

Three source parameters are treated as uncertain variables. The initial source mass used a triangular distribution with a minimum value of 2 mg/L, a most likely value of 6 mg/L, and a maximum value of 10 mg/L. This distribution has a mean value of 6 mg/L as used in model calibration and its range covers a big portion of field source well data (MW-30A). The initial source mass, M_0 , used a triangular distribution with a minimum value of 50 kg, a most likely value of 136 kg and a maximum value of 220 kg. This distribution has a mean of 136 kg as used in model calibration and its range reflects some uncertainty associated with reported value of M_0 . The power function exponent, Γ , used a

log-normal distribution with a geometric mean of 1 and a geometric standard deviation of 2. This distribution gives that a 5th percentile of Γ is 0.3 and a 95th percentile of Γ is 3.

Groundwater Darcy velocity, V_d , is the key transport parameter. The reported value ranges from 1.5 to 4.6 m/yr and the calibrated value is 8 m/yr. It can be seen that there is a large uncertainty associated with V_d , so it is treated as an uncertain parameter. V_d used a normal distribution with a mean of 8 m/yr and a stdv of 2.5m. This distribution gives that a 5th percentile of V_d is 2 m/yr and a 95th percentile of V_d is 14 m/yr. This range covers a large part of the uncertainty of V_d that could occur in the site. From model

Table 4.2 Stochastic parameters used in probabilistic simulation.

Parameter	Distribution	Value
Initial source concentration, C_0 (mg/l)	Triangular	min=2, most likely=6, max=10
Initial source mass, M_0 (kg)	Triangular	min=50, most likely=136, max=222
Power function exponent, Γ	Log-normal	geo mean =1, geo stdv=2
Darcy velocity, V_d (m/yr)	Normal	mean=8, stdv=2.5
TCE degradation rate in plume, λ (yr ⁻¹)	Triangular	min= 0.05, most likely= 0.125, max=0.2
Fraction of source mass removal (%)	Beta	mean=0.85, stdv = 0.08, min=0.6, max=0.99
TCE degradation rate in PRB wall, λ_{PRB} (yr ⁻¹)	Triangular	min=228, most likely=436, max=644

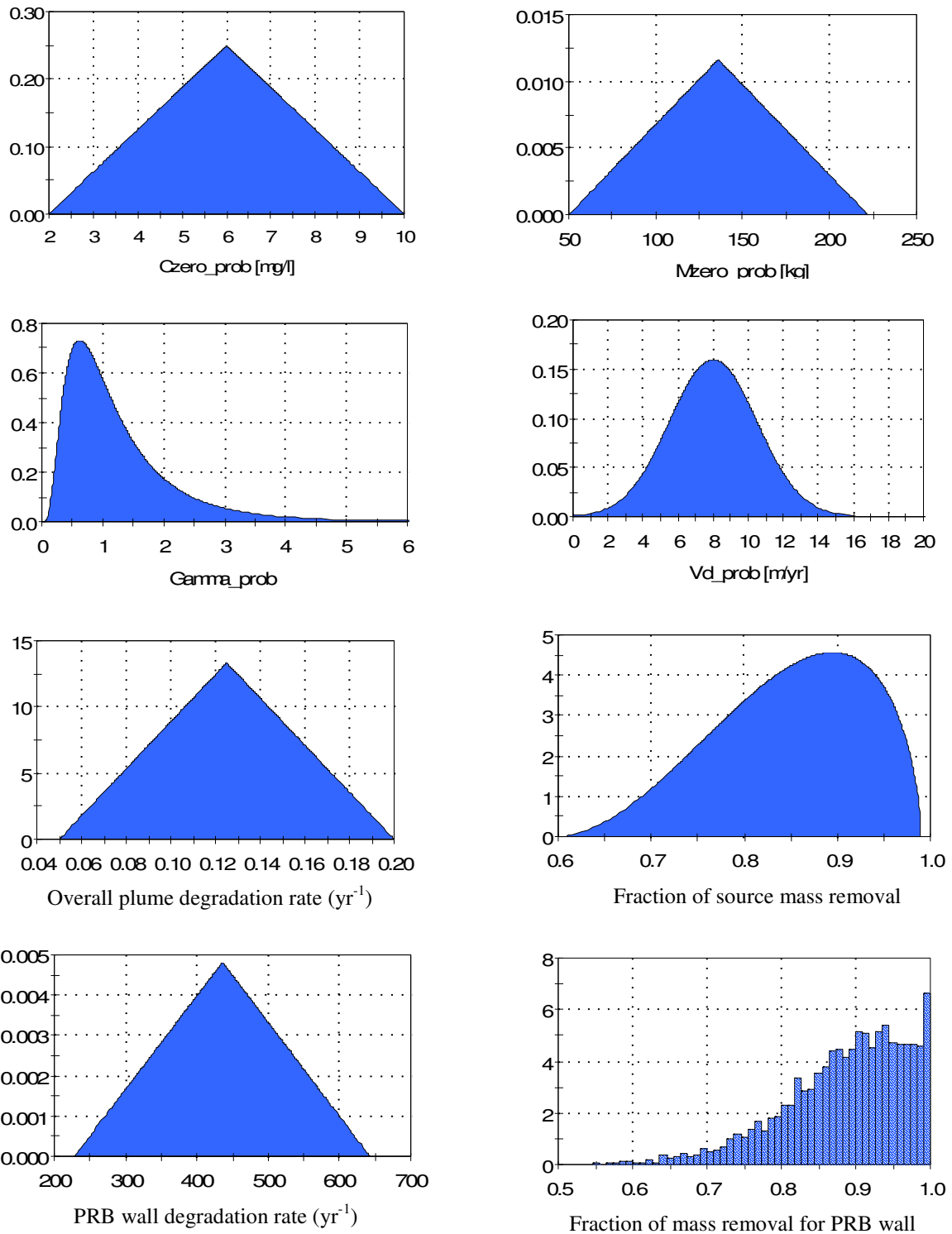


Figure 4.8 The PDFs of the stochastic variables used in the probabilistic simulation.

calibration, it is found that the averaged plume natural degradation rate affects plume concentration greatly if there is not any remediation effort. It also found that this averaged degradation rate has an uncertainty in some degree, so it is treated as an uncertain variable. It used a triangular distribution with a minimum value of 0.05 yr^{-1} (a half-life of 13.9 yrs), a most likely value of 0.125 yr^{-1} (a half-life of 5.5yrs), and a maximum value of 0.2 yr^{-1} (a half-life of 3.5 yrs). This distribution has a mean of 0.125 yr^{-1} as used in model calibration and its range captures some degree of uncertainty.

The remediation efficiency obviously plays the key role in the effectiveness of the remediation effort. The source mass removal efficiency and enhanced degradation rate for plume PRB wall are treated as the uncertain parameters. During the probabilistic simulation, the source ZVI treatment is modeled by removing a fraction of TCE mass from the source zone in a period of 11 months. The starting time of source ZVI treatment was 1999, which is 32 years from estimated initial release. Although source mass removal was reported as 95%, wells in the source zone have not seen large reductions in concentration. There is large uncertainty associated with this source mass removal efficiency. In the model, the efficiency of source mass removal is treated as an uncertain variable. It used a beta distribution derived earlier based on the data reported by McGuire et al., [2006]. During the simulation, a mean of 85% and a standard deviation of 8% were used. A minimum value of 60% and a maximum value of 99% were used in the model.

The plume PRB treatment is modeled by assigning a very high first-order degradation rate for TCE in a narrow reaction zone (as shown in Figure 4.9). The other eight reaction zones use the background degradation rate, which has a mean of 0.125 1/yr

estimated from the previous model calibration. The reported effective thickness of the PRB wall is from four to six inches [CRG, 2002]. The model uses the average value of 5 inches as the length of the PRB treatment zone. In the model, the PRB treatment zone starts from 89 m and ends at 89.127 m [CRG, 2002].

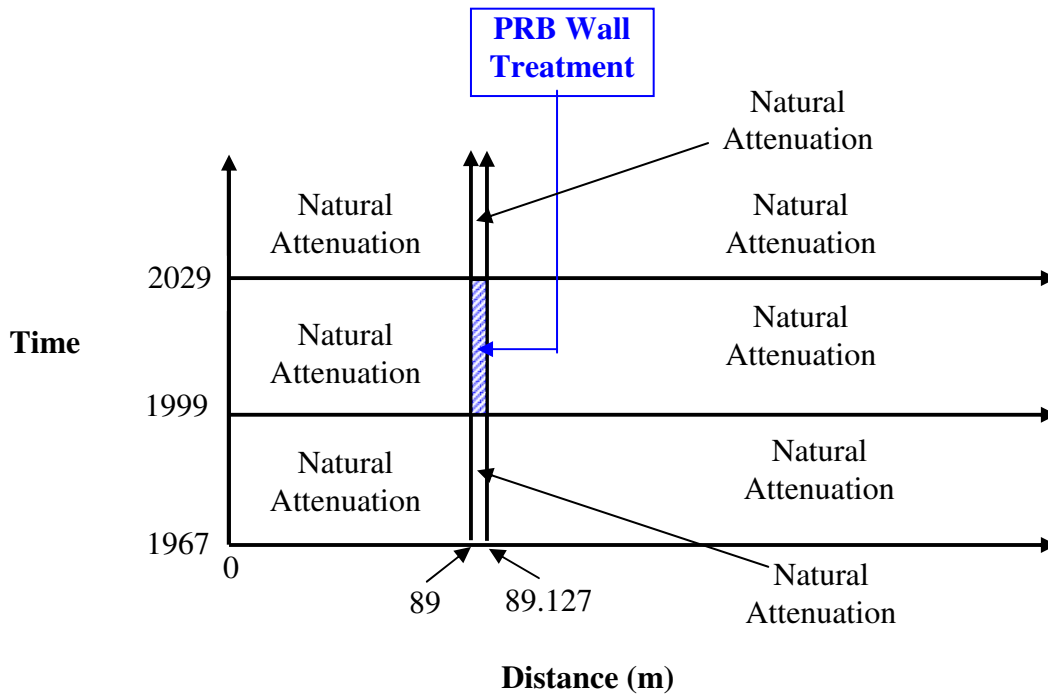
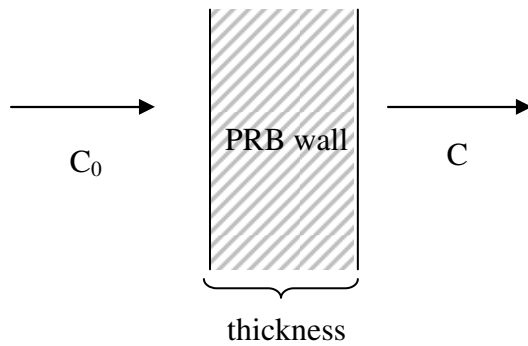


Figure 4.9 Plume reaction zones, including the PRB treatment, simulated in the model.

The bench scale half-life of TCE by ZVI treatment was reported as less than 4 hrs [DERS, 1998]. A half-life of 4 hrs is equivalent to a degradation rate of 1518 yr^{-1} . However, the field condition is much more complicated than the lab condition. The field

degradation rate of TCE inside the PRB wall might not achieve the bench scale level due to heterogeneity of the wall. Instead of using the bench-scale half-life of TCE due to ZVI treatment to estimate the degradation rate for plume PRB treatment, a more realistic approach is used in the model. This relates the percent of mass removal across the PRB wall to the degradation rate inside the PRB wall.

As illustrated in below, when contaminated groundwater passes through the PRB wall, the dissolved contaminant will be degraded by ZVI. As a result, the contaminant concentration leaving the PRB wall will be much lower than that of entering the PRB wall. Since PRB wall is very thin, the effects on the concentration due to dispersion should be small inside the PRB wall. By assuming a first-order reaction in aqueous phase, the concentration reduction across the wall after PRB treatment, X_{remain} , is given by Equation (28).



$$X_{remain} = 1 - X_{removal} = \frac{C}{C_0} = e^{\frac{-x}{v} \lambda_{PRB}} = e^{\frac{-x\phi}{V_d} \lambda_{PRB}} \quad (28)$$

where C_0 and C are the aqueous concentrations entering and leaving the PRB wall, λ_{PRB} is the degradation rate, x is the thickness of the PRB wall, v is the pore velocity, Vd is the Darcy velocity, and ϕ is the porosity. The degradation rate inside the PRB wall, λ_{PRB} , can be estimated from the percent of mass removal, $X_{removal}$, by Equation (29),

$$\lambda_{PRB} = -\frac{\ln(C/C_0)}{x\phi/V_d} = -\frac{\ln(1 - X_{removal})}{x\phi/V_d} \quad (29)$$

The deterministic values of Darcy velocity and porosity based on the model calibration are used to calculate the corresponding decay rates for different PRB wall removal efficiencies (as shown in Table 4.3). A degradation rate of 436 yr^{-1} corresponds to a mass removal efficiency of 90% for the PRB wall. If a degradation rate of 1518 yr^{-1} (equal to a half-life of 4 hrs) is used, the corresponding removal efficiency for the PRB wall would be 99.9%, which seems overly optimistic.

During the probabilistic simulation, the degradation rate for PRB wall is treated as an uncertainty parameter. It used a triangular distribution with a minimum value of 228 yr^{-1} (a half-life of 26.7 hrs), a most likely value of 436 yr^{-1} (a half-life of 13.9 hrs), and a maximum value of 643 yr^{-1} (a half-life of 9.4 hrs). The corresponding mass removal percentages are 70%, 90% and 97% respectively.

As shown in Equation (29), the PRB degradation rate used in model is derived from the mass removal percentage. If all parameters in Equation (29) are deterministic, then a specific mass removal percent will correspond to a single degradation rate. On the

Table 4.3 Percentage of mass removal and corresponding degradation rate for PRB wall used in probabilistic simulation.

Percent of Mass Removal (%)	Percent of Mass remaining (%)	Degradation Rate, λ_{PRB} (yr ⁻¹)
0.00	100.00	0.00
5.00	95.00	9.70
25.00	75.00	54.42
50.00	50.00	131.12
70.00	30.00	227.75
90.00	10.00	435.57
95.00	5.00	566.69
96.00	4.00	608.90
97.00	3.00	663.32
98.00	2.00	740.02
99.00	1.00	871.14
99.90	0.10	1306.71
99.99	0.01	1742.28
99.999	0.00	2177.85
99.9999	0.0001	2613.42
99.99999999	1.00E-09	4791.27
100	0	infinite

other hand, if one or more parameters are stochastic, then a range of mass removal percentages correspond to a single decay rate due to uncertain parameters. During the probabilistic simulation, Darcy velocity and degradation rate are treated as the stochastic variables. So the distribution of mass removal percentage for PRB wall results from the distributions of Darcy velocity and PRB degradation rate used in the model (Figure 4.8).

4.3.2 Probabilistic Simulation Results and Discussions

Based on the model settings and parameters discussed in previous section, probabilistic simulation are conducted to evaluate the effectiveness of source remediation and plume PRB wall installation in Kinston TCE site. During the probabilistic simulation, multiple realizations were run. For each realization, the model simultaneously sampled different values for seven uncertain parameters. The simulated TCE concentrations are assembled into the probabilistic statistics. The mean behavior of the TCE plume in 1999, prior to source remediation or plume PRB installation is shown in Figure 4.10 and that in 2009, 10 years after source remediation and plume PRB wall installation is shown in Figure 4.11. The comparisons of TCE concentration between modeled results and field sampling data for monitoring wells in different locations in source area and plume are shown. The monitoring wells compared here are those used in model calibration, including a source well MW-30A, along with plume wells MW-29, MW-35, MW-37, MW-38 and MW-36, and others with available field data, including a source well MW-47, along with plume wells MW-59, MW-58, MW-60 and MW-58 (see Figure 4.1). The comparisons and model predictions are shown from Figure 4.12 to Figure 4.22.

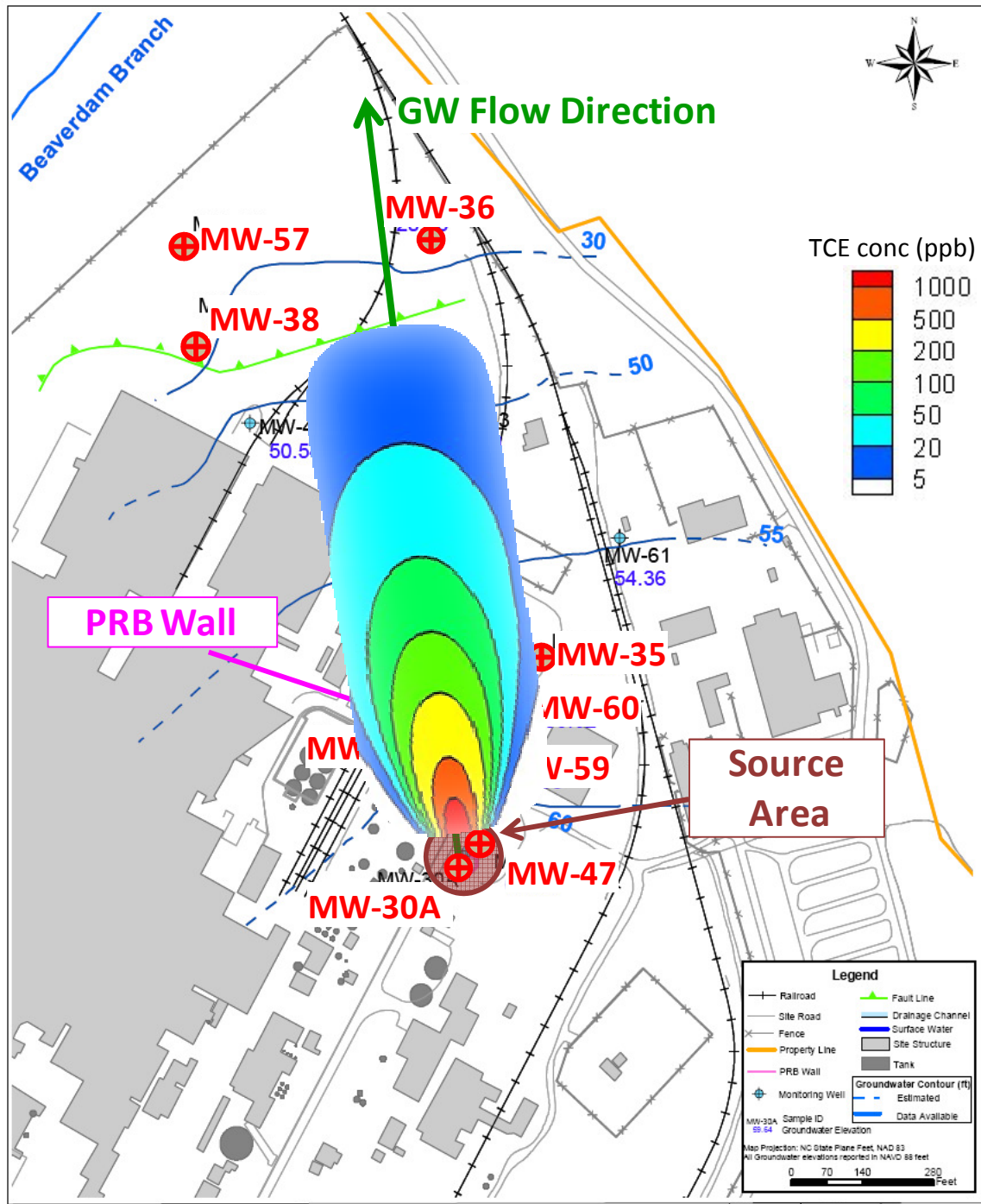


Figure 4.10 Simulated mean behavior of TCE concentrations in 1999 prior to source remediation or plume PRB wall installation from probabilistic simulation.

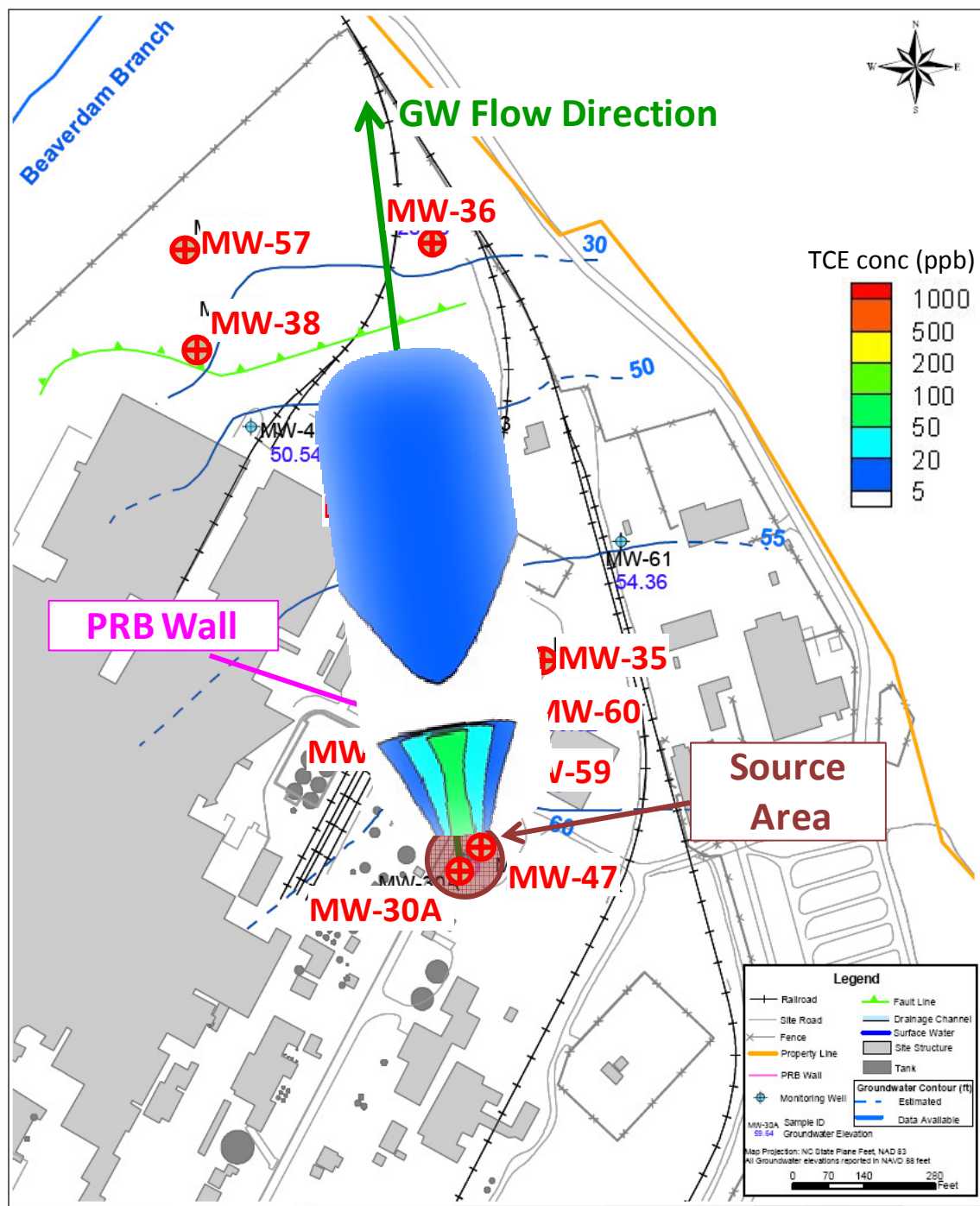


Figure 4.11 Simulated mean behavior of TCE concentrations in 2009 from probabilistic simulation.

The probabilistic simulation results and comparison of TCE concentrations over time for source well MW-30A are shown in Figure 4.12. The simulation duration time is from 1967 to 2027. Simulated TCE concentrations are shown as the probabilistic time histories from the 5th percentile to the 95th percentile. The solid black line is the median of simulated TCE concentrations. From the median line upward, the outline of the light dot filled area is the 75th percentile and the outline of light upward diagonal filled area is the 95th percentile respectively. From the median line downward, the outline of the light dot filled area is the 25th percentile and the outline of light upward diagonal filled area is the 5th percentile respectively. The red dots are the field sampling data. The overall uncertainty in TCE concentration propagates over time. Some field data points are off from simulated TCE concentrations. This indicates that uncertainties in seven parameters might reflect the site condition for this well in a limited degree. Nonetheless, simulated concentrations are shown in a range from 5th percentile to 95th percentile. It is possible that some of those off points could be covered by the upper bound and lower bound. On the other hand, field data from this source well show a large fluctuation over time, ranging from a few ppb to 10,000 ppb. This indicates that there is a large uncertainty associated with the field data. Field data in this well have not show large concentration reductions after the source remediation.

The probabilistic simulation results and comparison of TCE concentrations over time for source well MW-47 are shown in Figure 4.13. The simulated TCE concentrations are shown from the 5th percentile to the 95th percentile. Simulated TCE concentrations cover most of field data. This indicates that uncertainties in seven

parameters reflect the site condition for this well. Those very few off points very possibly could be covered by the upper bound and lower bound. Field data from this source well also have not show large concentration reductions after the source remediation.

Probabilistic simulation results and comparison of TCE concentrations over time for plume well MW-59 are shown in Figure 4.14. Simulated TCE concentrations cover all of field data and the simulated median concentrations match most field data. This indicates that uncertainties in seven input parameters capture the site condition for this well in a high degree. Field data from this source well have shown some reductions in concentration after source remediation. Probabilistic simulation results and comparison of TCE concentrations over time for plume well MW-58 are shown in Figure 4.15. Simulated TCE concentrations cover half of field data and all the field data are below the simulated median. This indicates that uncertainties in seven input parameters reflect the site condition for this well in a limit degree and model might underestimate the TCE concentrations over time.

Probabilistic simulation results and comparison of TCE concentrations over time for plume well MW-29 are shown in Figure 4.16. Simulated TCE concentrations cover most field data and they are around the simulated median. This indicates that uncertainties in seven input parameters capture the site condition for this well in a high degree. MW-29 is very close to the plume PRB wall, so as expected, both field data and simulated TCE concentration show a sharp drop due to PRB wall treatment and the overall uncertainty in TCE concentration is reduced greatly right after plume PRB wall installation.

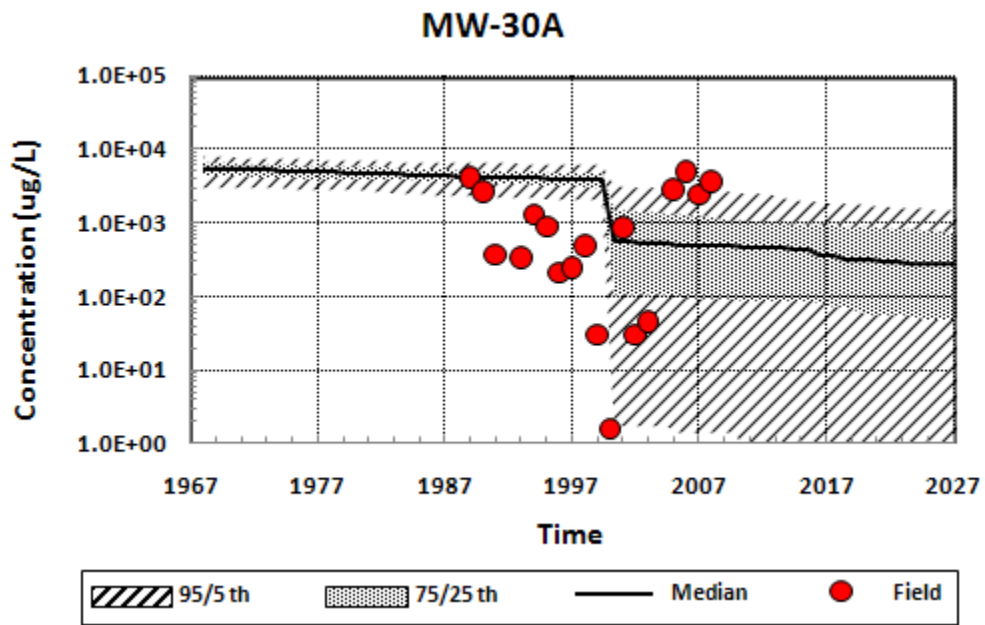


Figure 4.12 Comparison of TCE concentrations between modeled results and field data for MW-30A (probabilistic simulation).

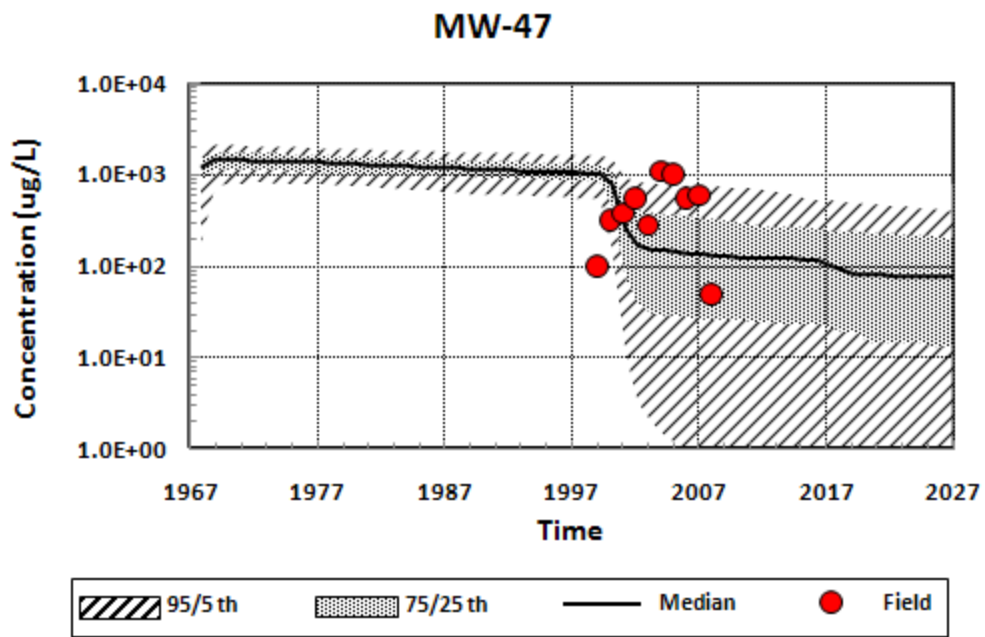


Figure 4.13 Comparison of TCE concentrations between modeled results and field data for MW-47 (probabilistic simulation).

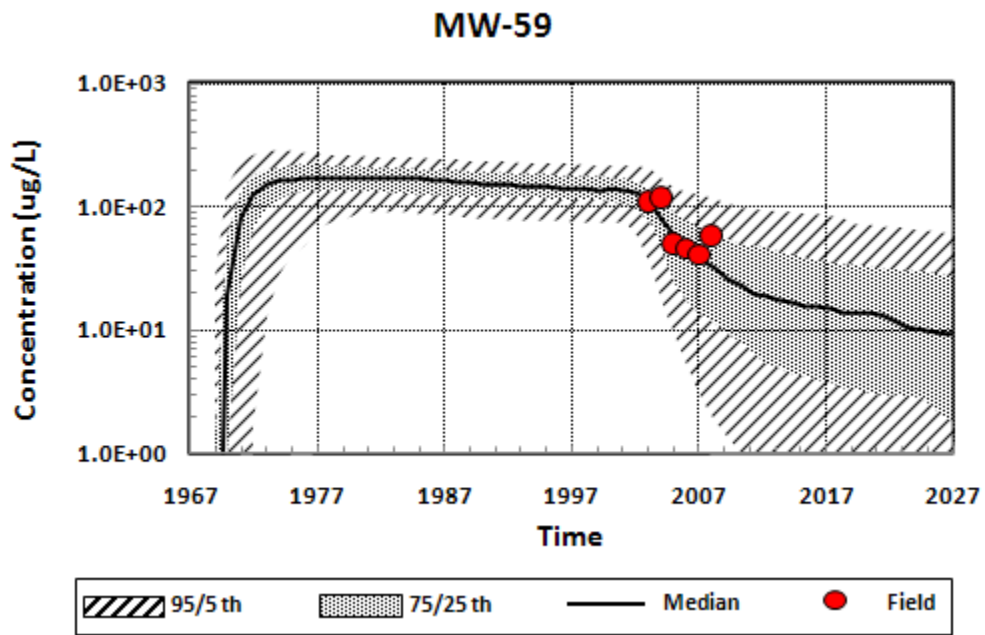


Figure 4.14 Comparison of TCE concentrations between modeled results and field data for MW-59 (probabilistic simulation).

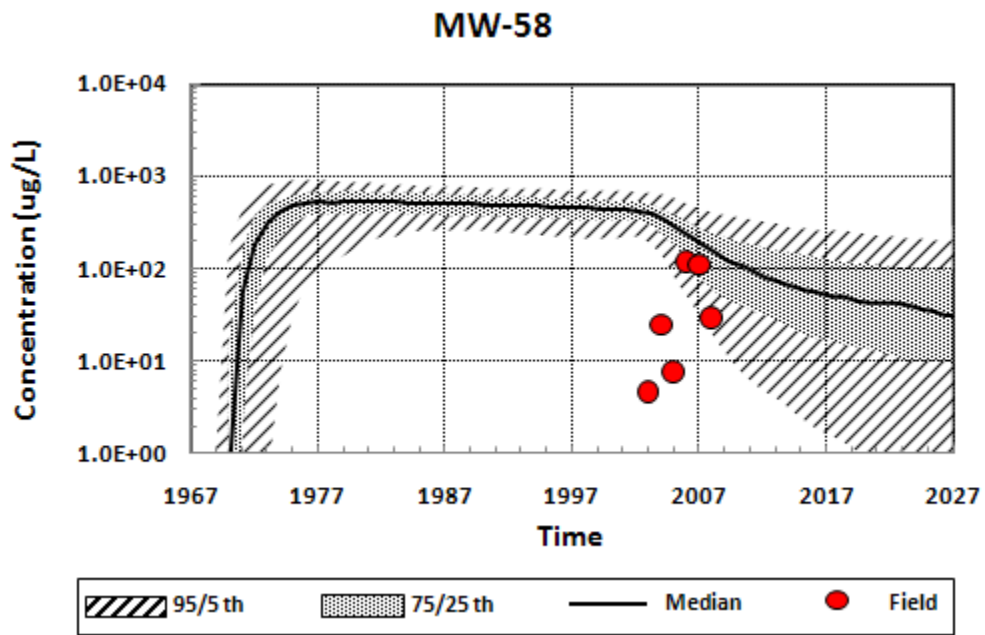


Figure 4.15 Comparison of TCE concentrations between modeled results and field data for MW-58 (probabilistic simulation).

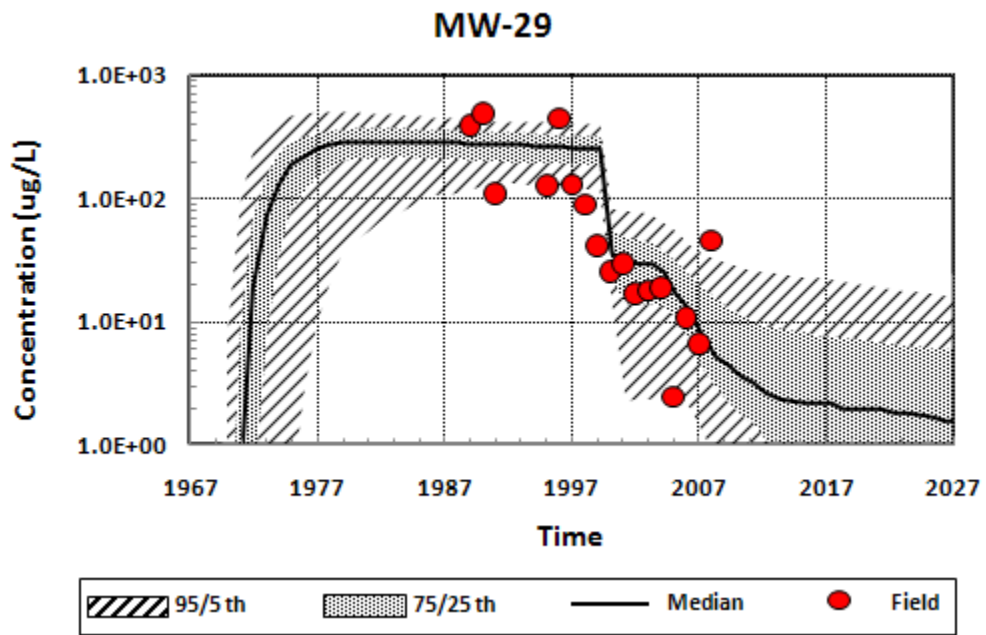


Figure 4.16 Comparison of TCE concentrations between modeled results and field data for MW-29 (probabilistic simulation).

Probabilistic simulation results and comparison of TCE concentrations over time for plume well MW-60 are shown in Figure 4.17. The overall uncertainty in TCE concentration propagates over time. The simulated TCE concentrations are lower than most field data. This indicates that uncertainties in seven parameters might underestimate the site condition for this well. Probabilistic simulation results and comparison of TCE concentrations over time for plume well MW-35 are shown in Figure 4.18. A large portion of field data are covered by simulated TCE concentrations. This indicates that uncertainties in parameters might reflect the site condition for this well in some degree.

Probabilistic simulation results and comparison of TCE concentrations over time for plume well MW-37 are shown in Figure 4.19. The simulated TCE concentrations cover most field data. This indicates that uncertainties in parameters reflect the site condition for this well in a high degree.

Probabilistic simulation results and comparison of TCE concentrations over time for plume well MW-38 are shown in Figure 4.20. More than half of the field data are covered by simulated TCE concentrations and almost all of the field data are above the simulated median. This indicates that uncertainties in parameters reflect the site condition for this well in some degree and model might overestimate the concentration. Probabilistic simulation results and comparison of TCE concentrations over time for plume well MW-36 is shown in Figure 4.21. Simulated TCE concentrations cover all of the field data but they are below the median. This indicates that uncertainties in parameters reflect the site condition for this well in some degree but model might underestimate the TCE concentration. Probabilistic simulation results and comparison of

TCE concentrations over time for plume well MW-57 are shown in Figure 4.22. The comparison between simulated TCE concentration and field data is similar to MW-60.

Based on above results and discusses, it can be summarized that the overall uncertainty in TCE concentration propagates over time given uncertainties in seven input parameters. Among eleven monitoring wells, the probabilistic model considering uncertainties in seven key parameters reflects the site conditions for MW-59, MW-29, MW-37 and MW-47 to a high degree. The probabilistic model reflects the site conditions for MW-35, MW-38 and MW-26 to a reasonable degree. For MW-30A, MW-58, MW-60 and MW-57, the probabilistic model reflects the site conditions to a limited degree.

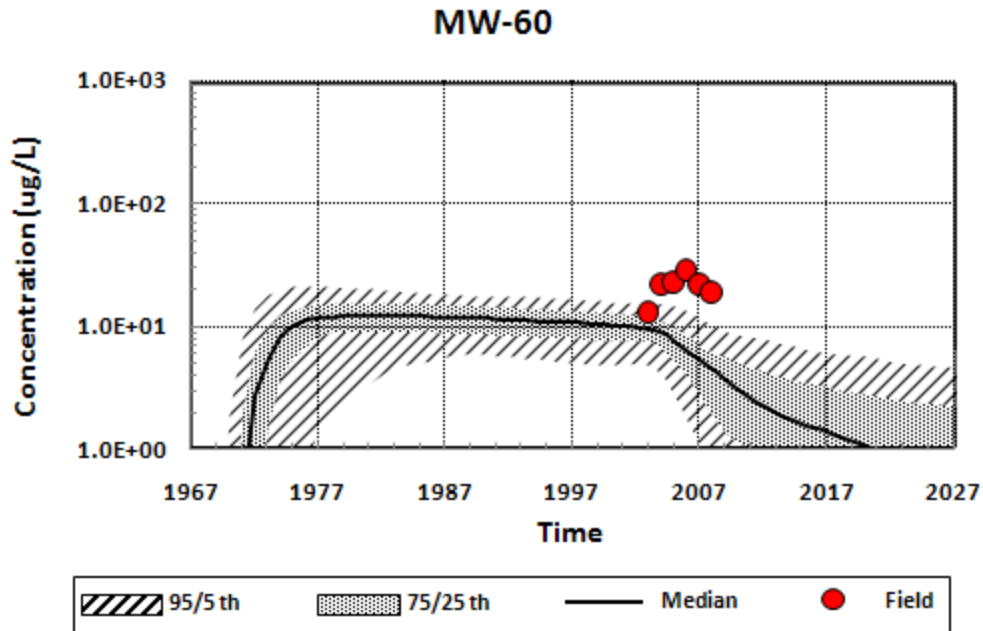


Figure 4.17 Comparison of TCE concentrations between modeled results and field data for MW-60 (probabilistic simulation).

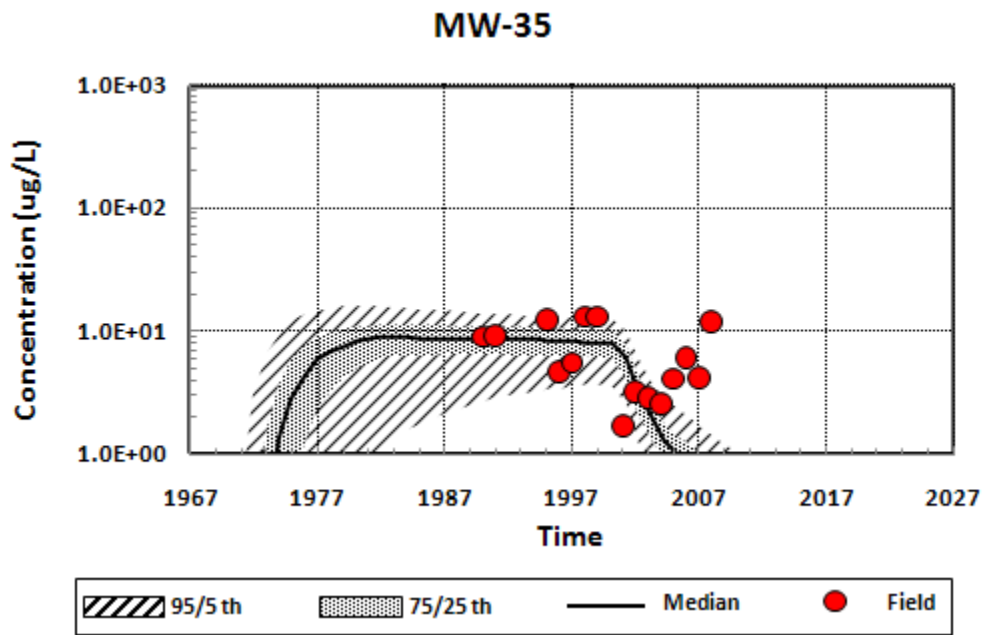


Figure 4.18 Comparison of TCE concentrations between modeled results and field data for MW-35 (probabilistic simulation).

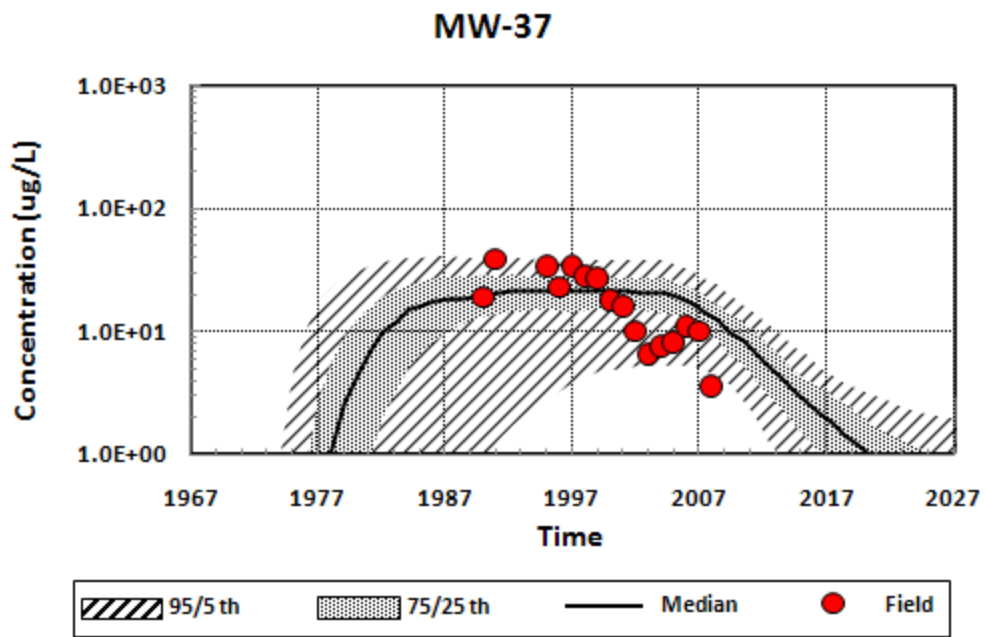


Figure 4.19 Comparison of TCE concentrations between modeled results and field data for MW-37 (probabilistic simulation).

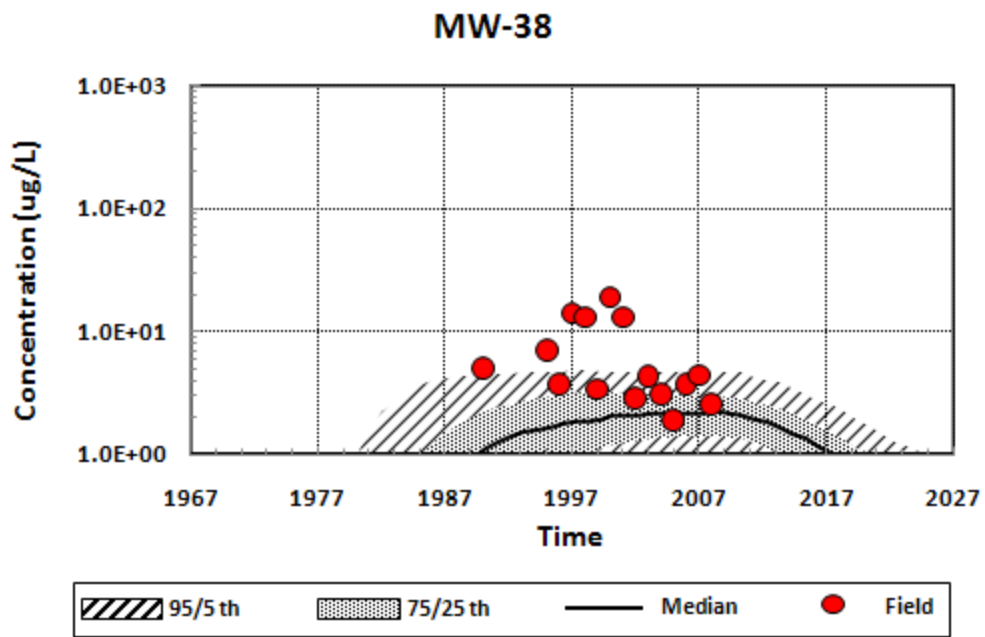


Figure 4.20 Comparison of TCE concentrations between modeled results and field data for MW-38 (probabilistic simulation).

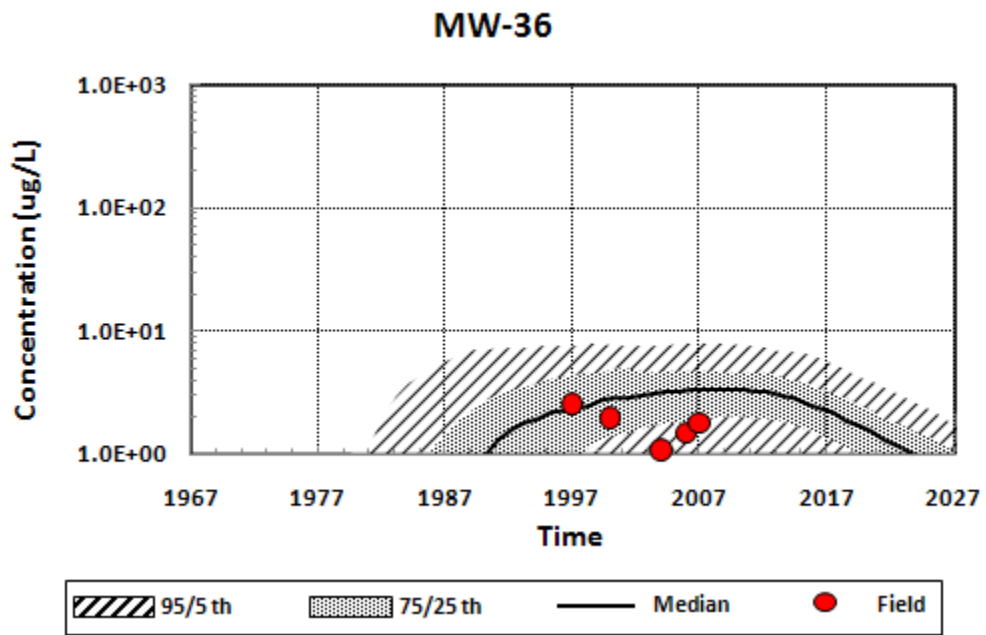


Figure 4.21 Comparison of TCE concentrations between modeled results and field data for MW-36 (probabilistic simulation).

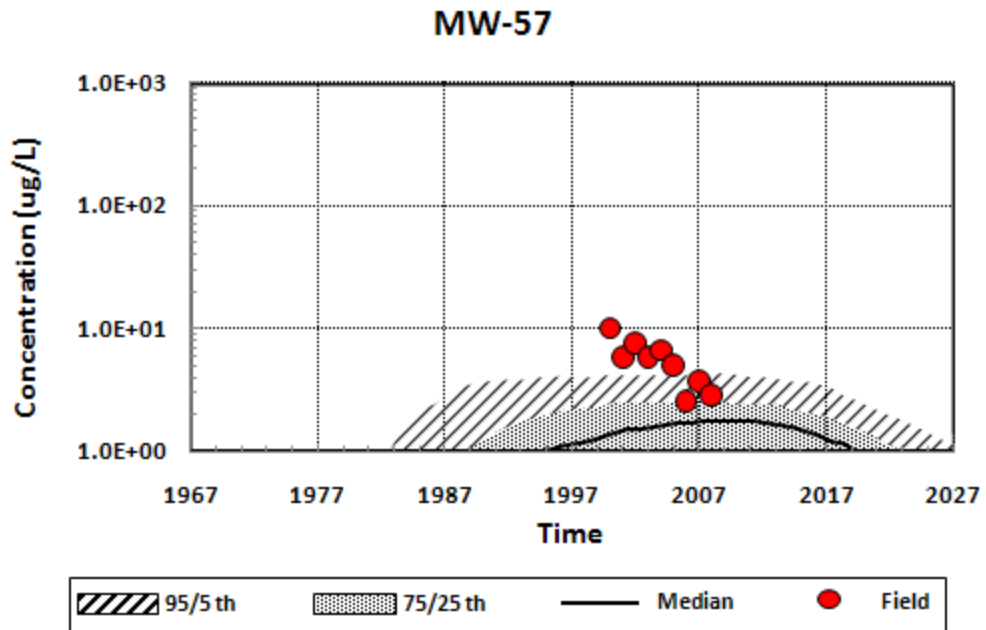


Figure 4.22 Comparison of TCE concentrations between modeled results and field data for MW-57 (probabilistic simulation).

CHAPTER 5

SENSITIVITY ANALYSIS FOR DIFFERENT PLUME TYPES

5.1 Introduction

Chlorinated solvents source and plume remediation are complex processes due to the many uncertain controlling variables, such as hydrogeological variables, geochemical variables and cost variables. These factors play different roles on the effectiveness of source and plume remediation efforts. Also, the influence of parameters on the effectiveness of remediation for different types of sites are different as well. In this chapter, the PREMChlor model is used to conduct sensitivity analyses by assessing the influence or relative importance of input variables on the target output (e.g. contaminant mass concentration at a control plane) in terms of different plume types.

The site behavior can be divided into three types in terms of the aqueous plume behavior: a shrinking plume, a stable plume and a growing plume. For shrinking/stable plumes with the contaminant mass mostly in the source zone, the target output may be mostly sensitive to the removal efficiency of the source treatment. The growing plume is more complicated. For the scenario with the contaminant mass partly in the source zone and partly in the dissolved plume, the target output may be sensitive to the efficiency of both source removal and plume treatment. The sensitivity analysis explores the different importance of input variables to the plume behavior for different types of plumes.

There are several possible ways to perform sensitivity analyses. The most common approach is sampling-based in which the model is executed repeatedly for

combinations of values sampled from the probabilistic distributions. In this study, sensitivity analysis is conducted by running the probabilistic simulation multiple times, making an input variable stochastic and sampling it over its specified PDF, while holding all of the other input variables constant. The resulting target output is also a probability distribution and it solely reflects the uncertainty in that single stochastic input variable. Such probabilistic simulations are repeated for every important input variable. This analysis can determine how different values of each input variable will impact the target output.

The target output specified in the sensitivity analysis is the contaminant mass concentration in plume. Ten key input variables are used to conduct the sensitivity analysis, consisting of the initial source concentration (C_0), initial source mass (M_0), power function exponent (Γ), Darcy velocity (V_d), porosity (ϕ), retardation factor (R), dispersivity parameters (longitudinal (α_x), transverse (α_y) and vertical (α_z), plume overall degradation rate without remediation (λ), source removal fraction (X_{rem}) and plume treatment rate (λ_{rem}). In PREMChlor, the longitudinal, transverse and vertical dispersivities are all scale-dependent. Each of them equals to a different dispersivity parameter times the travel distance.

In this study, three cases are tested: I. A stable plume connected to the source where the contaminant mass is partly in the source zone and partly in the plume; II. A growing plume that is disconnected from the source, where the most of the contaminant mass is in the plume; and III. A growing plume that is connected to the source, where contaminant mass is partly in the source zone and partly in the plume. These cases are

presented in following three sections, respectively. Each case includes the description of the deterministic plume setting (referred as base case) and the sensitivity analysis that is conducted based on the base case.

5.2 Case I: Stable Plume Connected to the Source

5.2.1 Base Case Description (Case I)

In this case, the Kinston TCE site from the model application section is used as a representative site to conduct the sensitivity analysis focusing on the TCE concentration. Daughter compounds, cis 1,2-DCE and VC are not considered here because DCE concentrations in plume were below the detection limit or less than 5 ug/L and VC concentrations in plume were below the detection limit according to the field sampling data. As described earlier in the model application chapter, the groundwater Darcy velocity is about 8 m/yr and an average porosity is about 0.33. The source zone has dimensions of about X=8 m, Y=8 m and Z=3.5 m. The source is assumed to behave according to the power function with an exponent, Γ , of 1. The release was estimated to have occurred in 1967, the initial source mass is believed to be roughly 136 kg, and the initial source concentration is about 6 mg/L, leading to an initial source discharge of 1.3 kg of TCE per year.

The overall degradation rate of TCE in dissolved plume without remediation was estimated to be 0.125 yr^{-1} , which corresponds to a half life of 5.54 yr. The retardation factor was estimated to be 2, the longitudinal dispersivity is scale-dependent and was estimated to be 0.05 times the travel distance. The transverse dispersivity was 1/2.5 of the longitudinal dispersivity, and the vertical dispersivity was 1/50 of the longitudinal

dispersivity. A source remediation with a removal percentage of 85% and a plume PRB treatment with an enhanced degradation rate of 436 yr^{-1} (a half life of 13.93 hr) are considered here. Values of ten key parameters are shown in Table 5.1 as the base case. Base case refers to the deterministic site condition. Note here that only the longitudinal dispersivity parameter is shown in Table 5.1 because for the sensitivity analysis, the transverse and vertical dispersivity parameters are set as 1/2.5 and 1/50 of the longitudinal dispersivity parameter, respectively.

The plume evolution over time without any remediation is shown in Figure 5.1. The plume is defined by 5 ppb TCE concentration. From these two different time snapshots, it can be seen that this site behaves as a stable plume if there is not any remediation. The percentages of TCE mass remaining in the source zone are calculated to be about 74% after 30 years from the initial release and about 50% after 70 years from the initial release.

Table 5.1 Input parameters tested in sensitivity analysis (Case I).

Parameters	Base Case	Sensitivity Analysis	
		Distributions	Distribution Parameters
C_0 (mg/l)	6	Triangular	min=2, most likely=6, max=10
M_0 (kg)	136	Triangular	min=50, most likely=136, max=222
Γ	1	Log-normal	geo mean =1, geo stdv=2
X_{rem}	0.85	Beta	mean=0.85, stdv = 0.08, min=0.6, max=0.99
V_d (m/yr)	8	Normal	mean=8, stdv=2.5
ϕ	0.33	Triangular	min=0.28, most likely=0.33, max=0.41
R	2	Triangular	min=1.5, most likely=2, max=2.5
α_x	$x/20$	Triangular	min= $x/100$, most likely= $x/20$, max= $x/10$
λ_{TCE} (yr ⁻¹)	0.125	Triangular	min= 0.05, most likely= 0.125, max=0.2
λ_{TCE_rem} (yr ⁻¹)	436	Triangular	min=228, most likely=436, max=644

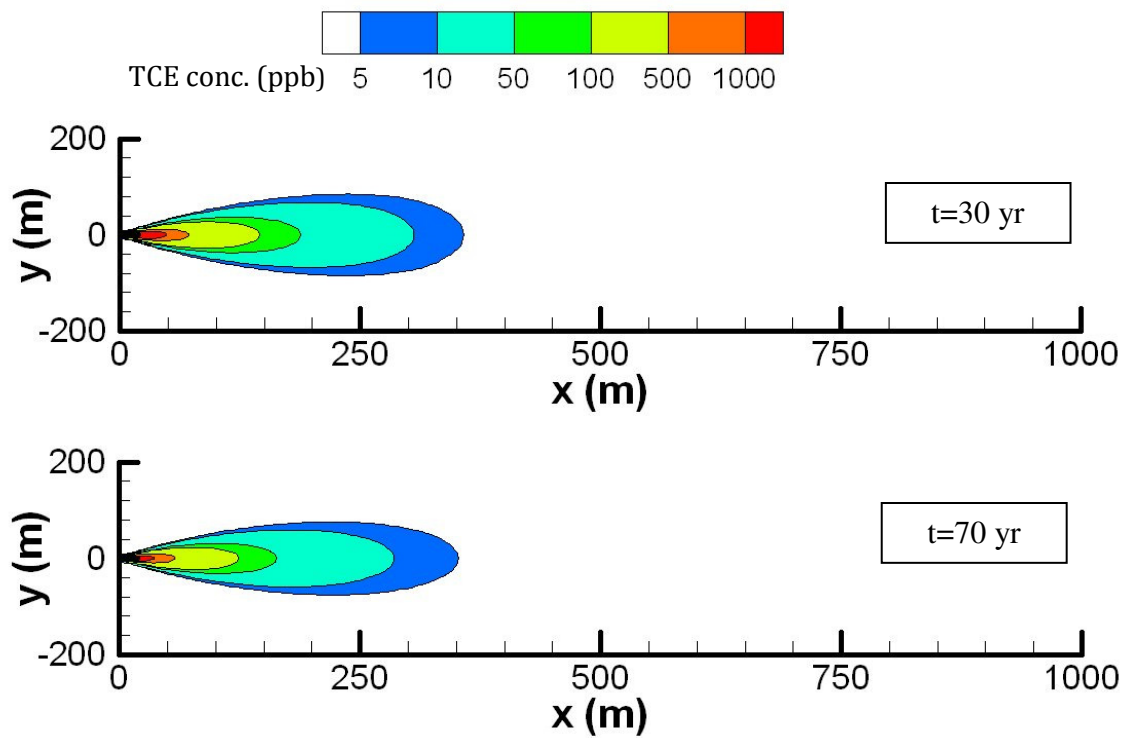


Figure 5.1 Plume evolution over time without remediation (Case I).

5.2.2 Sensitivity Analysis (Case I)

Based on the base case, ten probabilistic simulations are run for conducting sensitivity analysis. During each probabilistic simulation, the model samples the tested single input variable over its PDF, holding all of the other input variables constant using their base case values. The base case values and the PDF types and parameter values of tested input variables are shown in Table 5.1. The power function exponent (Γ) has a log-normal distribution, groundwater Darcy velocity (V_d) is assumed to have a normal distribution, and source removal fraction (X_{rem}) has a beta distribution. Several other input variables, including the initial source concentration (C_0), initial source mass (M_0), porosity (ϕ), retardation factor (R), longitudinal dispersivity parameter (α_x), plume overall degradation rate without remediation (λ_{TCE}), and plume treatment rate (λ_{TCE_rem}) for TCE are assumed to have the triangular distributions. The ranges of these distributions are estimated and the mean behavior keeps close to the base case. The exact distributions of tested input parameters are shown in Figure 5.2 & 5.3.

After all ten input variables are tested, the TCE concentration from different simulations are compared and presented in two ways. One way is to show the TCE concentration ranging from the 5th percentile to the 95th percentile due to the uncertainty in each tested input variable. As shown in Figure 5.4, TCE variations are plotted in a descending order from top to bottom (referred to as a Tornado chart [GoldSim User's Guide (v9.60), 2007]). The width of the range (horizontal bar) reflects the sensitivity of the TCE concentration to the input variable. Generally speaking, the wider of the range, the more sensitive the TCE concentration to that input variable.

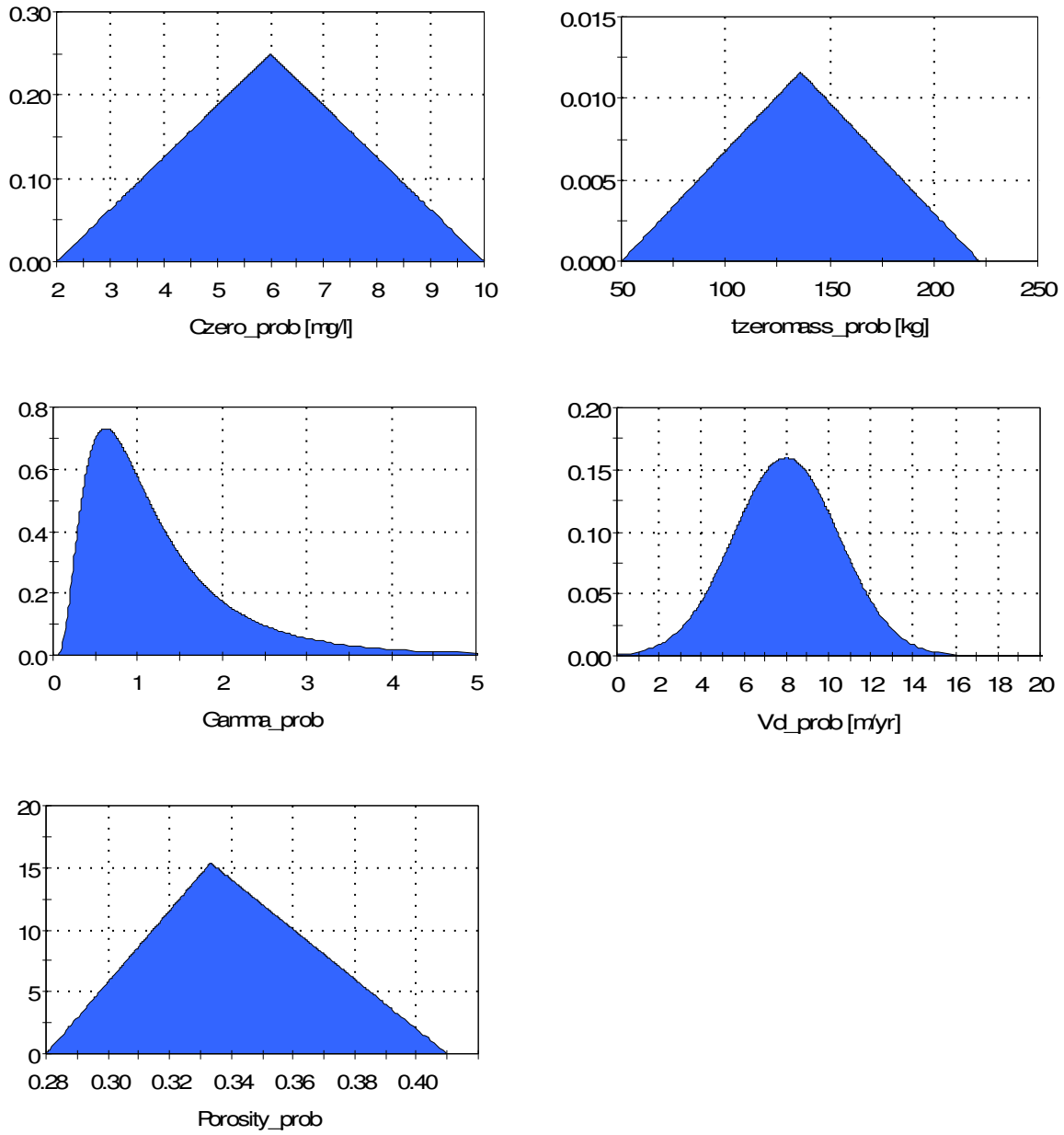


Figure 5.2 Distributions of input parameters: C_0 , M_0 , Γ , V_d , ϕ . (Case I).

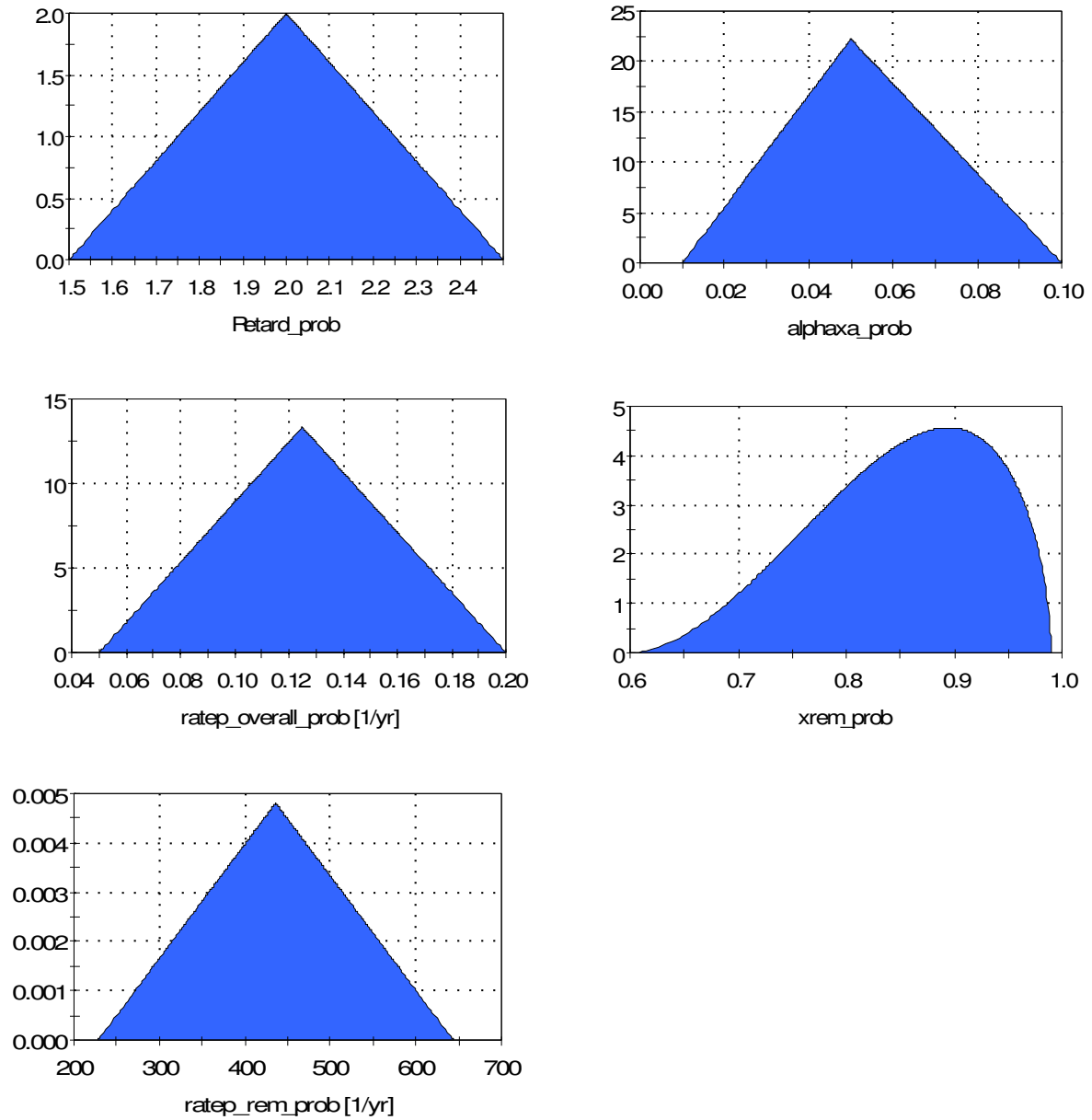


Figure 5.3 Distributions of input parameters (cont.): R , α_x , X_{rem} , λ_{TCE} , λ_{TCE_rem} . (Case I).

Case I: $x=100\text{m}, y=0\text{m}, z=0\text{m}, t=32\text{yr}$

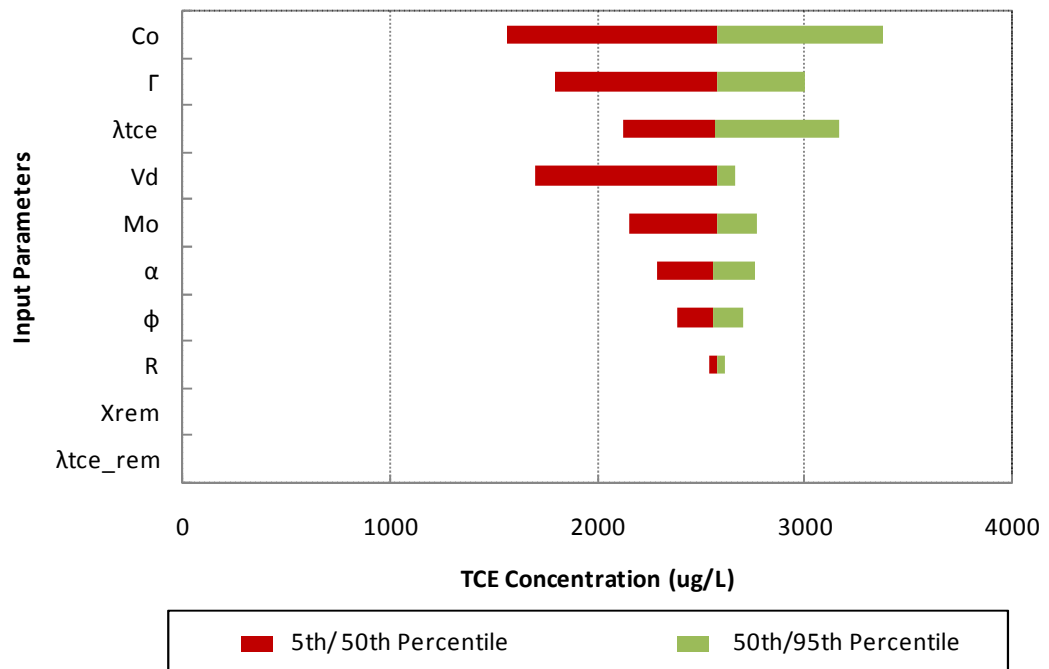


Figure 5.4 Tornado chart of TCE concentration variation at $x=100\text{m}$ and $t=32\text{ yr}$ (Case I).

TCE concentration variations at a distance of 100 m from the source and 32 years after the initial release are shown in Figure 5.4. It shows that TCE concentration is most sensitive to the initial source concentration (C_0), then to the power function exponent (Γ), Darcy velocity (V_d), plume overall degradation rate (λ_{TCE}), initial source mass (M_0), dispersivity parameter (α_L), porosity(ϕ) and retardation factor (R), in a descending order. It also shows that TCE concentration is not sensitive to the source removal fraction and the plume treatment rate, due to the fact that before and at the time of the 32nd yr, no remediation has been conducted.

Without any remediation effort, the contaminant mass concentration level in plume mainly depends on the contaminant concentration leaving the source zone, contaminant travel velocity, the plume overall degradation, and the dispersion processes. In this case, the TCE travel velocity and the plume overall degradation rate are relatively low, so the source concentration plays the key role. Source concentration is mainly determined by the initial source concentration and the power function exponent. The tested range of retardation factor is relatively small from 1.5 to 2.5, and TCE concentration shows the least sensitivity to it.

TCE concentrations at the same location (100 m) but at the time of 42 years, which is ten years from source remediation and plume PRB treatment, are shown in Figure 5.5 with two different scales. In Figure 5.5, the top chart uses a large scale which is the same as that used in Figure 5.4 for comparison purpose, while the bottom chart uses a smaller scale in order to more clearly show the concentration variations. Compared to the concentration variation before remediation (Figure 5.4), the variability of

concentration after remediation (top chart in Figure 5.5) shows a great reduction for all tested parameters. It indicates the remediation effort results in a large uncertainty reduction as well as a concentration reduction. For example, before the remediation (Figure 5.4), TCE concentration variation due to an uncertain Γ is from 1800 ug/L at the 5th percentile to 3000 ug/L at the 95th percentile. After the remediation (Figure 5.5), TCE concentration variation due to the same uncertain Γ is from 15 ug/L at the 5th percentile to 190 ug/L at the 95th percentile.

This Figure (bottom chart in figure 5.5) shows that TCE concentration is most sensitive to the power function exponent (Γ), then to the plume PRB treatment rate ($\lambda_{\text{TCE_rem}}$), source removal fraction (X_{rem}), Darcy velocity (V_d), retardation factor (R), initial source concentration (C_0), plume overall degradation rate (λ_{TCE}), initial source mass (M_0), porosity (ϕ) and dispersion parameter (α_L) in descending order.

Since this location (100m) is close to the plume PRB wall (89m) and the PRB treatment rate is very high (see Table 5.1), TCE concentration should be sensitive to the plume treatment rate and simulation results indicate this clearly. However, it is surprising that TCE concentration is most sensitive to the power function exponent. This is because the source behavior is described by the power function and the source remediation removed a large fraction of the source mass.

Another way to analyze the sensitivity is to compare the change of TCE concentration per unit change in input parameter. The input variables have different units and different absolute ranges. In order to compare them in a general way, the ratio of the 95th percentile to the 5th percentile of each input parameter is computed. This is then

done for the resulting TCE concentration (Table 5.2). If a large ratio of the TCE concentration (95th/5th percentiles) results from a small ratio of the input parameter (95th/5th percentiles), it indicates that the TCE concentration is very sensitive to that input parameter.

From top to bottom (Table 5.2), the parameters are ϕ , X_{rem} , R , λ_{TCE_rem} , λ_{TCE} , M_0 , C_0 , Vd , α_L , and Γ as the ratio of 95th/5th percentiles for each parameter increasing. At t=32 yr, C_0 has a ratio of 2.68 (95th/5th percentiles) and results in a ratio of 2.17 for TCE concentration, which is the largest ratio for TCE concentration. At the same time, Γ has a ratio of 9.88, which is the largest ratio among tested input parameters, and results in a ratio of 1.67 for TCE concentration. The change of TCE concentration per unit change in C_0 is greater than the change of TCE concentration per unit change in Γ , so TCE concentration is more sensitive to C_0 than Γ . This result is consistent with the TCE variation observation (Figure 5.4). At t=42 yr, Γ has a ratio of 9.88, which is the largest ratio among tested input parameters, and results in the largest ratio for TCE concentration with a value of 12.7, so TCE concentration is most sensitive to Γ . This agrees with the TCE variation observation (Figure 5.5).

Case: x=100m,y=0m,z=0m,t=42yr

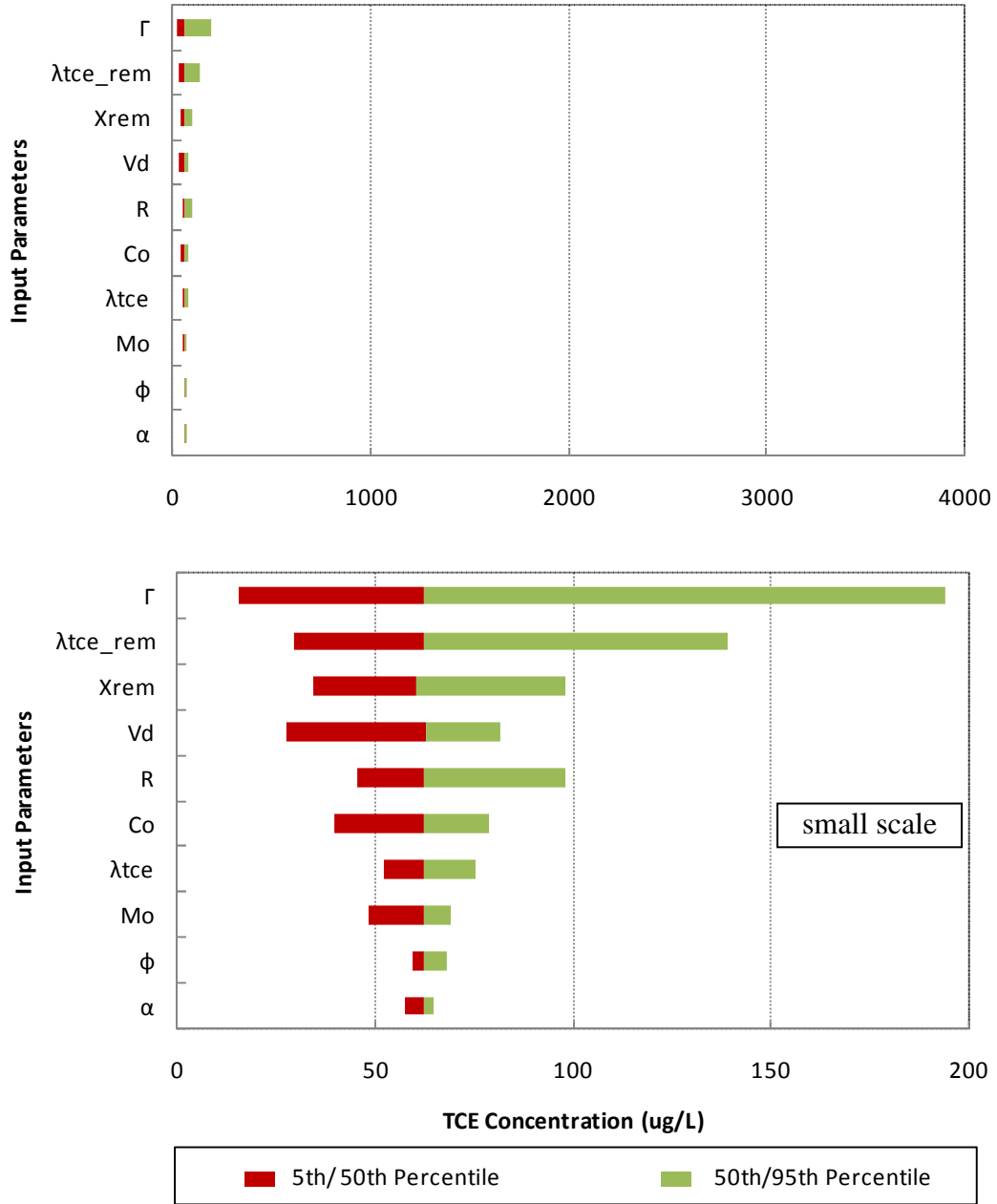


Figure 5.5 Tornado chart of TCE concentration variation at x=100m and t=42 yr (Case I).

Table 5.2 Ratio of 95th/5th percentiles for input parameters and resulting TCE concentration (Case I).

Input Parameters		TCE Concentration (95 th /5 th Percentiles)	
Name	95 th /5 th Percentiles	t=32yr	t=42yr
ϕ	1.30	1.13	1.14
X_{rem}	1.37	1.00	2.84
R	1.42	1.03	2.15
λ_{TCE_rem}	1.96	1.00	4.68
λ_{TCE}	2.41	1.49	1.44
M_0	2.55	1.29	1.42
C_0	2.68	2.17	1.99
V_d	3.14	1.57	2.94
α_s	3.63	1.20	1.13
Γ	9.88	1.67	12.70

5.3 Case II: Growing Plume Disconnected from the Source

5.3.1 Base Case Description (Case II)

In this case, a hypothetical 1,2-DCA site is used as the representative site to conduct the sensitivity analysis. It assumed that a 324 kg release of 1, 2-DCA occurred, with a groundwater Darcy velocity of 20 m/yr, and an average porosity of 0.33. The source zone has dimensions of X=10 m, Y=10 m and Z=3 m. The source is assumed to behave according to Equation (2), with an exponent, Γ , of 1. The release was assumed to have occurred in 1980, and the initial source concentration was 100 mg/l, leading to an initial source discharge of 60 kg of 1,2-DCA per year. The contaminant mass was flushed into plume quickly due to this high mass discharge.

1,2-DCA and its reductive dehalogenation daughter product, chloroethane (CA) were assumed to undergo natural attenuation with a degradation rate of 0.1 yr^{-1} , which corresponds to a half life of 6.93 yr. The compounds were specified a retardation factor of 2, the longitudinal dispersivity is scale-dependent and was equal to 0.01 times the travel distance. The transverse dispersivity was 1/10 of the longitudinal dispersivity, and the vertical dispersivity was 1/100 of the longitudinal dispersivity. Note here that only the longitudinal dispersivity parameter is shown in the table 5.3.

A source remediation with a removal percentage of 90% was assumed to be conducted ten years after the initial release. The source remediation period was one year. An enhanced reductive dechlorination for 1,2-DCA and CA conducted in the first 200 m from the 10th yr to the 30th yr. 1,2-DCA and CA shared same enhanced degradation rate of 1 yr^{-1} , which yields a half life of 0.69 yr.

The plume evolution over time without any remediation is shown in Figure 5.6. The plume is defined by 1 ppb total contaminant concentration. It can be seen that plume starts growing fast after the initial release, and eventually detaches from the source zone due to the high source discharge. The percentage of 1,2-DCA mass remaining in the source zone is estimated to be about 16% after ten years from the initial release and about 3% after 20 years from the initial release.

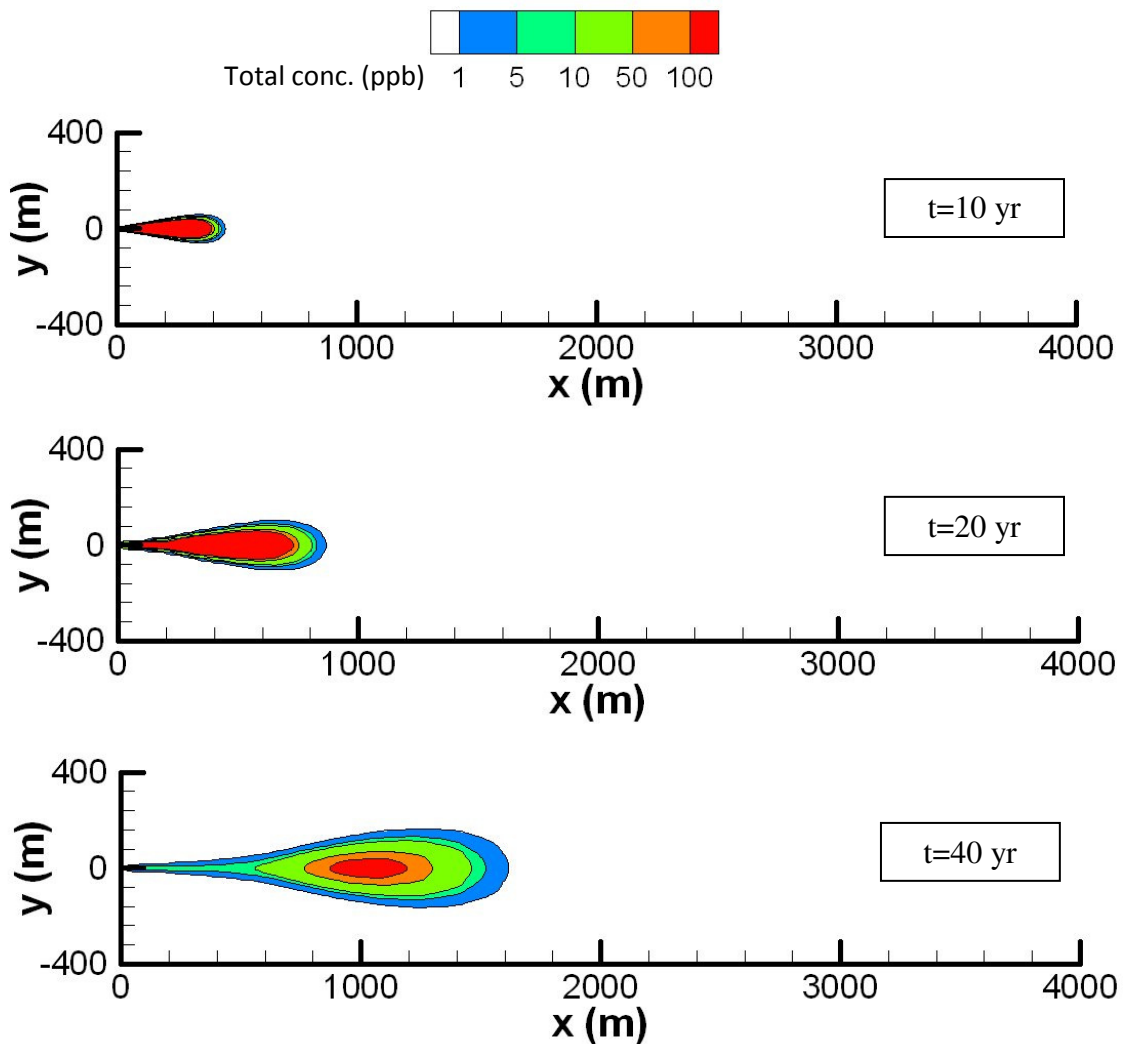


Figure 5.6 Plume evolution over time without remediation (Case II).

Table 5.3 Input parameters tested in sensitivity analysis (Case II).

Parameters	Base Case	Sensitivity Analysis	
		Distributions	Distribution Parameters
C_0 (mg/l)	100	Triangular	min=50, most likely=100, max=150
M_0 (kg)	324	Triangular	min=162, most likely=324, max=486
Γ	1	Log-normal	geo mean =1, geo stdv=1.52
X_{rem}	0.9	Beta	mean=0.9, stdv = 0.0, min=0.7, max=0.99
V_d (m/yr)	20	Normal	mean=20, stdv=3
ϕ	0.33	Triangular	min=0.28, most likely=0.33, max=0.41
R	2	Triangular	min=1.5, most likely=2, max=2.5
α_x	x/100	Triangular	min=x/200, most likely=x/100, max=x/67
λ (yr ⁻¹)	0.1	Triangular	min= 0.05, most likely= 0.1, max=0.15
λ_{rem} (yr ⁻¹)	1	Triangular	min=0.5, most likely=1, max=1.5

5.3.2 Sensitivity Analysis (Case II)

The sensitivity analysis is conducted in the similar way as in Case I. The target variable is the centerline total contaminant mass concentration in the plume and same ten input variables are tested. As shown in Table 5.3, the distribution types of tested input parameters are the same as in Case I but values and ranges are different except for the porosity and retardation factor. The ranges of these distributions are estimated and the mean behavior keeps close to the base case.

After all ten input variables are tested, the total concentration from different simulations are compared and presented in a similar way as in Case I. The Tornado chart of the total concentration variation at a distance of 250 m from the source and at the 10th yr after the initial release is shown in Figure 5.7. As discussed before, the width of the range (horizontal bar) reflects the sensitivity of the total concentration to the input variable. The total concentration is mostly sensitive to Darcy velocity (V_d), then to the initial source concentration (C_0), power function exponent (Γ), porosity (ϕ), retardation factor (R), initial source mass (M_0), dispersion parameter (α_L) and plume overall degradation rate (λ) in a descending order. It also shows that total concentration is not sensitive to the source removal fraction (X_{rem}) and plume treatment rate (λ_{rem}). This agrees with the fact that before and at the time of 10nd yr, no remediation has been conducted.

At a distance of 250 m, the moving front has not arrived when $t=10$ yr for some low values of V_d , and the contaminant concentration is very low. On the other hand, for some high values of V_d , the moving front has arrived or passed this location at same time,

Case II: x=250m, y=0m, z=0m, t=10yr

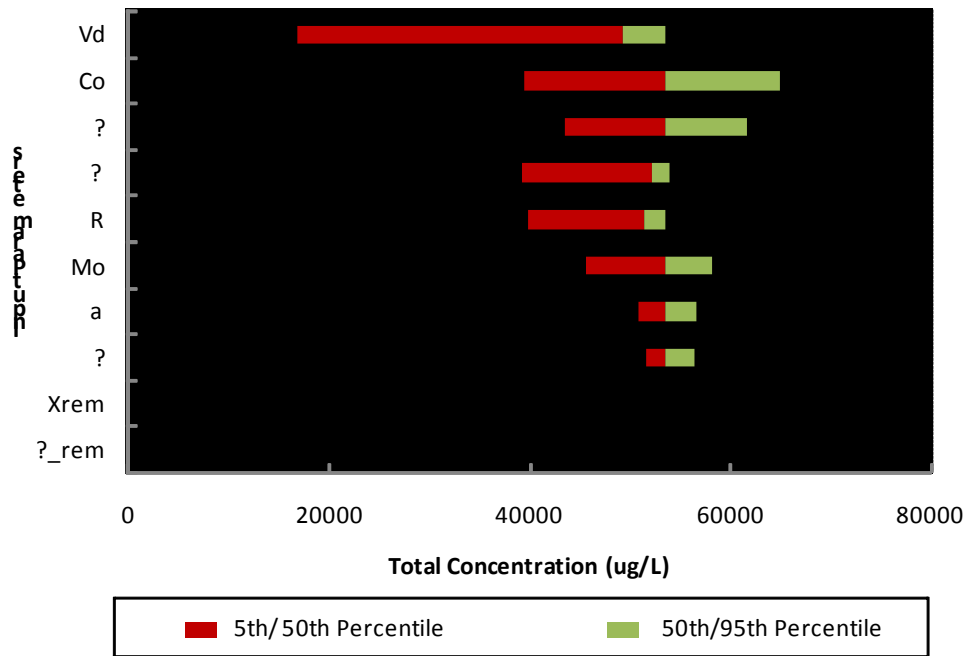


Figure 5.7 Tornado chart of total concentration variation at x=250m and t=10 yr (Case II).

and contaminant mass concentration is relatively high. Combining the effects of low V_d and high V_d results in the largest variation in the concentration. As discussed in Case I, without any remediation effort, the contaminant mass concentration in the plume mainly depends on the initial source concentration (C_0) and the power function exponent (Γ), so concentration is sensitive to these two parameters following the Darcy velocity. Porosity (ϕ) and retardation factor (R) also show some sensitivity because they affect the contaminant travel velocity. The dispersion parameter (α_L) with a low value does not affect the centerline concentration much, and it shows little sensitivity. The plume overall degradation rate (λ) is relatively low, and it shows the least sensitivity.

The Tornado chart of the total concentrations variation at the same location (250m) but at the 20th yr, which is 10 years from the source and plume remediation, is shown in Figure 5.8 with two different scales. In Figure 5.8, the top chart uses a large scale which is the same as in Figure 5.7 for comparison purposes, and the bottom chart uses a small scale in order to more clearly show the concentration variation. Compared to the concentration variation before remediation (Figure 5.7), the overall uncertainty of the concentration after remediation (top chart in Figure 5.8) shows a great reduction for all tested parameters. It indicates the remediation effort results in a large uncertainty reduction as well as a concentration reduction.

Shown in the bottom chart in Figure 5.8, the total concentration is mostly sensitive to the Darcy velocity (V_d), then to the retardation factor (R), porosity (ϕ), plume treatment rate (λ_{rem}), initial source mass (M_0), power function exponent (Γ), source removal fraction (X_{rem}), initial source concentration (C_0), dispersivity parameter (α_L), and

the plume overall degradation rate (λ) in the descending order. After the source and plume remediation, the total concentration at $x=250\text{m}$ is greatly affected by chemical travel velocity. At $t=20$ yr, about 97% of the initial source mass is flushed into the plume, so source parameters play a less important role in the plume concentration. α_L and λ are relatively low, so they affect the plume concentration in a low degree.

The ratios of 95th/5th percentiles for total concentration and corresponding input variables are computed as in Table 5.4. From top to bottom, input parameters are X_{rem} , ϕ , R , V_d , λ , λ_{rem} , α_L , C_0 , M_0 and Γ as the ratio of 95th/5th percentiles for each parameter increasing. At $t=10$ yr, V_d has a ratio of 1.66 (95th/5th percentiles) and results in a ratio of 3.18 for the total concentration, which is the largest ratio for the total concentration. At the same time, C_0 has a ratio of 2.04, which is larger than V_d ratio, and results in a ratio of 1.65 for the total concentration. The change of total concentration per unit change in V_d is greater than that per unit change in C_0 , so the total concentration is more sensitive to V_d than C_0 . This result is consistent with the total concentration variation observation (Figure 5.7). At $t=20$ yr, V_d results in the largest ratio for the total concentration with a value of 16.19, so the total concentration is most sensitive to V_d . This agrees with the total concentration variation observation (Figure 5.8).

Case II: $x=250\text{m}$, $y=0\text{m}$, $z=0\text{m}$, $t=20\text{yr}$

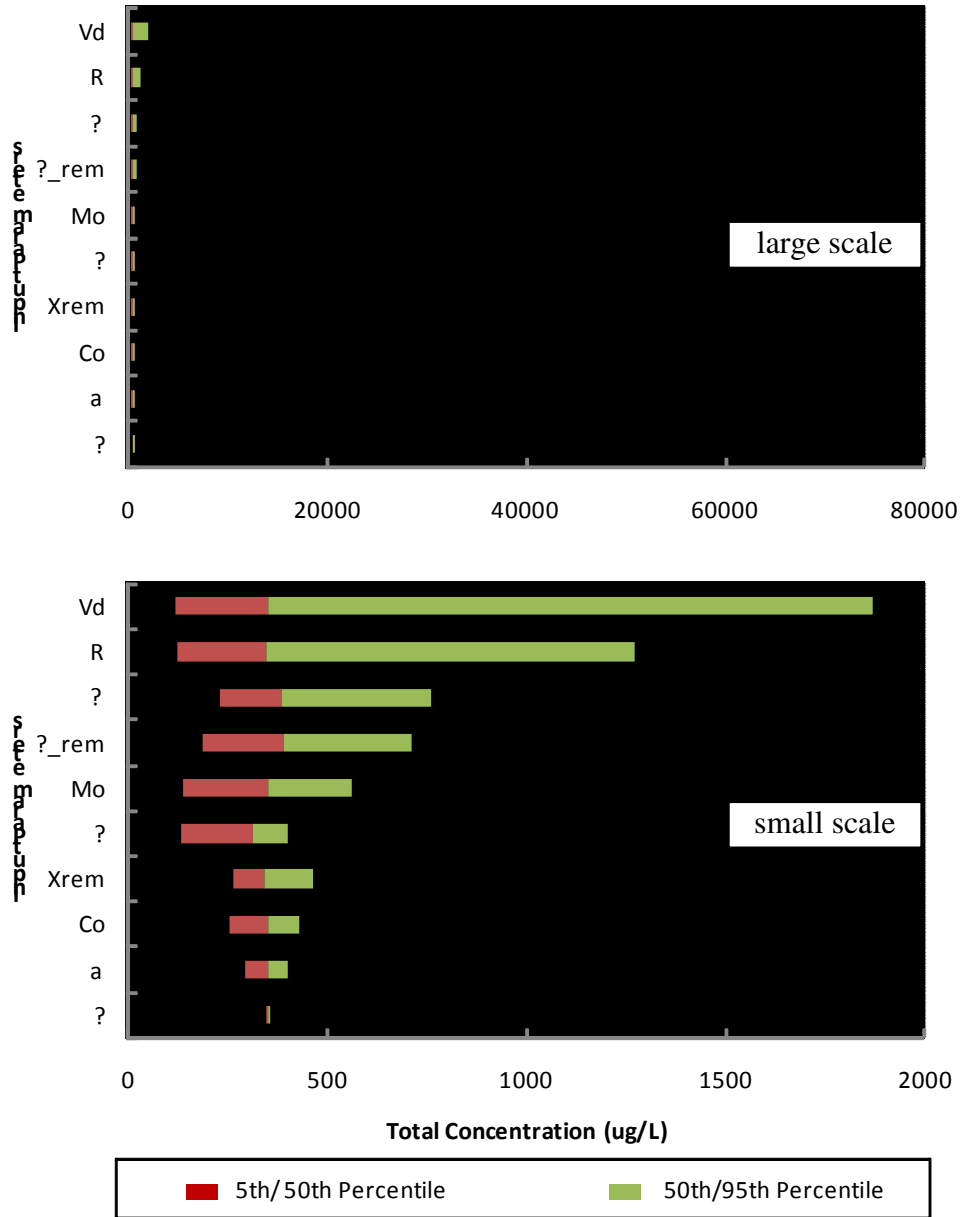


Figure 5.8 Tornado chart of total concentration variation at $x=250\text{m}$ and $t=25\text{yr}$ (Case II).

Table 5.4 Ratio of 95th/5th percentiles for input parameters and resulting total concentration (Case II).

Input Parameters		Total Concentration (95 th /5 th Percentiles)	
Name	95 th /5 th Percentiles	t=10yr	t=20yr
X_{rem}	1.20	1.00	1.76
ϕ	1.30	1.37	3.31
R	1.42	1.34	10.25
V_d	1.66	3.18	16.19
λ	2.03	1.09	1.01
λ_{rem}	2.03	1.00	3.82
α_x	2.04	1.11	1.38
C_0	2.04	1.65	1.69
M_0	2.06	1.28	4.09
Γ	3.99	1.42	3.05

5.4 Case III: Growing Plume Connected to the Source

5.4.1 Base Case Description (Case III)

In this case, a hypothetical complex PCE site based on the example in Falta [2008] is used as the representative site to conduct the sensitivity analysis. It assumed a 1620 kg release of PCE from the source zone, The groundwater Darcy velocity is 10 m/yr, and the average porosity is 0.33. The source zone has dimensions of X=10 m, Y=10 m and Z=3 m. The source behaves according to the power function, with an exponent, Γ , of 1. The release was assumed to have occurred in 1975, and the initial source concentration was 100 mg/l, leading to an initial source discharge of 30 kg of PCE per year [Falta, 2008].

PCE and its daughter products, TCE, DCE and VC were assumed to undergo natural attenuation. According to Wiedemeier et al. [1999], the typical values of the first-order sequential decay rate is 0.07 ~ 1.2 yr⁻¹ for PCE, 0.05 ~ 10.9 yr⁻¹ for TCE, 0.18 ~ 13.3 yr⁻¹ for cis-1, 2-DCE, and 0.12 ~ 2.16 yr⁻¹ for VC. In the model, the degradation rate of PCE was set to 0.4 yr⁻¹, TCE was set to 0.15 yr⁻¹, DCE was set to 0.1 yr⁻¹ and VC was set to 0.2 yr⁻¹[Falta, 2008]. These background degradation rates are low and would represent a weak attenuation site condition [Wiedemeier et al. 1999; Aziz et al. 2002]. The compounds were specified a retardation factor of 2, the longitudinal dispersivity is scale-dependent and was equal to 0.005 times the travel distance. The transverse dispersivity was 1/10 of the longitudinal dispersivity, and the vertical dispersivity was 1/100 of the longitudinal dispersivity. Note here that only the longitudinal dispersivity parameter is shown in the table 5.5.

The EPA drinking water standards for PCE, TCE, DCE, and VC are 5, 5, 70, and 2 ug/L, respectively. VC is a well known human carcinogen and may cause cancer (http://www.epa.gov/TEACH/chem_summ/VC_summary.pdf). Therefore remediation is focused on managing the VC plume and the VC concentration is set to be the target variable during the sensitivity analysis. Source remediation with a removal percentage of 90% of PCE was assumed to be conducted 30 years after the initial release. The source remediation period was one year.

It is known that PCE and TCE degradation may be enhanced through the reductive dechlorination, while DCE and VC degradation may be enhanced through the aerobic process downgradient from the reductive dechlorination zone [Wiedemeier et al. 1999; NRC 2000; Alvarez and Illman 2006]. In the model, plume treatment includes an enhanced reductive dechlorination for PCE and TCE in the first 200 m and an enhanced aerobic degradation for DCE and VC from 200 m to 500 m. Following Falta [2008], the PCE decay rate was increased from 0.4 yr^{-1} to 1.4 yr^{-1} (a half life from 1.73 yr to 0.5 yr) and TCE decay rate was increased from 0.15 yr^{-1} to 1.5 yr^{-1} (a half life from 4.62 yr to 0.46 yr) in the first 200 m only. The decay rate of DCE was enhanced from 0.1 yr^{-1} to 3.5 yr^{-1} (a half life from 6.93 yr to 0.2 yr), and VC decay rate was increased from 0.2 yr^{-1} to 3.6 yr^{-1} (a half life from 3.47 to 0.19 yr) from 200 m to 500 m only. The plume treatment started at the same time when source remediation started and the treatment period is 30 years for both the enhanced reductive dechlorination of PCE and TCE in the first 200 m, and the enhanced aerobic degradation for DCE and VC from 200 m to 500 m.

The plume evolution over time without any remediation is shown in Figure 5.9. The plume is defined by 1ppb as the VC concentration. It can be seen that VC plume continues growing as the source mass is flushed into plume continuously and the parent-daughter reactions occur. The percentage of PCE mass remaining in the source zone is estimated to be about 57% after 30 years from the initial release, about 33% after 60 years, and 19% after 90 years from the initial release.

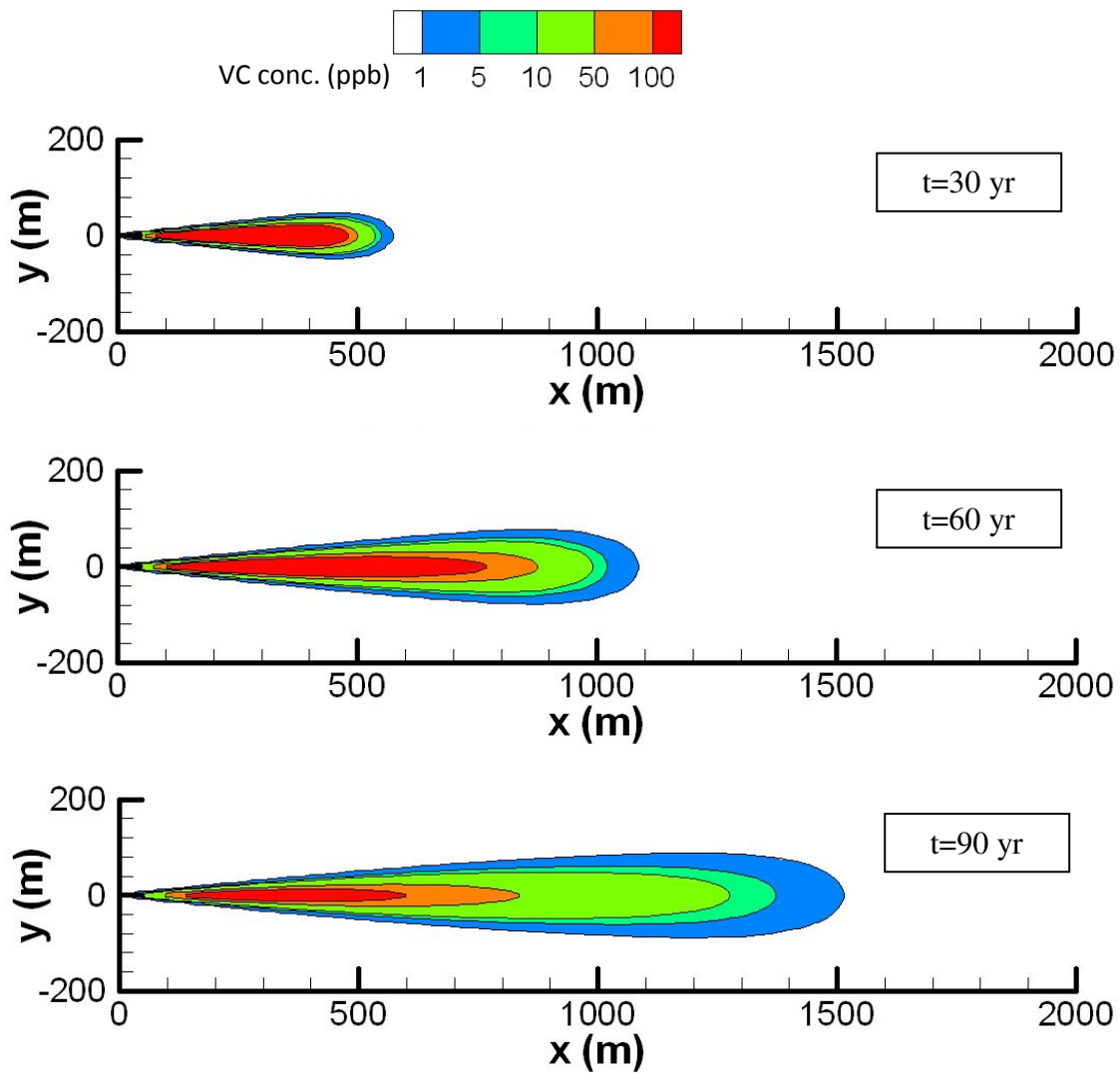


Figure 5.9 Plume evolution over time without remediation (Case III).

Table 5.5 Input parameters tested in sensitivity analysis (Case III).

Parameters	Base Case*	Sensitivity Analysis	
		Distributions	Distribution Parameters
C_0 (mg/l)	100	Triangular	min=33, most likely=100, max=167
M_0 (kg)	1620	Triangular	min=540, most likely=1620, max=2700
Γ	1	Log-normal	geo mean =1, geo stdv=1.52
X_{rem}	0.9	Beta	mean=0.9, stdv = 0.05, min=0.7, max=0.99
V_d (m/yr)	10	Normal	mean=10, stdv=2
ϕ	0.33	Triangular	min=0.25, most likely=0.33, max=0.45
R	2	Triangular	min=1.5, most likely=2, max=2.5
α_x	x/200	Triangular	min=x/500, most likely=x/200, max=x/125
λ_{PCE} (yr ⁻¹)	0.4	Triangular	min= 0.13, most likely= 0.4, max=0.67
λ_{TCE} (yr ⁻¹)	0.15	Triangular	min= 0.05, most likely= 0.15, max=0.25
λ_{DCE} (yr ⁻¹)	0.1	Triangular	min= 0.03, most likely= 0.1, max=0.17
λ_{VC} (yr ⁻¹)	0.2	Triangular	min= 0.07, most likely= 0.2, max=0.33
$\lambda_{PCE_{rem}}$ (yr ⁻¹)	1.4	Triangular	min= 0.47, most likely= 1.4, max=2.33
$\lambda_{TCE_{rem}}$ (yr ⁻¹)	1.5	Triangular	min= 0.5, most likely= 1.5, max=2.5
$\lambda_{DCE_{rem}}$ (yr ⁻¹)	3.5	Triangular	min= 1.17, most likely= 3.5, max=5.83
$\lambda_{VC_{rem}}$ (yr ⁻¹)	3.6	Triangular	min=1.2, most likely=3.6, max=6

* base case values from Falta [2008].

5.4.2 Sensitivity Analysis (Case III)

The sensitivity analysis is conducted in the similar way as in previous cases. The target variable is the VC concentration at a distance of 300m from the source along the centerline. A total of 16 input parameters are tested in this case. The source parameters and transport parameters, C_0 , M_0 , Γ , X_{rem} , V_d , ϕ , R and α_L , are tested. The natural degradation rates and enhanced decay rates are different for four compounds, so these decay rates are tested separately. The natural degradation rates for PCE, TCE, DCE and VC are labeled as λ_{PCE} , λ_{TCE} , λ_{DCE} and λ_{VC} , respectively, and they are applied to entire plume. The enhanced decay rates for PCE and TCE are labeled as λ_{PCE_rem} and λ_{TCE_rem} , respectively, and they are applied to the first 200 m only. The enhanced decay rates for DCE and VC are labeled as λ_{DCE_rem} and λ_{VC_rem} , respectively, and they are applied to from 200 m to 500 m only. The distributions and exact values are shown in Table 5.5. The ranges of these distributions are estimated and the mean behavior keeps close to the base case.

After all 16 input parameters are tested, the VC concentration from different simulations are compared and presented in a similar way as in the previous cases. The Tornado chart of the VC concentration variation at a distance of 300 m from the source and at the 30th yr after the initial release is shown in Figure 5.10. It can be seen that the VC concentration is most sensitive to the Darcy velocity (V_d), then to the initial source concentration (C_0), DCE natural degradation rate (λ_{DCE}), porosity (ϕ), natural degradation rate of TCE (λ_{TCE}), VC (λ_{VC}), and PCE (λ_{PCE}), and then to power function exponent (Γ), initial source mass (M_0), retardation factor (R) and dispersion parameter

Case III: $x=300\text{m}$, $y=0\text{m}$, $z=0\text{m}$, $t=30\text{yr}$

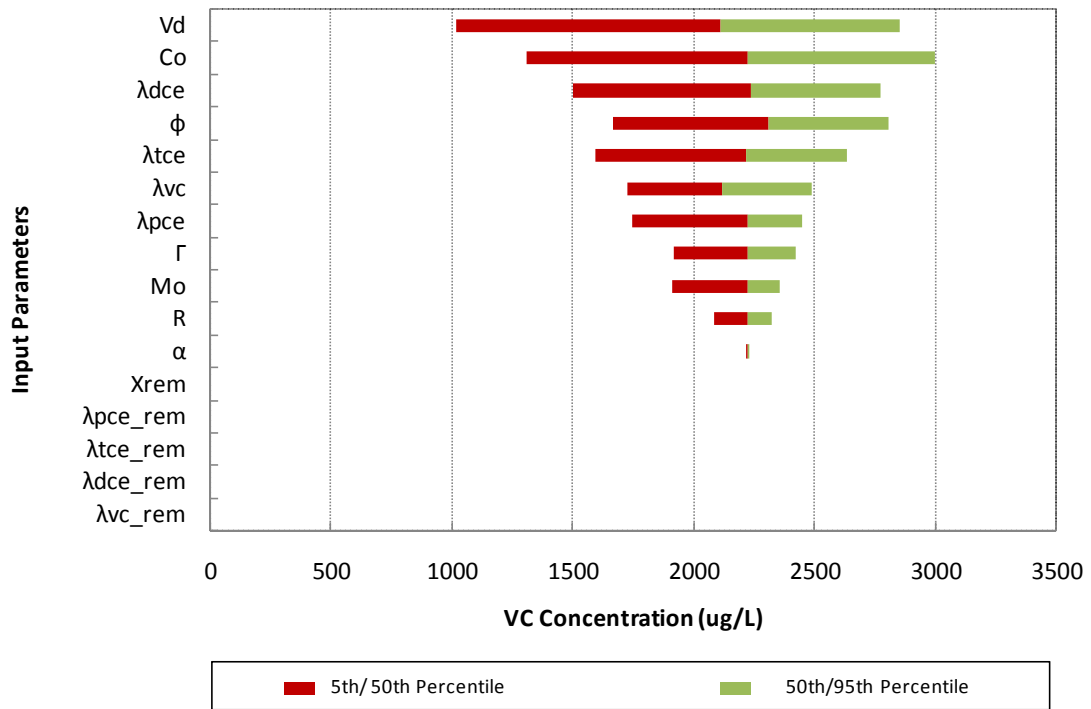


Figure 5.10 Tornado chart of VC concentration variation at $x=300\text{m}$ and $t=30\text{ yr}$ (Case III).

(α_L) in descending order. Since there is no remediation conducted before this time, VC concentration is not affected by either the source removal fraction or the plume treatment rates.

The influence of V_d , ϕ , C_0 and Γ has been discussed in previous cases. The biggest influence posed by V_d is partly due to the fact that the moving front has not arrived because of some low velocities. From Figure 5.10, it can be seen that parent and daughter natural degradation rates play different roles in the VC concentration. VC is directly yielded from DCE, so the DCE natural degradation rate (λ_{DCE}) shows a very strong influence on the VC concentration. DCE is yielded from TCE, so TCE natural degradation (λ_{TCE}) also shows a big influence on VC concentration. Obviously, VC concentration is also dependent on its own degradation rate (λ_{VC}). As the ultimate parent, PCE degradation rate (λ_{PCE}) also shows influence on VC concentration. The dispersion parameter (α_L) was small and it shows the least influence.

The Tornado chart of the VC concentration variation at the same location (300 m) but at the 55th yr, which is 25 years from the source and plume remediation, is shown in Figure 5.11. By comparing the scales used in Figure 5.10 and Figure 5.11, it can be seen that the overall uncertainty of VC concentration after remediation (Figure 5.13) shows a great reduction for all 16 tested parameters by approximately three orders of magnitude. It indicates the remediation effort results in a large uncertainty reduction as well as a concentration reduction.

Case III: $x=300\text{m}$, $y=0\text{m}$, $z=0\text{m}$, $t=55\text{yr}$

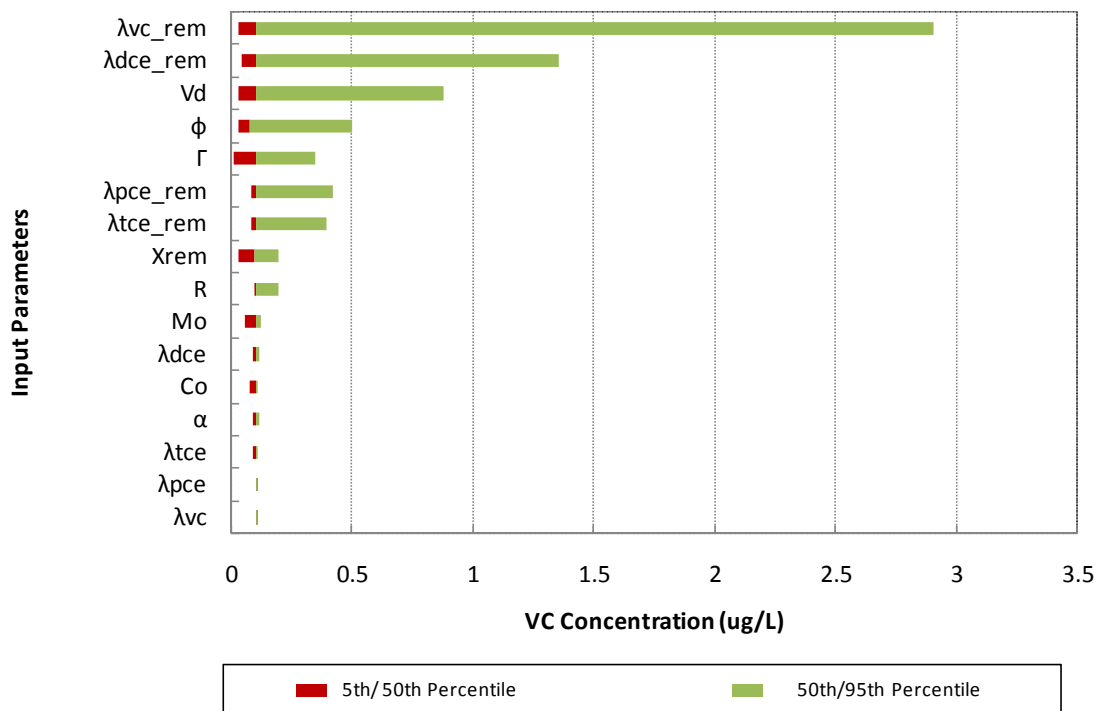


Figure 5.11 Tornado chart of VC concentration variation at $x=300\text{m}$ and $t=55\text{ yr}$ (Case III).

Shown in Figure 5.11, the VC concentration is mostly sensitive to its own treatment rate (λ_{VC_rem}), then to the DCE enhanced degradation rate (λ_{DCE_rem}), Darcy velocity (V_d), porosity (ϕ), power function exponent (Γ), PCE enhanced degradation rate (λ_{PCE_rem}), TCE enhanced degradation rate (λ_{TCE_rem}), source removal fraction (X_{rem}), retardation factor (R), initial source mass (M_0), DCE natural degradation rate (λ_{DCE}), initial source concentration (C_0), dispersion parameter (α_L), TCE natural degradation rate (λ_{TCE}), PCE natural degradation rate (λ_{PCE}), and VC natural degradation rate (λ_{VC}) in descending order.

From Table 5.4, it can be seen that the VC decay rate is increased by a factor of 18 (from 0.2 yr^{-1} as the natural decay rate to 3.6 yr^{-1} for the mean behavior) from 200 m to 500m for a treatment period of 20 years (from a time of 30 years to 50 years). The observed VC concentration is at a time of 10 years after this enhanced biodegradation of VC and a distance of 300 m, Ten years after this enhanced VC degradation, a large reduction of VC concentration is expected in the treated zone. The tested range of VC enhanced decay rate (λ_{VC_rem}) is from 1.2 yr^{-1} to 6 yr^{-1} , combining the effects of both the low and high ends of λ_{VC_rem} , it plays the biggest role on the VC concentration.

The pathway of PCE reductive dechlorination is $\text{PCE} \rightarrow \text{TCE} \rightarrow \text{DCE} \rightarrow \text{VC}$. VC is directly yielded from DCE, so the DCE enhanced degradation rate (λ_{DCE_rem}) shows a very strong influence on the VC concentration. The higher λ_{DCE_rem} , the more VC yielded from DCE. TCE yields DCE and PCE is the ultimate parent, so λ_{PCE_rem} and λ_{TCE_rem} also affect the VC concentration greatly. V_d and ϕ contribute to the chemical travel velocity, so they effect the VC concentration greatly.

Following the enhanced parent/daughter degradation rates and transport parameters, source parameters, C_0 , Γ , M_0 , and the source removal fraction (X_{rem}) show certain influence on the VC concentration. Among those, Γ plays the bigger role than X_{rem} , M_0 , and C_0 . It is surprising that Γ , X_{rem} , M_0 , and C_0 show relatively less importance on VC concentration. This observation can be explained by the fact that in the source zone, only the ultimate parent PCE is present. Source parameters play important role on the PCE concentration. However, there are two breakdown products between PCE and VC, so Γ , M_0 , and C_0 are relatively less important to the VC concentration. The source remediation removed some fraction of PCE source mass, the effect of PCE mass removal on the VC concentration is relatively smaller than enhanced parent/daughter degradation rates and transport parameters. Nonetheless, the influence of X_{rem} on the VC concentration is greater than R , M_0 , λ_{DCE} , C_0 , α_L , λ_{TCE} , λ_{PCE} , and λ_{VC} . The parent/daughter natural degradation rates are low, so they show less importance to the VC concentration.

The ratios of 95th/5th percentiles for total concentration and corresponding input variables are computed as in Table 5.6. From top to bottom, input parameters are X_{rem} , R , ϕ , V_d , α_L , λ_{VC} , $\lambda_{DCE_{rem}}$, $\lambda_{TCE_{rem}}$, $\lambda_{PCE_{rem}}$, λ_{TCE} , C_0 , λ_{PCE} , $\lambda_{VC_{rem}}$, M_0 , λ_{DCE} and Γ as the ratio of 95th/5th percentiles for each parameter increasing. At $t=30$ yr, V_d has a ratio of 1.99 (95th/5th percentiles) and results in a ratio of 2.81 for the VC concentration, which is the largest ratio for the VC concentration. At the same time, C_0 has a ratio of 2.7, which is larger than V_d ratio, and results in a ratio of 2.29 for the VC concentration. The change of the VC concentration per unit change in V_d is greater than that per unit change in C_0 ,

so the VC concentration is more sensitive to V_d than C_0 . This result is consistent with the VC concentration variation observation (Figure 5.10).

At $t=55$ yr, λ_{VC_rem} , which has a ratio of 2.7 (95th/5th percentiles), results in the largest ratio for the VC concentration with a value of 88.55 (95th/5th percentiles), so the total concentration is most sensitive to λ_{VC_rem} . This agrees with the total concentration variation observation (Figure 5.11). At $t=55$ yr, λ_{DCE_rem} has a ratio of 2.64 (95th/5th percentiles) and results in a ratio of 29.12 for the VC concentration. At the same time, Γ has a ratio of 3.99 and results in a ratio of 39.24 for the VC concentration. The change of the VC concentration per unit change in λ_{DCE_rem} is greater than that per unit change in Γ , so the VC concentration is more sensitive to λ_{DCE_rem} than Γ . This also is consistent with the VC concentration variation observation (Figure 5.11).

Based on the sensitivity analysis from above three different cases, it is found that degree of the influence of different input parameters on the plume response are not equal. The observations for three plume types are summarized in Table 5.7. For a stable plume that is connected to the source and a growing plume that is disconnected from the source, the parent compound concentration or the total concentration in the downgradient plume is primarily sensitive to the initial source concentration, the power function exponent, the plume degradation rate, and the chemical travel velocity, which is determined by groundwater Darcy velocity, porosity and retardation factor. For a growing plume that is connected to the source, the concentration of a daughter compound (VC) is greatly affected by its degradation rate, the degradation rate of its direct parent (DCE) and transport parameters. For this case, source parameters are less important compared to

enhanced parent/daughter degradation rates and transport parameters. Nonetheless, the power function exponent affects the VC concentration greatly and source removal fraction plays more important role than several other parameters.

It is also observed that for all three different plume types, the overall uncertainty of contaminant mass concentration is reduced greatly by remediation effort as well as the concentration itself. The reduction can be in several orders magnitude. Such sensitivity analysis would be useful in terms of finding out key parameters that affect remediation effectiveness, thereafter to support to select or determine the remediation alternatives.

Table 5.6 Ratio of 95th/5th percentiles for input parameters and resulting VC concentration (Case III).

Input Parameters		VC Concentration (95 th /5 th Percentiles)	
Name	95 th /5 th Percentiles	t=30yr	t=55yr
X_{rem}	1.20	1.00	6.37
R	1.42	1.12	2.09
ϕ	1.50	1.68	16.88
V_d	1.99	2.81	26.65
α_x	2.39	1.01	1.34
λ_{VC}	2.60	1.44	1.01
$\lambda_{DCE_{rem}}$	2.64	1.00	29.12
$\lambda_{TCE_{rem}}$	2.64	1.00	4.65
$\lambda_{PCE_{rem}}$	2.65	1.00	5.07
λ_{TCE}	2.68	1.65	1.15
C_0	2.70	2.29	1.48
λ_{PCE}	2.70	1.40	1.01
$\lambda_{VC_{rem}}$	2.70	1.00	88.55
M_0	2.71	1.23	2.15
λ_{DCE}	2.81	1.85	1.37
Γ	3.99	1.26	39.24

Table 5.7 Summary of sensitivity analysis for three plume types.

Sensitivity	Case I		Case II		Case III	
	Before remediation	After remediation	Before remediation	After remediation	Before remediation	After remediation
Most	C_0	Γ	V_d	V_d	V_d	λ_{vc_rem}
	Γ	λ_{tce_rem}	C_0	R	C_0	λ_{dce_rem}
	λ_{tce}	X_{rem}	Γ	ϕ	λ_{dce}	V_d
	V_d	V_d	ϕ	λ_{rem}	ϕ	ϕ
	M_0	R	R	M_0	λ_{tce}	Γ
	α_x	C_0	M_0	Γ	λ_{vc}	λ_{pce_rem}
	ϕ	λ_{tce}	α_x	X_{rem}	λ_{pce}	λ_{tce_rem}
	R	M_0	λ	C_0	Γ	X_{rem}
	X_{rem}	ϕ	X_{rem}	α_x	M_0	R
	λ_{tce_rem}	α_x	λ_{rem}	λ	R	M_0
					α_x	λ_{dce}
					X_{rem}	C_0
					λ_{pce_rem}	α_x
					λ_{tce_rem}	λ_{tce}
					λ_{dce_rem}	λ_{pce}
Least					λ_{vc_rem}	λ_{vc}

CHAPTER 6

SUMMARY AND CONCLUSIONS

In this research, a new probabilistic remediation model, Probabilistic Remediation Evaluation Model for Chlorinated solvents sites (PREMChlor), has been developed. This is achieved through linking the analytical model REMChlor to a Monte Carlo modeling simulation package GoldSim via a FORTRAN Dynamic Link Library (DLL) application. PREMChlor can simultaneously evaluate the effectiveness of source and plume remediation considering uncertainties in all major parameters. In PREMChlor, all of the key input parameters, including source parameters, transport parameters and remediation parameters, are treated as uncertain parameters represented by probability density functions (PDFs). The outputs from the PREMChlor model, including contaminant mass concentration, contaminant mass discharge, cancer risk posed by a contaminant over time at a specific location and remediation costs, are also probability distributions and probability statistics. Such results are much more useful to decision-makers who utilize the simulation results.

PREMChlor considers common technologies for DNAPL source removal, including thermal treatments, surfactant/cosolvent flooding, chemical oxidation/reduction and enhanced bioremediation. Also considered are dissolved plume treatments, mainly enhanced biodegradation and permeable reactive barriers (PRBs). In the PREMChlor model, graphical user interfaces have been built to allow other users to easily enter the input values, run the model and view the results. A license-free GoldSim player file

containing the graphical user interface has been generated to make the PREMChlor model available to potential users who are not familiar with details of the probabilistic model and the GoldSim simulation environment.

This probabilistic simulation model has been applied to a TCE plume in a shallow aquifer at a manufacturing plant. The calibrated model using a deterministic approach is able to match the pre-remediation site conditions. Probabilistic simulations predicting the effects of remediation show that the overall uncertainty in TCE concentration propagates over time by given uncertainties in seven key input parameters: the initial source concentration, initial source mass, power function exponent, Darcy velocity, overall plume degradation rate, source removal efficient, and the plume PRB treatment rate. The probabilistic simulations capture most uncertainties in key parameters and reflect the site conditions based on estimated PDFs.

The PREMChlor model has also been used to conduct the sensitivity analyses by assessing the influence or relative importance of each important input parameter on the contaminant mass concentration for three different plume types. It is found that the degree of the influence of different input parameters on the plume response vary widely. For both a stable plume that is connected to the source and a growing plume that is disconnected from the source, the parent compound concentration or the total concentration in the plume is highly sensitive to the initial source concentration, the power function exponent, the plume degradation rate, and the chemical travel velocity, which is determined by groundwater Darcy velocity, porosity and retardation factor. For a growing plume that is connected to the source, the concentration of a daughter

compound (VC) is greatly affected by its degradation rate, the degradation rate of its direct parent (DCE) and the transport parameters. For this case, source parameters are less important compared to enhanced parent/daughter degradation rates and transport parameters. Nonetheless, the power function exponent affects the VC concentration greatly and source removal fraction plays more important role than several other parameters.

It is also observed that for all three different plume types, the overall uncertainty of contaminant mass concentration is reduced greatly by remediation effort as well as the concentration itself. The reduction can be in several orders magnitude. Such sensitivity analysis would be useful in terms of finding out key parameters that affect remediation effectiveness, thereafter to support to select or determine the remediation alternatives.

Based on the earlier discussion and the above summary, the following conclusions are made:

- A probabilistic remediation model, Probabilistic Remediation Evaluation Model for Chlorinated solvents sites (PREMChlor), has been developed. PREMChlor can simultaneously evaluate the effectiveness of source and plume remediation considering the inherent uncertainties in all major parameters.
- This probabilistic model can quickly simulate different combinations of source and plume remediation scenarios to find a robust remediation design considering uncertainties in input parameters.

- The calibrated model using a deterministic approach has been shown to closely match the pre-remediation condition at a real TCE site.
- The PREMChlor model is capable of capturing uncertainties in key parameters and reflecting the site conditions based on the estimated PDFs.
- For both a stable plume that is connected to the source and a growing plume that is disconnected from the source, the parent compound concentration or the total concentration in plume is greatly sensitive to the initial source concentration, the power function exponent, the plume degradation rate, and the chemical travel velocity.
- For a growing plume that is connected to the source, the concentration of a daughter compound (VC) is greatly affected by its degradation rate, the degradation rate of its direct parent (DCE) and the transport parameters. Source parameters are less important compared to enhanced parent /daughter degradation rates and the transport parameters. Nonetheless, the power function exponent and the source removal fraction plays more important role than several other parameters.
- For all three plume types considered in this study, the overall uncertainty of contaminant mass concentration is reduced greatly by remediation efforts as well as the contaminant mass concentration. The reduction can be in several orders of magnitudes.

APPENDIX

FORTRAN DLL Source Code

```
c---modify source plume function to generate dll to link it to GoldSim, 5/7/07, liang
c Analytical solution for advection, retardation and decay with variable
c source concentration, including remediation. Plume rates are stepwise variable
c in space (x) and time.
c Falta 7/29/05
c Input variables -----
c
c czero = initial source zone concentration, kg/m^3 or g/l
c tzeromass= initial source zone mass, kg
c gamma = exponent on mass vs conc. relationship: C/Co=(M/Mo)^gamma
c xremove = fraction of source mass removed (remediated) between times t1 and t2
c t1 = time when remediation starts, yr
c t2 = time when remediation ends, yr
c
c rates = source zone decay rate const. due to processes other than flushing, 1/yr
c ysource = source width, m
c zsource = source thickness, m
c vd=darcy velocity, m/yr
c
c porosity = porosity (effective)
c retard = retardation factor
c sigmav = standard deviation of normalized pore velocity (vbar=1), dimensionless
c vmin = minimum normalized velocity (>+=0), dimensionless
c vmax = maximum normalized velocity, dimensionless
c ntubes = number of stream tubes considered
c alphax = transverse dispersivity, m. If alphax<0, transverse dispersivity is scale
c dependent, with a value of abs(alphax)*x
c alphaz = vertical dispersivity, m (one-direction only). If alphaz<0, vertical
c dispersivity is scale dependent, with a value of abs(alphaz)*x
c
c x1 = length of zone 1 for plume decay rate (m)
c x2 = length of zone 2 for plume decay rate (m)
c
c tplume1 = length of period 1 for plume decay, y
c tplume2 = length of period 2 for plume decay, y
c
c slopef(1) = lifetime cancer risk oral slope factor for component 1, risk per (mg/kg) per day
c slopef(2) = lifetime cancer risk oral slope factor for component 2, risk per (mg/kg) per day
c slopef(3) = lifetime cancer risk oral slope factor for component 3, risk per (mg/kg) per day
c slopef(4) = lifetime cancer risk oral slope factor for component 4, risk per (mg/kg) per day
c
c slopefh(1) = lifetime cancer risk inhalation slope factor for component 1, risk per (mg/kg) per day
c slopefh(2) = lifetime cancer risk inhalation slope factor for component 2, risk per (mg/kg) per day
c slopefh(3) = lifetime cancer risk inhalation slope factor for component 3, risk per (mg/kg) per day
c slopefh(4) = lifetime cancer risk inhalation slope factor for component 4, risk per (mg/kg) per day
c
c yield21 = yield of daughter 2 from parent 1, 1 is ultimate parent
```

```

c yield32 = yield of daughter 3 from parent 2
c yield43 = yield of daughter 4 from parent 3
c
c **** For Component 1, the ultimate parent compound *****
c ratep(1,1,1) = plume decay rate const. in zone 1, period 1 1/yr
c ratep(1,1,2) = plume decay rate const. in zone 1, period 2 1/yr
c ratep(1,1,3) = plume decay rate const. in zone 1, period 3 1/yr
c
c ratep(1,2,1) = plume decay rate const. in zone 2, period 1 1/yr
c ratep(1,2,2) = plume decay rate const. in zone 2, period 2 1/yr
c ratep(1,2,3) = plume decay rate const. in zone 2, period 3 1/yr
c
c ratep(1,3,1) = plume decay rate const. in zone 3, period 1 1/yr
c ratep(1,3,2) = plume decay rate const. in zone 3, period 2 1/yr
c ratep(1,3,3) = plume decay rate const. in zone 3, period 3 1/yr
c
c **** For Component 2, the first daughter compound *****
c ratep(2,1,1) = plume decay rate const. in zone 1, period 1 1/yr
c ratep(2,1,2) = plume decay rate const. in zone 1, period 2 1/yr
c ratep(2,1,3) = plume decay rate const. in zone 1, period 3 1/yr
c
c ratep(2,2,1) = plume decay rate const. in zone 2, period 1 1/yr
c ratep(2,2,2) = plume decay rate const. in zone 2, period 2 1/yr
c ratep(2,2,3) = plume decay rate const. in zone 2, period 3 1/yr
c
c ratep(2,3,1) = plume decay rate const. in zone 3, period 1 1/yr
c ratep(2,3,2) = plume decay rate const. in zone 3, period 2 1/yr
c ratep(2,3,3) = plume decay rate const. in zone 3, period 3 1/yr
c
cc **** For Component 3, the second daughter compound *****
c ratep(3,1,1) = plume decay rate const. in zone 1, period 1 1/yr
c ratep(3,1,2) = plume decay rate const. in zone 1, period 2 1/yr
c ratep(3,1,3) = plume decay rate const. in zone 1, period 3 1/yr
c
c ratep(3,2,1) = plume decay rate const. in zone 2, period 1 1/yr
c ratep(3,2,2) = plume decay rate const. in zone 2, period 2 1/yr
c ratep(3,2,3) = plume decay rate const. in zone 2, period 3 1/yr
c
c ratep(3,3,1) = plume decay rate const. in zone 3, period 1 1/yr
c ratep(3,3,2) = plume decay rate const. in zone 3, period 2 1/yr
c ratep(3,3,3) = plume decay rate const. in zone 3, period 3 1/yr
c
cc **** For Component 4, the final (third) daughter compound *****
c ratep(4,1,1) = plume decay rate const. in zone 1, period 1 1/yr
c ratep(4,1,2) = plume decay rate const. in zone 1, period 2 1/yr
c ratep(4,1,3) = plume decay rate const. in zone 1, period 3 1/yr
c
c ratep(4,2,1) = plume decay rate const. in zone 2, period 1 1/yr
c ratep(4,2,2) = plume decay rate const. in zone 2, period 2 1/yr
c ratep(4,2,3) = plume decay rate const. in zone 2, period 3 1/yr

```

```

c
c  ratep(4,3,1) = plume decay rate const. in zone 3, period 1 1/yr
c  ratep(4,3,2) = plume decay rate const. in zone 3, period 2 1/yr
c  ratep(4,3,3) = plume decay rate const. in zone 3, period 3 1/yr
c
c
c  nx = number of x locations
c  xmin = min x, m
c  xmax = max x, m
c
c
c  ny = number of y locations
c  ymin = min y, m
c  ymax = max y, m
c
c
c  nz = number of z locations
c  zmin = min z (not less than zero), m
c  zmax = max z, m
c
c
c  nt = number of times
c  tmin = min time, years
c  tmax = max time, years
c
c
cc----head for GoldSim, Liang
      subroutine source_plume_streamtube_chain (method, state, in, out)

!DEC$ ATTRIBUTES dllexport, c  :: source_plume_streamtube_chain
!DEC$ ATTRIBUTES value        :: method
!DEC$ ATTRIBUTES reference :: state
!DEC$ ATTRIBUTES reference :: in
!DEC$ ATTRIBUTES reference :: out

cc----declare variable method for GoldSim, Liang *****
cc  common/tran/tres(3,3),retard,velp,x1,x2,tplume1,tplume2
      Integer(4) method, state
      real in(*), out(*)
      real tres(3,3)
      real retard, velp,x1,x2,tplume1,tplume2
      real ratep(4,3,3)
      real weight(5000),vel(5000),treact(5),rate1(5),rate2(5),rate3(5),
      &rate4(5),conc1(5),conc2(5),conc3(5),conc4(5),slopef(4), slopefh(4)
cc---reduce 3D array to scalar due to taking off x,y and z loops, liang
      real fy,fz,concc1,concc2,concc3,concc4,concn1,concn2,concn3,
      &concn4
      real czero,tzeromass,gamma,xremove,t1,t2,rates,
      &ysource,zsource,vd,porosity,sigmav,vmin,vmax,
      &alphay,alphaz,yield21,yield32,yield43,
      &xmin,xmax,ymin,ymax,zmin,zmax,tmin,tmax,t,x
      real sumdishch1, sumdishch2,sumdishch3,sumdishch4
      real csource,dischtot

```

```

real concn1t(5000),concn2t(5000),concn3t(5000),concn4t(5000)

cc *****
cc Initialize, report version for GoldSim, liang
cc *****
  if (method.eq.0) then      !Initialize
    continue
  elseif (method.eq.2) then  !Report version
    out(1) = 1.0
cc---Dummy output file for error messages
  open (unit=15, file='FortranDLLoutput.txt')
  elseif (method.eq.3) then  !Report arguments
    out(1) = 74              !74 incoming arguments
    out(2) = 15             !15 outgoing argument: at one single x,y,z
  elseif (method.eq.1) then  !Calculate
cc---Assign values from GoldSim inputs to 74 input parameters in Fortran, liang
    czero = in(1)
    tzeromass = in(2)
    gamma = in(3)
    xremove = in(4)
    t1 = in(5)
    t2 = in(6)
    rates = in(7)
    ysource = in(8)
    zsource = in(9)
    vd = in(10)
    porosity = in(11)
    retard = in(12)
    sigmav = in(13)
    vmin = in(14)
    vmax = in(15)
    ntubes = in(16)
    alphay = in(17)
    alphaz = in(18)
    x1 = in(19)
    x2 = in(20)
    tplume1 = in(21)
    tplume2 = in(22)
    do i=1,4
      slopef(i)=in(i+22)
      slopefh(i)= in(i+26)
    end do
    yield21 = in(31)
    yield32 = in(32)
    yield43 = in(33)
    do k=1,3
      ratep(1,1,k) = in(k+33)
      ratep(1,2,k) = in(k+36)
      ratep(1,3,k) = in(k+39)

```

```

        ratep(2,1,k) = in(k+42)
        ratep(2,2,k) = in(k+45)
        ratep(2,3,k) = in(k+48)
        ratep(3,1,k) = in(k+51)
        ratep(3,2,k) = in(k+54)
        ratep(3,3,k) = in(k+57)
        ratep(4,1,k) = in(k+60)
        ratep(4,2,k) = in(k+63)
        ratep(4,3,k) = in(k+66)
    end do
    t = in(70)
    x = in(71)
    y = in(72)
    z = in(73)
    deltt = in(74)
c   end of 74 inputs
c
c-----adjust parameters that lead to singulatities in solution
c   eps is a numerical "zero" that is very small
c
    eps=1.e-4
        eps2=1.e-6
        eps3=0.01
c-----when gamma=.5, mass and Cs can "rebound" from zero
    if (gamma.eq.0.5) gamma=0.5+eps2
c-----solution is singular for gamma=1. Avoid values very close to 1
    if (abs(1.-gamma).le.eps3) gamma=1.+eps3
        if (rates.lt.eps2) rates=eps2
        if (t1.eq.t2) t2=t1+eps
c-----avoid very small transverse dispersivities
    if (abs(alphay).lt.eps2) alphay=eps2
    if (abs(alphaz).lt.eps2) alphaz=eps2
c
c-----the plume rate constants must be unique from each other in each x,t space
c
    do 500 i=1,3
        do 600 j=1,3
            if (ratep(1,i,j).eq.ratep(2,i,j)) ratep(1,i,j)=ratep(1,i,j)+eps
            if (ratep(1,i,j).eq.ratep(3,i,j)) ratep(1,i,j)=ratep(1,i,j)+eps
                if (ratep(1,i,j).eq.ratep(4,i,j)) ratep(1,i,j)=ratep(1,i,j)+eps
                    if(ratep(2,i,j).eq.ratep(3,i,j)) ratep(2,i,j)=ratep(2,i,j)+1.5*eps
                    if(ratep(2,i,j).eq.ratep(4,i,j)) ratep(2,i,j)=ratep(2,i,j)+1.5*eps
                    if(ratep(3,i,j).eq.ratep(4,i,j)) ratep(3,i,j)=ratep(3,i,j)+2.5*eps
        c
        600 continue
    500 continue
c
c
cc----take off x,y and z loops, liang
c ----- compute the Domenico terms fy, fz for transverse and vertical dispersion

```

```

c ---- these are now done outside of time loop since they only depend on x,y,z 8/24
c   x loop
cc  do 701 i=1,nx
cc    x=((xmax-xmin)/(nx-1))*(i-1)+xmin
cc  xx(i)=x
c-----allow for scale dependent transverse dispersion falta 7/19/07
  alphay=alphay
    if (alphay.lt.0.) alphay=abs(alphay)*x
    alphaz=alphaz
    if(alphaz.lt.0.) alphaz=abs(alphaz)*x
c **** y loop
cc  do 702, j=1,ny
cc    if (ny.gt.1) y=((ymax-ymin)/(ny-1))*(j-1)+ymin
cc    if (ny.eq.1) y=(ymax+ymin)/2.
cc    yy(j)=y
c-----calculate y dispersion
c
  d1=(y+ysource/2.)/(2.*sqrt(alphay*x))
  d2=(y-ysource/2.)/(2.*sqrt(alphay*x))
cc  fy(i,j)=.5*(erf(d1)-erf(d2))
  fy=.5*(erf(d1)-erf(d2))
c 702 continue
c
c **** z loop
c
cc  do 703, k=1,nz
c
cc  deltz=(zmax-zmin)/nz
cc    z=deltz/2.+(k-1)*deltz
cc    zz(k)=z
c
c-----calculate z dispersion
  e1=(z+zsource)/(2.*sqrt(alphaz*x))
  e2=(z-zsource)/(2.*sqrt(alphaz*x))
cc  fz(i,k)=.5*(erf(e1)-erf(e2))
  fz=.5*(erf(e1)-erf(e2))

c 703 continue
c 701 continue

c
cc  take off time loop, liang
c  calculate time step for calculation and for risk assessment integral
c    deltt=(tmax-tmin)/nt
c
c  assume a 30 year exposure period for risk assessment integral
c
c  nriskt=30./deltt
c  sums used in risk assessment integral for average conc

```

```

c  sumc1=0.
c      sumc2=0.
c      sumc3=0.
c      sumc4=0.
c
c
c----- This part for source function remains unchanged --- 7/29
c-----source area
      area=ysource*zsource
c-----pore velocity -- this is now the average pore velocity 8/5/
      vp=vd/porosity
c
c%%%%%%%%%%%%%%%%%%%%%%%%%%%%%%%%%%%%%%%%%%%%%%%%%%%%%%%%%%%%%%%%%%%%%%%%
c%%%%%%%%%%%%%%%%%%%%%%%%%%%%%%%%%%%%%%%%%%%%%%%%%%%%%%%%%%%%%%%%%%%%%%%%
c Calculate stream tube statistics: weights and velocities, using a
c normally distributed velocity field
c
      deltav=(vmax-vmin)/ntubes
c
      do 301 i=1,ntubes
c      these are all normalized velocities where vave=vp
          vlow=vmin+(i-1)*deltav
          vhigh=vlow+deltav
          arglow=(vlow-1.)/(sigmav*sqrt(2.))
          arghigh=(vhigh-1.)/(sigmav*sqrt(2.))
c --- use erf relationship to integral of PDF from Abramowitz and Stegun
          problow=0.5*(1.+erf(arglow))
          probhigh=0.5*(1.+erf(arghigh))
          weight(i)=probhigh-problow
c      this is the actual velocity for the streamtube of weight(i)
          vel(i)=vp*((vlow+vhigh)/2.)
c
      301 continue

c%%%%%%%%%%%%%%%%%%%%%%%%%%%%%%%%%%%%%%%%%%%%%%%%%%%%%%%%%%%%%%%%%%%%%%%%
c%%%%%%%%%%%%%%%%%%%%%%%%%%%%%%%%%%%%%%%%%%%%%%%%%%%%%%%%%%%%%%%%%%%%%%%%
c*****
c calculate constants used in source function
c constants for t<t1
c
      cs4a=vd*area*czero
      cs4b=rates*tzeromass**gamma
      if(cs4b.eq.0) cs4b=eps2
      cs4=cs4a/cs4b
      cs3=tzeromass**(1.-gamma)
      cs2=-cs4
      cs6=1./(1.-gamma)
c

```



```

c mass remaining at t1
c
  cs5=(gamma-1.)*rates*t1
  arg=cs2+(cs3+cs4)*expd(cs5)
  if(arg.lt.0.) arg=0.
  t1mass=arg**cs6
c
c mass at t2 following remediation
c
  t2mass=(1.-xremove)*t1mass
c
c check to make sure t2mass < no remediation case
c
  cs5norem=(gamma-1.)*rates*t2
  argnorem=cs2+(cs3+cs4)*expd(cs5norem)
  if(argnorem.lt.0.) argnorem=0.
  t2massnorem=argnorem**cs6
c   if(t2massnorem.lt.t2mass) then
c     print *, ' natural remediation is faster than specified removal',
c     & ' IGNORE SOURCE REMEDIATION !!!!!!!!!!!!!!!'
c     & ' program terminating execution'
c     stop
c   endif
c
c concentration at t2
  if(tzeromass.gt.0.) then
    ctwo=czero*(t2mass/tzeromass)**gamma
  else
    ctwo=0.
  endif
c
c constants used in source function for t>t2
c
  css4a=vd*area*ctwo
  css4b=rates*t2mass**gamma
  if(css4b.eq.0.) css4b=eps2
  css4=css4a/css4b
  css3=t2mass**(1.-gamma)
  css2=-css4
c
c*****
cc time loop*****
cc assign value for t from GoldSim, so no need of time loop, liang
c*****
c   do 100, l=1,nt
c     t=deltt*l
c     tt(l)=t
c*****
c x loop *****

```



```

c
c
c ***** now identify the non-zero residence time zones
c   This is needed for the parent-daughter reactions
c   These are stored in order -- nreact=1 is first,
c   nreact=2 is second, up to max of nreact=5
c
c   Also store corresponding reaction rates in a local array raten(nreact)
c
c   nreact=0
c     do 90 m=1,3
c       do 91 n=1,3
c
c         if(tres(m,n).gt.0.) then
c           nreact=nreact+1
c           treat(nreact)=tres(m,n)
c
c
c----- divide these local rates by retard so simplify solution (assumes reaction only in water)
c       rate1(nreact)=ratep(1,m,n)/retard
c       rate2(nreact)=ratep(2,m,n)/retard
c       rate3(nreact)=ratep(3,m,n)/retard
c       rate4(nreact)=ratep(4,m,n)/retard
c     endif
91 continue
90 continue
c
c   nreacttot=nreact
c
c
c   now construct solutions
c   start with reaction zone 1, and proceed to reaction zone nreacttot
c
c!!!!!!! reactor loop !!!!!!!
c*****
c   do 110 nr=1,nreacttot
c     first reactor uses csource for c1(0), zero for c2(0),c3(0), c4(0)
c     if(nr.eq.1) then
c
c       conc1(1)=csource*exp(-rate1(1)*treact(1))
c
c       conc2(1)=csource*f2(rate1(1),rate2(1),yield21,treact(1))
c
c       conc3(1)=csource*f3(rate1(1),rate2(1),rate3(1),yield32,yield21,
c       & treact(1))
c
c       conc4(1)=csource*f4(rate1(1),rate2(1),rate3(1),rate4(1),
c       & yield43,yield32,yield21,treact(1))
c
c     endif
c

```

```

c   for second and subsequent reactors, use nr-1 concentrations as c(0)
c
c   if(nr.gt.1) then
c
c       conc1(nr)=conc1(nr-1)*exp(-rate1(nr)*treact(nr))
c
c       conc2(nr)=conc1(nr-1)*f2(rate1(nr),rate2(nr),yield21,treact(nr))+
& conc2(nr-1)*exp(-rate2(nr)*treact(nr))
c
c       conc3(nr)=conc1(nr-1)*f3(rate1(nr),rate2(nr),rate3(nr),yield32,
& yield21,treact(nr))+conc2(nr-1)*f2(rate2(nr),rate3(nr),yield32,
& treact(nr))+conc3(nr-1)*exp(-rate3(nr)*treact(nr))
c
c       conc4(nr)=conc1(nr-1)*f4(rate1(nr),rate2(nr),rate3(nr),rate4(nr),
& yield43,yield32,yield21,treact(nr))+conc2(nr-1)*f3(rate2(nr),
& rate3(nr),rate4(nr),yield43,yield32,treact(nr))+conc3(nr-1)*f2(
& rate3(nr),rate4(nr),yield43,treact(nr))+
& conc4(nr-1)*exp(-rate4(nr)*treact(nr))
c
c       endif
c ***** end of reactor loop *****
110 continue
c
c***** get partial contribution from streamtube
c   plume concentration in ug/l
c
c   tube1=weight(j)*conc1(nreacttot)*1.e6
c       tube2=weight(j)*conc2(nreacttot)*1.e6
c       tube3=weight(j)*conc3(nreacttot)*1.e6
c       tube4=weight(j)*conc4(nreacttot)*1.e6
c
c they are all zero ahead of the front
c   if (x.gt.velp*t/retard) then
c       tube1=0.0
c       tube2=0.
c       tube3=0.
c       tube4=0.
c   endif
c----- sum up the weighted streamtubes
c
c       sumtubes1=sumtubes1+tube1
c       sumtubes2=sumtubes2+tube2
c       sumtubes3=sumtubes3+tube3
c       sumtubes4=sumtubes4+tube4
c
c-----discharge calculations -- discharge from each tube
c
c   dischtube1=porosity*area*velp*weight(j)*conc1(nreacttot)
c   dischtube2=porosity*area*velp*weight(j)*conc2(nreacttot)
c   dischtube3=porosity*area*velp*weight(j)*conc3(nreacttot)

```



```

cc  end if
cc  end if
cc  end if
cc  54 Format (A2,f8.3)
c
c---- concentrations with transverse and vertical dispersion
cc----reduce 3D array to scalar for concen1/2/3/4 due to taking off x, y and z loops, liang
    concen1=sumtubes1*fy*fz
        concen2=sumtubes2*fy*fz
        concen3=sumtubes3*fy*fz
        concen4=sumtubes4*fy*fz
    conctot=concen1+concen2+concen3+concen4
c
c---- output
cc  print 51, x,y,z,concen1,concen2,concen3,concen4,conctot
cc
cc  51 format (f8.3,1x,f8.3,1x,f8.3,5(1x,e12.6))
cc  write (12,52) t,',x,',y,',z,',
cc  & concen1,',concen2,',concen3,',concen4,',conctot
cc  52 format(f8.3,A1,f8.3,A1,1x,f8.3,A1,1x,f8.3,5(A1,1x,e12.6))

c
c---- write concentrations to an array for use in risk calculations
cc----reduce 3D array to scalar for concc1/2/3/4 due to taking off x, y and z loops, liang
c  now concc1=concen1
    concc1=concen1
        concc2=concen2
        concc3=concen3
        concc4=concen4

c
c*****
c***  end z loop
c*****
c 450 continue
c*****
c  end y loop
c*****
c 350 continue
c
c*****
c  end x loop
c*****
c
c 200 continue
c
c- -- compute average conc at each x-y location for risk calc.
c  average concentration values over well
cc----take off x,y and z loops, liang
cc  do 921 i=1,nx
cc      do 922 j=1,ny

```

```

        sum1z=0.
        sum2z=0.
        sum3z=0.
        sum4z=0.
c
cc      do 923 k=1,nz
c  now concn1=concc1=concen1 because only one z used here, liang
        sum1z=sum1z+concc1
        sum2z=sum2z+concc2
        sum3z=sum3z+concc3
        sum4z=sum4z+concc4
c
c 923  continue
        concn1=sum1z
        concn2=sum2z
        concn3=sum3z
        concn4=sum4z
c 922  continue
c 921  continue
c
c*****
c  end time loop
c*****
c 100  continue
c
c
c
c *****
c  RISK ASSESSMENT CALCULATION -- ingestion
c  calculate average concentration during a 30 year
c  exposure period, then convert that to a 70 year
c  lifetime average dose by multiplying by 2 l/d,
c  and dividing by 70 kg and 70 years. Then multiply
c  by slope factor. Conc. units are converted to mg/l
c
c  RISK Assessment calculation -- inhalation
c  include risk due to offgassing in shower, bathroom and house
c  using standard EPA methodology, and implemented in Maxwell et al., 1998
c  hardwire all inhalation parameters except for slope factors
c  note that water-air transfer efficiencies are slightly chemical
c  dependent, depending mainly on the aqueous diffusion coefficient
c
c  continue to use 30 year exposure period
c
c
c  another time loop to get 30 year exposures from concentration array
c----- write concentrations to an array for use in risk calculations, liang
c
c  do 950 l=1,nt      ! take off time loop
c

```



```

!-----zeroout the initial vaules for arrays, liang
!   do mm=1, nt           ! get nt from GoldSim run properties
!       concn1t(mm)=0.
!       concn2t(mm)=0.
!       concn3t(mm)=0.
!       concn4t(mm)=0.
!   enddo
!-----get deltt from GoldSim run properties
      nrisk=30/deltt
      l=t/deltt
      concn1t(l)=concn1
      concn2t(l)=concn2
      concn3t(l)=concn3
      concn4t(l)=concn4

      nbot=l-nrisk
      if(l.lt.nrisk) nbot=0
      ntop=l
!---- trapezoidal rule integraion, max of 30 years
c   do 951 i=1,nx      ! take off x loop
c   do 952 j=1,ny      ! take off y loop
      sumc1=0.
      sumc2=0.
      sumc3=0.
      sumc4=0.
c
      do 960 m=nbot+1, ntop
        if(m.eq.1) then
          sumc1=sumc1+deltt*concn1t(m)/2.
          sumc2=sumc2+deltt*concn2t(m)/2.
          sumc3=sumc3+deltt*concn3t(m)/2.
          sumc4=sumc4+deltt*concn4t(m)/2.
        endif
        if(m.gt.1) then
          sumc1=sumc1+deltt*(concn1t(m-1)+concn1t(m))/2.
          sumc2=sumc2+deltt*(concn2t(m-1)+concn2t(m))/2.
          sumc3=sumc3+deltt*(concn3t(m-1)+concn3t(m))/2.
          sumc4=sumc4+deltt*(concn4t(m-1)+concn4t(m))/2.
        endif
      960 continue
c
c   average of concentrations (mg/l)*t during past 30 years
      avec1=sumc1/(1000.*30.)
      avec2=sumc2/(1000.*30.)
      avec3=sumc3/(1000.*30.)
      avec4=sumc4/(1000.*30.)
c
c*****
c   ingestion risk -- 2 liters per day, 70 kg person, 70 year averaging period
c   30 year exposure period

```

```

c
c convert to dose normlized by 70 year lifetime, at 2 liters/d, 70 kg
c
doseg1=avec1*2.*30./(70.*70.)
doseg2=avec2*2.*30./(70.*70.)
doseg3=avec3*2.*30./(70.*70.)
doseg4=avec4*2.*30./(70.*70.)
c
c ingestion cancer risk-- use EPA RAGS exponential model
c
riskg1=1.-exp(-slopef(1)*doseg1)
riskg2=1.-exp(-slopef(2)*doseg2)
riskg3=1.-exp(-slopef(3)*doseg3)
riskg4=1.-exp(-slopef(4)*doseg4)
riskgtot=riskg1+riskg2+riskg3+riskg4
c
c
c
c*****
c inhalation risk -- shower, bathroom, house, 70 kg person, 70 year averaging period
c 30 year exposure period
c
c
c ----- convert average water concentration to gas concentration (mg/m**3) in shower, bathroom, house
c
c shower stall concentration
c water use rate is 480 L/hr; transfer efficiency is 0.5; air exchange rate is 12 m**3/hr
cairsh1=avec1*480.*0.5/12.
cairsh2=avec2*480.*0.5/12.
cairsh3=avec3*480.*0.5/12.
cairsh4=avec4*480.*0.5/12.
c
c bathroom concentration
c water use rate is 40 L/hr; transfer efficiency is 0.43; air exchange rate is 55 m**3/hr
caibr1=avec1*40.*0.43/55.
caibr2=avec2*40.*0.43/55.
caibr3=avec3*40.*0.43/55.
caibr4=avec4*40.*0.43/55.
c
c house concentration
c water use rate is 40 L/hr; transfer efficiency is 0.43; air exchange rate is 750 m**3/hr
cairhs1=avec1*40.*0.43/750.
cairhs2=avec2*40.*0.43/750.
cairhs3=avec3*40.*0.43/750.
cairhs4=avec4*40.*0.43/750.
c
c----- calculate inhalation dose in shower, bathroom, house, assume breathing rate of 13.25 m**3/d
c 70 kg person, 70 year life, and convert from hours to days
c
c shower stall dose, exposure time is 0.17 hr/d

```

```

dosehsh1=cairsh1*0.17*13.25*30./(70.*70.*24.)
dosehsh2=cairsh2*0.17*13.25*30./(70.*70.*24.)
dosehsh3=cairsh3*0.17*13.25*30./(70.*70.*24.)
dosehsh4=cairsh4*0.17*13.25*30./(70.*70.*24.)
c
c bathroom dose, exposure time is 0.32 hr/d
dosehbr1=caibr1*0.32*13.25*30./(70.*70.*24.)
dosehbr2=caibr2*0.32*13.25*30./(70.*70.*24.)
dosehbr3=caibr3*0.32*13.25*30./(70.*70.*24.)
dosehbr4=caibr4*0.32*13.25*30./(70.*70.*24.)
c
c house dose, exposure time is 15.9 hr/d
dosehhs1=cairhs1*15.9*13.25*30./(70.*70.*24.)
dosehhs2=cairhs2*15.9*13.25*30./(70.*70.*24.)
dosehhs3=cairhs3*15.9*13.25*30./(70.*70.*24.)
dosehhs4=cairhs4*15.9*13.25*30./(70.*70.*24.)
c
c----- add up inhalation dose for each compound
doseh1=dosehsh1+dosehbr1+dosehhs1
doseh2=dosehsh2+dosehbr2+dosehhs2
doseh3=dosehsh3+dosehbr3+dosehhs3
doseh4=dosehsh4+dosehbr4+dosehhs4
c
c inhalation cancer risk-- use EPA RAGS exponential model
c
riskh1=1.-exp(-slopefh(1)*doseh1)
riskh2=1.-exp(-slopefh(2)*doseh2)
riskh3=1.-exp(-slopefh(3)*doseh3)
riskh4=1.-exp(-slopefh(4)*doseh4)
riskhtot=riskh1+riskh2+riskh3+riskh4
c
c total risks -- sum of ingestion and inhalation
c
risk1=riskg1+riskh1
risk2=riskg2+riskh2
risk3=riskg3+riskh3
risk4=riskg4+riskh4
risktot=risk1+risk2+risk3+risk4
c
c 952 continue
c
c 951 continue
c time
c 950 continue
c
c
c*****
cc end time loop, no need of time loop, Liang
c*****
c 100 continue

```

```

c export discharges, concentrations, and cancer risks
  out(1)=sumdisch1    !unit: kg/yr
  out(2)=sumdisch2    !unit: kg/yr
  out(3)=sumdisch3    !unit: kg/yr
  out(4)=sumdisch4    !unit: kg/yr
  out(5)=dischtot     !unit: kg/yr
  out(6)=concn1       !unit: ug/l
  out(7)=concn2       !unit: ug/l
  out(8)=concn3       !unit: ug/l
  out(9)=concn4       !unit: ug/l
  out(10)=conctot     !unit: ug/l
  out(11)=risk1
  out(12)=risk2
  out(13)=risk3
  out(14)=risk4
  out(15)=risktot
c*****
cc assign value from Fortran to GoldSim output, Liang
c*****
c
c
c   elseif (method.eq.99) then    !Cleanup
c     close (unit=15)
c   else
c     write(15,*)'FortranDLL was called with an invalid argument'
c   endif
c
c
c   return
c   end subroutine
c
c
c
c
c   subroutine zone1(x,t,tres,retard,velp,x1,x2,tplume1,tplume2)
c   this subroutine computes the residence times for locations in zone 1
cc----take off the common block, re-declare arguments for zone1, liang
cc   common/tran/tres(3,3),retard,velp,x1,x2,tplume1,tplume2
cc   real retard,velp,x1,x2,tplume1,tplume2
cc     real tres(3,3)
cc     real x, t,ttravel,trelease
c   travel time to x
cc   ttravel=retard*x/velp
c   time of release from x=0
cc   trelease=t-ttravel
c   time in period 1
cc   if(t.le.tplume1) then
cc     tres(1,2)=0.
cc     tres(1,3)=0.
cc     tres(1,1)=ttravel

```

```

        endif
c   time in period 2
if((t.gt.tplume1).and.(t.le.tplume2)) then
    tres(1,3)=0.
    if(trelease.ge.tplume1) then
        tres(1,1)=0.0
        tres(1,2)=ttravel
    endif
    if(trelease.lt.tplume1) then
        tres(1,1)=tplume1-trelease
        tres(1,2)=t-tplume1
    endif
endif
c   time in period 3
if(t.gt.tplume2) then
    if(trelease.ge.tplume2) then
        tres(1,1)=0.
        tres(1,2)=0.
        tres(1,3)=ttravel
    endif
    if((trelease.ge.tplume1).and.(trelease.lt.tplume2)) then
        tres(1,1)=0.
        tres(1,2)=tplume2-trelease
        tres(1,3)=t-tplume2
    endif
    if(trelease.lt.tplume1) then
        tres(1,1)=tplume1-trelease
        tres(1,2)=tplume2-tplume1
        tres(1,3)=t-tplume2
    endif
endif
return
end subroutine zone1
c
c
c
subroutine zone2(x,t,tres,retard,velp,x1,x2,tplume1,tplume2)
c   this subroutine computes the residence times for locations in zone 2
cc----take off the common block, re-declare arguments for zone2, liang
cc   common/tran/tres(3,3),retard,velp,x1,x2,tplume1,tplume2
real retard,velp,x1,x2,tplume1,tplume2
real tres(3,3)
real x, t,ttravel,trelease
c   travel time from x1 to x
ttravel=retard*(x-x1)/velp
c   time of release from x=x1
trelease=t-ttravel
c   time in period 1
if(t.le.tplume1) then
    tres(2,2)=0.

```

```

        tres(2,3)=0.
        tres(2,1)=ttravel
    endif
c   time in period 2
    if((t.gt.tplume1).and.(t.le.tplume2)) then
        tres(2,3)=0.
        if(trelease.ge.tplume1) then
            tres(2,1)=0.0
            tres(2,2)=ttravel
        endif
        if(trelease.lt.tplume1) then
            tres(2,1)=tplume1-trelease
            tres(2,2)=t-tplume1
        endif
    endif
c   time in period 3
    if(t.gt.tplume2) then
        if(trelease.ge.tplume2) then
            tres(2,1)=0.
            tres(2,2)=0.
            tres(2,3)=ttravel
        endif
        if((trelease.ge.tplume1).and.(trelease.lt.tplume2)) then
            tres(2,1)=0.
            tres(2,2)=tplume2-trelease
            tres(2,3)=t-tplume2
        endif
        if(trelease.lt.tplume1) then
            tres(2,1)=tplume1-trelease
            tres(2,2)=tplume2-tplume1
            tres(2,3)=t-tplume2
        endif
    endif
c   calculate time when solute crossed x1 for zone1 subroutine call
c   this is the travel time to x1 plus the time of release from x=0
    tx1=retard*x1/velp+t-retard*x/velp
    call zone1(x1,tx1,tres,retard,velp,x1,x2,tplume1,tplume2)
c
    return
    end
c
c
c
    subroutine zone3(x,t,tres,retard,velp,x1,x2,tplume1,tplume2)
c   this subroutine computes the residence times for locations in zone 3
cc---take off the common block, re-declare arguments for zone1, liang
cc    common/tran/tres(3,3),retard,velp,x1,x2,tplume1,tplume2
    real retard,velp,x1,x2,tplume1,tplume2
    real tres(3,3)
    real x, t,ttravel,trelease

```

```

c   travel time from x2 to x
    ttravel=retard*(x-x2)/velp
c   time of release from x=x2
    trelease=t-ttravel
c   time in period 1
    if(t.le.tplume1) then
        tres(3,2)=0.
        tres(3,3)=0.
        tres(3,1)=ttravel
    endif
c   time in period 2
    if((t.gt.tplume1).and.(t.le.tplume2)) then
        tres(3,3)=0.
        if(trelease.ge.tplume1) then
            tres(3,1)=0.0
            tres(3,2)=ttravel
        endif
        if(trelease.lt.tplume1) then
            tres(3,1)=tplume1-trelease
            tres(3,2)=t-tplume1
        endif
    endif
c   time in period 3
    if(t.gt.tplume2) then
        if(trelease.ge.tplume2) then
            tres(3,1)=0.
            tres(3,2)=0.
            tres(3,3)=ttravel
        endif
        if((trelease.ge.tplume1).and.(trelease.lt.tplume2)) then
            tres(3,1)=0.
            tres(3,2)=tplume2-trelease
            tres(3,3)=t-tplume2
        endif
        if(trelease.lt.tplume1) then
            tres(3,1)=tplume1-trelease
            tres(3,2)=tplume2-tplume1
            tres(3,3)=t-tplume2
        endif
    endif
c   calculate time when solute crossed x2 for zone2 subroutine call
c   this is the travel time to x2 plus the time of release from x=0
    tx2=retard*x2/velp+t-retard*x/velp
    call zone2(x2,tx2,tres,retard,velp,x1,x2,tplume1,tplume2)
c
    return
end
c
c
c

```

```

function expd(x)
c arguments less than -170 return zero
expd=0.
  if(x.lt.-170.) return
  expd=exp(x)
  return
end
c
c
function erf(x)
c error function from abramowitz and stegun
  p=.3275911
  a1=.254829592
  a2=-.284496736
  a3=1.421413741
  a4=-1.453152027
  a5=1.061405429
  xx=abs(x)
  t=1./(1.+p*xx)
  erf=1.-(a1*t+a2*t**2+a3*t**3+a4*t**4+a5*t**5)*expd(-xx**2)
  if (x.lt.0.) erf = -erf
  return
end
c
c
function f2(r1,r2,y21,t)
cc----add declaration for arguments of function to avoid error during exporting to GoldSim, liang
  real r1, r2, y21, t
c function used in first daughter product
  f2=y21*r1*(exp(-r1*t)-exp(-r2*t))/(r2-r1)
  return
end
c
c
function f3(r1,r2,r3,y32,y21,t)
cc----add declaration for arguments of function to avoid error during exporting to GoldSim, liang
  real r1, r2,r3,y32,y21,t
c function used in second daughter product
  part1=y32*r2*y21*r1/((r2-r1)*(r3-r2)*(r1-r3))
  part2=(r3-r2)*exp(-r1*t)+(r1-r3)*exp(-r2*t)+(r2-r1)*exp(-r3*t)
  f3=-part1*part2
  return
end
c
c
function f4(r1,r2,r3,r4,y43,y32,y21,t)
cc----add declaration for arguments of function to avoid error during exporting to GoldSim, liang
  real r1,r2,r3,r4,y43,y32,y21,t
c function used in third daughter product
  part1=y43*r3*y32*r2*y21*r1/((r2-r1)*(r4-r3))

```



```
part2=(exp(-r1*t)-exp(-r3*t))/(r3-r1)-  
&(exp(-r1*t)-exp(-r4*t))/(r4-r1)-  
&(exp(-r2*t)-exp(-r3*t))/(r3-r2)+  
&(exp(-r2*t)-exp(-r4*t))/(r4-r2)  
f4=part1*part2  
return  
end
```

REFERENCES

- Alvarez, P.J.J., and W.A. Illman. 2006. *Bioremediation and Natural Attenuation*. Hoboken, New Jersey: Wiley-Interscience.
- Aziz, C.E., C.J. Newell, J.R. Gonzales, P. Hass, T.P. Clement, and Y. Sun, 2000. BIOCHLOR Natural Attenuation Decision Support System. User's Manual Version 1.0, *U.S. Environmental Protection Agency*, EPA/600/R-00/008.
- Aziz, C.E., C.J. Newell, and J.R. Gonzales, 2002. BIOCHLOR Natural Attenuation Decision Support System Version 2.2. User's Manual Addendum. <http://www.epa.gov/ada/download/models/biochlor22.pdf>.
- Bedient, P. B., H.S. Rifai, C.J. Newell, 1999. *Groundwater Contamination: Transport and Remediation*, 2nd ed. Prentice-Hall, 1999.
- Brown, C.L., G.A. Pope, L.M. Abriola, and K. Sepehrnoori, 1994. Simulation of Surfactant-Enhanced Aquifer Remediation. *Water Resource Research*, 30(11): 2959-2977.
- Brusseau, M.L., D.A. Sabatini, J.S. Gierke, and M.D. Annable, ed. 1999. *Innovative Subsurface Remediation, Field Testing of Physical, Chemical, and Characterization Technologies*, ACS Symposium Series 725. Washington, DC: American Chemical Society.
- Chang, S.S., 1999. Implementing Probabilistic Risk Assessment in USEPA Superfund Program. *Human and Ecological Risk Assessment: An International Journal*, Vol. 5, 737-754.
- Chapelle, F.H., M.A. Widdowson, J.S. Brauner, E. Mendez, and C.C. Casey, 2003. *Methodology for Estimating Times of Remediation Associated with Monitored Natural Attenuation*. USGS Water-Resources Investigation Report 03-4057. Reston, Virginia: USGS.
- Charbeneau, R.J. 2000. *Groundwater Hydraulics and Pollutant Transport*. Upper Saddle River, New Jersey: Prentice Hall.
- Corporate Remediation Group (CRG) (An Alliance between DuPont and URS Diamond), May 30, 2002. TCE Corrective Action Plan Modification Report for DuPont Kinston Plant.
- Corporate Remediation Group (CRG) (An Alliance between DuPont and URS Corporation-North Carolina), June 27, 2008. 2007 annual TCE Monitoring Report

- Delshad, M., G.A. Pope, and K. Sepehrnoori, 1996. A Compositional Simulator for Modeling Surfactant Enhanced Aquifer Remediation. *Journal of Contaminant Hydrology*, Vol. 23, No. 4, 303-327.
- DuPont Environmental Remediation Services (DERS), October, 1992. Soil Investigation and Characterization Study Electroosmosis/In-situ Bioremediation Project.
- DuPont Environmental Remediation Services (DERS), February, 1994. Kinston Plant Manufacturing Area Corrective Action Plan.
- DuPont Environmental Remediation Services (DERS), August, 1995. Baseline Conditions Report TCE Remediation System.
- DuPont Environmental Remediation Services (DERS), June, 1998. Plan For Implementing Zero Valent Iron Treatment In The Central Manufacturing Area.
- Falta, R.W., K. Pruess, I. Javandel, and P.A. Witherspoon. 1992. Numerical Modeling of Steam Injection for the Removal of Nonaqueous Phase Liquids from the Subsurface, I, Numerical Formulation. *Water Resources Research*, Vol. 28, No. 2, 433-449.
- Falta, R.W., P.S.C. Rao and N. Basu. 2005a. Assessing the impacts of partial mass depletion in DNAPL source zones: I. Analytical modeling of source strength functions and plume response. *Journal of Contaminant Hydrology*, Vol. 78, No. 4, 259-280.
- Falta, R.W., N. Basu. and P.S.C. Rao, 2005b. Assessing the impacts of partial mass depletion in DNAPL source zones: II. Coupling source strength functions and plume evolution. *Journal of Contaminant Hydrology*, Vol. 79, No. 1-2, 45-66.
- Falta, R.W., 2007. REMChlor User's Manual Beta Version 1.0.
- Falta, R.W., 2008. Methodology for comparing source and plume remediation alternatives. *Groundwater*, Vol. 46, No. 2, 272-285.
- Fetter, C. W., 1993. Contaminant Hydrogeology, Macmillan Publishing Co., New York, NY.
- Freeze, G.A., J.C. Fountain, and G.A. Pope, 1994. Modeling the surfactant-enhanced remediation of PCE at the Borden Test Site using the UTCHEM compositional simulator. *Toxic Substances and the Hydrologic Sciences*, 339-345.
- Fure, A.D., J.W. Jawitz, and M.D. Annable. 2005. DNAPL source depletion: Linking architecture and flux response. *Journal of Contaminant Hydrology*, Vol. 85, No. 3-4, 118-140.
- Gillham, R. W. and S. F. O'Hannesin, 1994. Enhanced degradation of halogenated aliphatics by zero-valent iron. *Ground Water*, vol.32, no.6: 958-967.
- GoldSim User's Guide (v9.60), 2007. GoldSim Technology Group.
- GoldSim Dashboard Authoring Module User's Guide (v9.60), 2007. GoldSim Technology Group,

- Hope, B. and M. Stock, 1998. Guidance for use of probabilistic analysis in human health risk assessments. Oregon Department of Environmental Quality, Portland OR.
- Interstate Technology & Regulatory Council (ITRC), 2006. Life Cycle Cost Analysis. RPO-2. Washington, D.C. pp4.
- Jawitz, J.W., A.D. Fure, G.G. Demmy, S. Berglund, and P.S.C.Rao. 2005. Groundwater contaminant flux reduction resulting from nonaqueous phase liquid mass reduction. *Water Resources Research*, Vol. 41, no. 10, W10408.
- Kaluarachchi, J.J., ed. 2001. Groundwater Contamination by Organic Pollutants, Analysis and Remediation. ASCE Manuals and Reports on Engineering Practice No. 100. Reston, Virginia: American Society of Civil Engineers.
- Li, J., H.G. Huang, G. Zeng, I. Maqsood, Y. Huang, 2007. An integrated fuzzy-stochastic modeling approach for risk assessment of groundwater contamination. *Journal of Environmental Management*, Vol. 82, 173–188.
- Liang, H., 2005. Multiphase Flow Modeling of Field Scale Cosolvent Flooding for DNAPL Remediation. M. S. Thesis, Dept. of Geological Science, Clemson University, Clemson, SC.
- Liang, H. and R.W. Falta, 2008. Modeling field-scale cosolvent flooding for DNAPL source zone remediation. *Journal of Contaminant Hydrology*, Vol. 96, No. 1-4, 1-16.
- Liu, L., S. Y. Cheng and H. C. Guo, 2004. A simulation-assessment modeling approach for analyzing environmental risks of groundwater contamination at waste landfill sites. *Human and Ecological Risk Assessment: An International Journal*, Vol. 10 (2), 373 — 388.
- Mackay, D.M., and J.A. Cherry, 1989. Groundwater contamination: Pump-and-treat remediation. *Environmental Science and Technology*, 23(6): 630-636.
- Mayer, A.S., and S.M. Hassanizadeh, ed. 2005. Soil and Groundwater Contamination: Nonaqueous Phase Liquids. Water Resources Monograph 17. Washington, DC: American Geophysical Union.
- McDade, J.M., T.M. McGuire, and C.J. Newell, 2005. Analysis of DNAPL source-depletion costs at 36 field sites, *Remediation*, Spring 2005, 9-18.
- McGuire, T.M., J.M. McDade, and C.J. Newell. 2006. Performance of DNAPL source depletion technologies at 59 chlorinated solvent-impacted sites. *Ground Water Monitoring and Remediation*, Vol. 26, No. 1, 73–84.
- National Research Council (NRC). 2000. Natural Attenuation for Groundwater remediation. Washington, DC: National Research Council, National Academy Press.

- Newell, C.J., R.K. McLeod, and J.R. Gonzales. 1996. BIOSCREEN Natural Attenuation Decision Support System User's Manual Version 1.3, EPA/600/R-96/087. Washington, DC: U.S. EPA National Risk Management Research Laboratory.
- Pankow, J.F., S. Feenstra, J. A. Cherry, and M.C. Ryan, 1996. Dense chlorinated solvents in groundwater, Background and history of the problem. In *Dense Chlorinated Solvents and other DNAPLs in Groundwater*. eds. J.F. Pankow and J.A. Cherry, 1-46. Waterloo, Ontario, Canada: Waterloo Press.
- Park, E. and J.C. Parker, 2005. Evaluation of an upscaled model for DNAPL dissolution kinetics in heterogeneous aquifers. *Advanced Water Resource*. Vol. 28, 1280-1291.
- Parker, J.C., and E. Park, 2004. Modeling field-scale dense nonaqueous phase liquid dissolution kinetics in heterogeneous aquifers. *Water Resources Research*, Vol. 40, W05109.
- Pope, G.A. and R.C. Nelson .1978. A chemical flooding compositional simulator. *Society of Petroleum Engineers Journal*, 18(5): 339-354.
- Rao, P.S.C., J.W. Jawitz, C.G. Enfield, R. Falta, M.D. Annable, and A.L. Wood. 2001. *Technology Integration for Contaminated Site Remediation: Cleanup Goals and Performance Metrics*. Sheffield, UK: Ground Water Quality.
- Rao, P.S.C., and J.W. Jawitz. 2003. Comment on “Steady-state mass transfer from single-component dense non-aqueous phase liquids in uniform flow fields” by T.C. Sale & D.B. McWhorter. *Water Resources Research*, Vol. 39, No. 3, 1068.
- Reddi, L.N., ed. 1996. Non-aqueous phase liquids (NAPLs) in subsurface environment: Assessment and remediation. In *Proceedings of the Specialty Conference held in Conjunction with the ASCE National Convention, November 12–14, 1996*. New York: American Society of Civil Engineers, 852.
- Robinson, B.A., C. Li, C.K. Ho, 2003. Performance assessment model development and analysis of radionuclide transport in the unsaturated zone, Yucca Mountain, Nevada. *Journal of Contaminant Hydrology*, 62-63, 249-268.
- Shoemaker, Steve, February 10, 2002. Draft. In Situ Treatment of a TCE Source Area Using a Jetted Slurry of ZVI and Clay.
- Slob, W and M.N. Pieters, 1998. A probabilistic approach for deriving acceptable human intake limits and human health risks from toxicological studies: General framework. *Risk Analysis*, Vol. 18, 787–798.
- U.S. Environmental Protection Agency (USEPA), 1989. *Risk Assessment Guidance for Superfund, Volume I, Human Health Evaluation Manual (Part A)*, PB90-155581, National Technical Information Service, Springfield, VA.
- U.S. Environmental Protection Agency (USEPA), 1997. *Cleanup of the Nation's Waste Sites: Markets and Technology Trends*. EPA 542-R-96-005. U.S. Environmental Protection Agency: U.S. Government Printing Office: Washington, DC.

- U.S. Environmental Protection Agency (USEPA), 2001. Risk assessment guidance for Superfund: Volume III – Part A, Process for conducting probabilistic risk assessment. US Environmental Protection Agency, Washington DC, report EPA/540/R-02/002.
- U.S. Environmental Protection Agency (USEPA). 2004a. Cleanup of the Nation's Waste Sites: Markets and Technology Trends. EPA 542-R-96-005. U.S. Environmental Protection Agency: U.S. Government Printing Office: Washington, DC.
- U.S. Environmental Protection Agency (USEPA), 2004b. The DNAPL Remediation Challenge: Is There a Case for Source Depletion? Kavanaugh, M. C. and P.S.C. Rao (editors), EPA/600/R-03/143, National Risk Management Research Laboratory, Office of Research and Development, U.S. Environmental Protection Agency, Cincinnati, Ohio, USA.
- Verschuere, Karel, Handbook of Environmental Data on Organic Chemicals, 2001, John Wiley & Sons.
- Wiedemeier, T.D., H.S. Rifai, C.J. Newell, and J.T. Wilson. 1999. Natural Attenuation of Fuels and Chlorinated Solvents in the Subsurface. New York: John Wiley and Sons Inc.
- Zhang, Y.Q., C.M. Oldenburg, S. Finsterle, G.S. Bodvarsson, 2007. System-level modeling for economic evaluation of geological CO₂ storage in gas reservoirs. *Energy Conversion and Management* 48, 1827–1833.
- Zhu, J., and J.F. Sykes, 2004. Simple screening models of NAPL dissolution in the subsurface, *Journal of Contaminant Hydrology*, Vol. 72, No. 1-4, pp245-258.